ISBN 978-82-326-5849-7 (printed ver.)
ISBN 978-82-326-5232-7 (electronic ver.)
ISSN 1503-8181 (printed ver.)
ISSN 2703-8084 (electronic ver.)

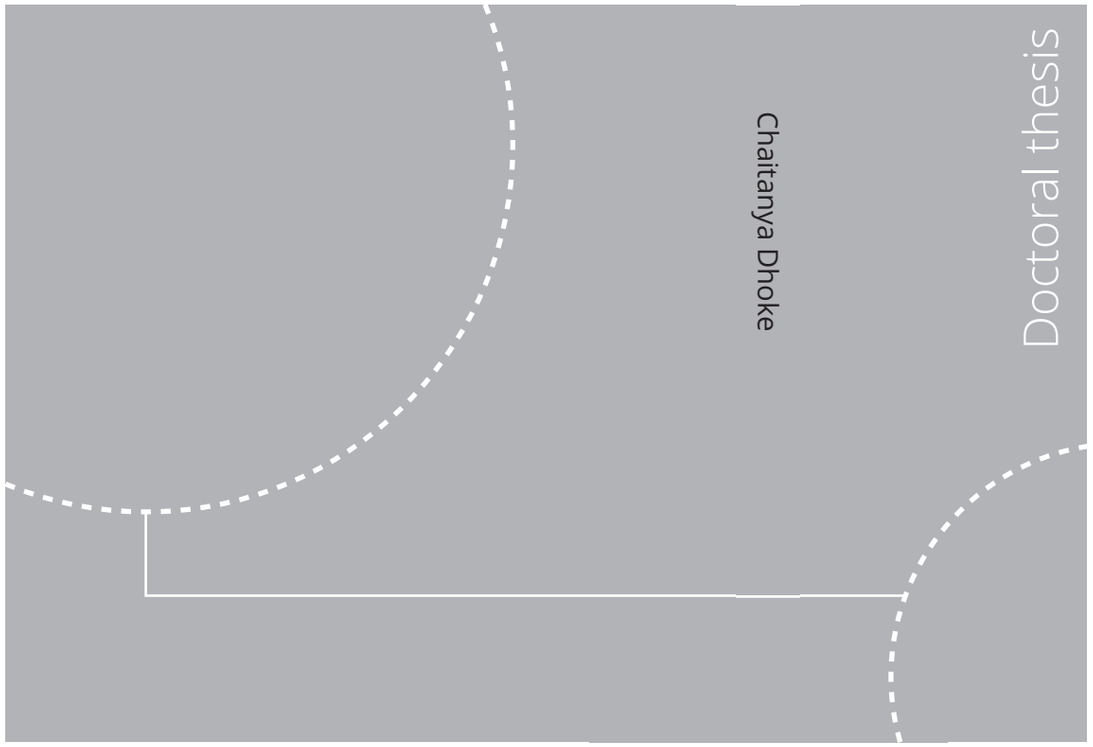

Doctoral theses at NTNU, 2021:148

Chaitanya Dhoke

Demonstration of Swing Adsorption Reactor Cluster (SARC) concept for CO_2 capture

Doctoral theses at NTNU, 2021:148

Chaitanya Dhoke
Doctoral thesis

NTNU
Norwegian University of Science and Technology
Thesis for the degree of Philosophiae Doctor

NTNU
Norwegian University of Science and Technology

NTNU
Norwegian University of Science and Technology

Chaitanya Dhoke

Demonstration of Swing Adsorption Reactor Cluster (SARC) concept for CO_2 capture

Thesis for the degree of Philosophiae Doctor

Trondheim, April 2021

Norwegian University of Science and Technology

NTNU
Norwegian University of
Science and Technology

NTNU
Norwegian University of Science and Technology

Thesis for the degree of Philosophiae Doctor

ISBN 978-82-326-5849-7 (printed ver.)
ISBN 978-82-326-5232-7 (electronic ver.)
ISSN 1503-8181 (printed ver.)
ISSN 2703-8084 (electronic ver.)

Doctoral theses at NTNU, 2021:148

PRINTED IN NORWAY
NO - 1598

NORDIC SWAN ECOLABEL
Printed matter
2041 0731

Printed by Skipnes Kommunikasjon AS

‘To my lovely daughter Srinidhi Dhoke for the love, understanding, and support’

Preface

This thesis is submitted in partial fulfillment of the requirement for the degree of Philosophiae Doctor (Ph.D.) at the Norwegian University of Science and Technology (NTNU). The work was carried out at the Department of Energy and Process Engineering, NTNU with close collaboration with SINTEF Industry under the supervision of Shahriar Amini and Abdelghafour Zaabout. This project (SARC) was possible due to the funding from the Research Council of Norway, under the CLIMIT program (grant no. 268507/E20).

Acknowledgement

I would like to express gratitude to my supervisor, Dr. Shahriar Amini for giving me the opportunity to work on this interesting project and I acknowledge your support during these three years. My sincere thanks go to my co-supervisor, Dr. Abdelghafour Zaabout for the guidance and involvement at every stage of this research. You are instrumental to every outcome of this work and I owe you more than I can acknowledge. Also, I would like to express my heartful thanks to Dr. Schalk Cloete who has been a great support and friend. His help, suggestions, comments, and discussions were phenomenal. He has helped me more than I could ever give him credit for.

This project would not have been possible without the financial support from the Research Council of Norway under the CLIMIT program (grant no. 268507/E20). I thank the project partners KRICT from South Korea and RTI from USA for the sorbent materials. I also thank the management of Equinor for the 2019 publication grants. The VATL Lab technicians at the Norwegian University of Science and Technology are equally acknowledged for constructing and maintaining the experimental setup. Reidar Tellebon and Håvard Rekstad are like friends to me; they always provide timely support and assistance. I am also grateful to Paul Svendsen, Martin Bustadmo, Aleksander Mosand, Bjørn, Bendik Sægrov for the technical support. Thank you Morten Grønli for providing the necessary support, approving my experiments, and responding swiftly to my request. I also thank Maxime Chauvet and Leyne Demoulin for the support during their internships.

Coming to Trondheim brought much progress in my life. Within this short period, I have met wonderful friends. I would like to thank Dr. Ambrose Ugwu for being there for me always. You have been like a family member in Trondheim. I would also like to thank Mogahid Osman, Mohammed Khan, Shareq Mohd Nazir, Giorgia Mondino and Jan Hendrik Cloete. You guys are always ready to help; the support, encouragement, and motivation from you cannot be overemphasized. We had great times together and I enjoyed sharing ideas with you. I also thank Dr. Shreenath Krishnamurthy, Dr. Hwimin Seo, Dr. Ignacio Luz, Dr. Mustapha Soukri, Dr. Yong-ki Park, Dr. Richard Blom, Dr. Dr. Kiwoong Kim for the discussion and technical suggestion.

I do have many other important people to thank and I will try not to miss anyone. Let me start with my ex-colleagues at SABIC, Dr. Prasanna Pathak and Dr. P. Manikandan whom I have worked under. They have instilled immense motivation in me to pursue a Ph.D. They have shown me, what a good scientist (and person) should be. My experience at SABIC has helped to sustain me here.

Thank you, Sandeep Negi, Arun T P, Harsha Dharwad, Deepak Pal, Akash Mittal, Nicky Dandwani, Neeraj Meerani, Rakesh K, Makarand D and Ajit Dubey for the friendship and support. Vishal and Shirish Abhyankar are equally not forgotten. I also thank Dr. Sanjib Das and Dr. Sandesh Deshmukh for technical advice and discussions.

One of the greatest things is the opportunity to work with Prof. B Viswanathan, Prof Dr. Sivasankar, Prof Dr. Krishnamurthy and Prof Dr. Selvam as part of my master's course. They have always continued to keep in touch and played their role as mentors even after all these years and distance. I have gained much knowledge and experience working with all of them during my course work as well as my master's thesis.

Lastly, I owe everything to my family members for their constant support and encouragement whenever needed, without them, it would have been impossible for me to complete this work. I would like to thank my parents of whom their love and guidance are with me in whatever I pursue. They are my ultimate role models. My brother Praful Dhoke has always been there for me, providing support and love to make this journey a success. To my other cousins and in-laws, I appreciated you all for the encouragement, love, and support. I wish to thank my loving and supportive wife, Rajalakshmi for being a great confidant, providing me strength and constant encouragement. Most importantly I would like to thank my wonderful daughter Srinidhi, it is her smiling face that always brings happiness to me.

Content

Abstract

Adsorption-based post-combustion CO_2 capture is enjoying significant research attention due to its wide applicability within the power and industrial sectors and its ability to retrofit existing infrastructure. Important research focus areas include reduction in energy penalty, cost and environmental impact. This thesis is focused on the experimental demonstration of the Swing Adsorption Reactor Cluster (SARC) for CO_2 capture. The SARC concept combines a temperature and vacuum swings for sorbent regeneration. A heat pump is used for transferring heat from the exothermic carbonation reaction to the endothermic regeneration reaction. Sorbent regeneration under vacuum allows for a small temperature difference between carbonation and regeneration, leading to a high heat pump efficiency, thereby minimizing the resulting energy penalty of CO_2 capture. This key principle behind the SARC concept was experimentally demonstrated in a bench-scale prototype and, subsequently, in a standalone multistage reactor with inbuilt heat transfer surfaces designed and constructed at the Norwegian University of Science and Technology (NTNU) in close collaboration with SINTEF Industry. The final research outcome of this thesis was achieved in four different campaigns as follows:

- **Proof of concept for hybrid mode of regeneration (VTSA):** The experiments were carried out in a bench-scale reactor designed for demonstrating the working principle of the SARC hybrid regeneration mode. This study compares combined vacuum and temperature swing adsorption (VTSA) to pure temperature swing adsorption (TSA). The comparison study showed that 50 mbar vacuum (VTSA) can reduce the required temperature swing by 30-40 °C compared to the TSA. A complete SARC cycle comprising of carbonation, evacuation, regeneration and cooling steps was successfully demonstrated, and the concept performed largely as expected. The study was completed using polyethyleneimine

supported (PEI) on silica sorbent supplied by the project partner KRICT (Korean research institute of chemical technology, South Korea).

- **Sorbent screening:** The main objective of this study was to identify the best performing sorbent for the Swing Adsorption Reactor Cluster (SARC) concept. The screening results of four sorbents indicated two PEI sorbents to be good candidates for the SARC application: a PEI sorbent functionalized with 1,2-epoxybutane supported on silica (referred to as EB-PEI in the rest of the document) and a PEI sorbent supported on mesoporous silica containing confined metal organic framework nanocrystals (referred to as PEI-MOF in the rest of the document). Though PEI-MOF working capacity was higher than EB-PEI sorbent, the large-scale reactor simulation suggested that it did not result in an efficiency advantage relative to EB-PEI, mainly due to the higher vacuum pump power consumption of PEI-MOF.
- **Demonstration of the Novel Swing Adsorption Reactor Cluster (SARC) Concept in a multistage fluidized bed with heat transfer surfaces:** A multistage fluidized bed lab-scale reactor with inbuilt heat exchangers was designed for the experimental demonstration of the novel SARC concept. The study showed 90% CO_2 capture from an N_2/CO_2 mixture approximating a coal power plant flue gas fed at 200 Nl/min, representing a CO_2 capture capacity up to 24 kg-CO_2/day. The lab-scale reactor utilized a vacuum pump and a heating oil loop (emulating the heat pump) to demonstrate the SARC concept. Experiments revealed that 1) the polyethyleneimine sorbent employed imposes no kinetic limitations in CO_2 adsorption and only minor non-idealities in regeneration, 2) a high heat transfer coefficient in the range of 307-489 W/m^2 K is achieved on the heat transfer surfaces inside the reactor, and 3) perforated plate separators inserted along the height of the reactor can achieve the plug-flow characteristics required for high CO_2 capture efficiency while maintaining good

fluidization conditions to maximize heat transfer. Finally, a sensitivity analysis revealed the expected improvements in CO_2 capture efficiency with increased pressure and temperature swings, and shorter carbonation times, demonstrating predictable behaviour of the SARC reactor. This study provides a sound basis for further scale-up of the SARC concept.

- **Reactor validation and techno-economic assessment of the SARC concept applied to a cement plant for CO_2 capture:** The experimental results from the multistage fluidized bed reactor were used to validate a SARC reactor model developed by SINTE. The previous assumptions made in the model for the pressure drop, the heat transfer coefficient and the number of CSTR were revised based on the lab scale experimental results. The reactor model reasonably predicted the experimentally observed CO_2 capture. Subsequently, industrial scale reactor modelling (using the adjusted model assumptions) and process simulations were completed. Two process schemes for SARC integration to cement plant were evaluated and new techno-economic assessments based on revised assumptions were completed for 6 new cases (compared to previously published). By combining the high experimentally observed heat transfer coefficient and the proven effectiveness of simple perforated separators for minimizing axial mixing with a new heat integration layout and shorter reactors, the CO_2 avoidance cost was reduced from a previously published value of 50.7 €/ton to 38.7 €/ ton of CO_2. This makes SARC not only the simplest option for retrofitting existing cement plants but also the most economical CO_2 capture solution for new plants.

Thesis outline

The thesis consists of 7 chapters with five of the chapters adapted from journal publications of the research outcome. Chapter 1 (introduction) gives an overview of the project, the motivation, the state-of-the-art, collaborations, the objectives, the scope, the method, and the contributions of the research. The technical background with a brief review about different reactor configurations is presented in Chapter 2. The demonstrations of SARC are reported in Chapters 3 – 6. Chapter 3 presents the successful bench-scale demonstration of the SARC working principle using the EB-PEI sorbent. Chapter 4 reports the screening study with the different sorbents to identify an efficient sorbent for this concept. Based on the learnings from the bench-scale reactor, a standalone multistage fluidized bed reactor was designed for demonstrating the continuous operation of the SARC concept. The study related to experimental demonstration with the previously identified sorbent candidate (EB-PEI) is presented in Chapter 5. Chapter 6 reports the reactor validation against results from the multistage fluidized bed reactor. This chapter also presents the process models and the techno-economic performance for two process schemes proposed for SARC integration to a cement plant. Finally, a distinct conclusion of the work and recommendations for future work are given in Chapter 7.

1 Introduction

The Swing Adsorption Reactor Cluster (SARC) concept is an adsorption-based process that aims to minimize both the energy penalty and process complexity related to CO_2 capture. It utilizes low-temperature solid sorbents and brings special advantages to retrofits in existing coal power plants and industrial applications such as cement and steel plants. The combined effect of heat and vacuum pump in the SARC concept significantly reduces the energy penalty (one of the important element of CO_2 capture cost). This concept provides an alternative to the interconnected circulating reactors (CFB) that present a challenge in getting the desired degree of CO_2 capture because of significant back mixing. This Ph.D. research project is focused on technical and economic demonstration of the SARC concept and is funded by the Research Council of Norway, under the CLIMIT program (grant no. 268507/E20).

1.1 Overview of the project approach

The project contains elements of experiments and techno-economic assessment. Experimental work was focused on understanding the reaction system, demonstrating the technical feasibility of the SARC concept and providing validation data to the phenomenological model that was used for the thermodynamic assessment of the full-scale SARC process [1]. The thermodynamic modelling work was conducted for the purpose of finding the optimized reactor design, the combination between the temperature and pressure swings, and operating conditions. The economic potential of the SARC process was evaluated for the integration of the SARC through dedicated economic assessment work.

1.2 Research tasks

The project has the following 5 tasks driven by four project partners as mentioned in *Table **1-1***. The basic characterization of the reaction equilibrium and kinetics was carried out at SINTEF Industry, Norway. The proof of technical feasibility was carried out at NTNU, Norway in close collaboration with SINTEF Industry by dedicated experimental work. The thermodynamic and economic assessment of the project was completed in collaboration between POLIMI, Italy, SINTEF Industry, Norway and NTNU, Norway. The sorbents were prepared by two project partners; KRICT, South Korea and RTI, USA. The overall project was managed and coordinated by SINTEF Industry, Norway.

*Table **1-1**: SARC project task breakdown and task owner.*

Project work task	**Task owner**
Basic characterization of reaction equilibria and kinetics	SINTEF Industry, Norway
Demonstration of technical feasibility	NTNU, Norway
Thermodynamic and economic assessments	POLIMI
Sorbent preparation	KRICT, South Korea and RTI, USA
Management and dissemination	SINTEF Industry, Norway

1.3 Motivation

Greenhouse gas (GHG) emission has adversely affected our environment and has resulted in serious climate change with consequences such as heatwaves, wildfire, acidifying oceans, etc. With the current emission rate, a 1.5 °C increase in global temperature relative to the preindustrial level would be attained by 2040 [2]. Thus, urgent actions are required to prevent irreversible damages to planetary ecosystems.

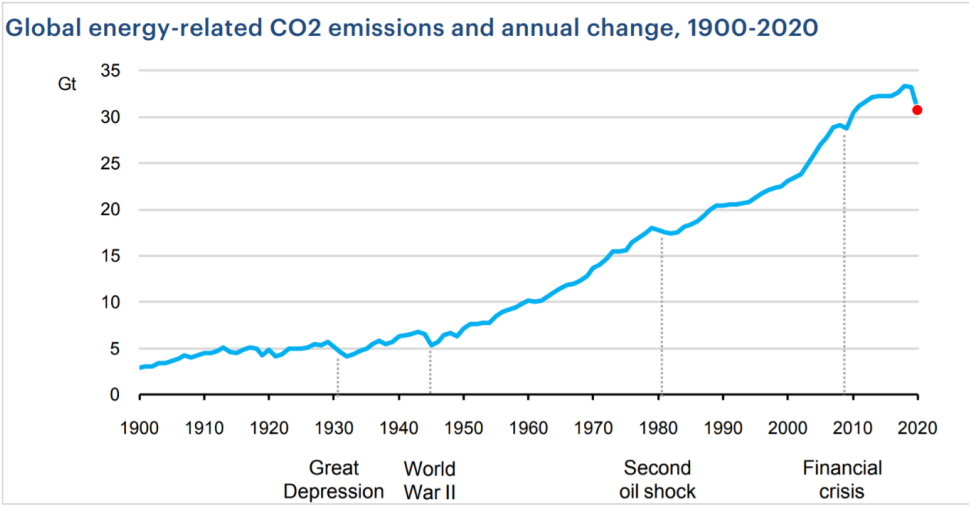

*Figure **1-1**: Global CO_2 emission till 2020 [3].*

The GHG emissions are mainly associated with the energy production based on fossil-fuel and industrial application such as cement and steel industries. As seen in *Figure **1-1***, CO_2 emissions from the energy sector has already reached a historic 33.1 gigatons (Gt) in 2018 [4]. Although the emissions slowed down in the first quarter of 2020 due to the lockdown of COVID-19 which lowered the global energy demand by ~ 3.8% relative to the first quarter of 2019, it is expected that the emissions trend will recover when the lockdown is relaxed [3].

CO_2 capture, utilization, and storage (CCUS) is considered a vital approach and is recommended by the IPCC report (2014) to control the anthropogenic CO_2 emission [5]. In CCUS, amine scrubbing is the most mature process for CO_2 capture, but it imposes a high energy penalty [6-9] that results in very high CO_2 avoidance cost (in the range of 60-140 £/ton of CO_2 from cement plant based on various process integration) [10]. Moreover, this process is not considered as green as it generates and emits hazardous chemicals such as nitrosamines to the environment [11-13]. Owing to these challenges, adsorption-based post-combustion CO_2 capture is enjoying significant research attention due to its potential for significant reductions in energy penalty, cost and

environmental impact. This thesis is focused on the development of an adsorption-based CO_2 capture technology aiming to reduce the high energy penalty associated with the conventional amine-based process. This adsorption process runs on electricity which makes it highly suitable to retrofits in power and industrial plants without any requirement of process integration. However, it should be noted that adsorption process has its own challenges, especially with the stability of sorbent particles and achieving high capture rate with CO_2 purity.

1.4 Objectives

The overall aim of the project is to accelerate the scale-up of the SARC concept and the specific objectives of this Ph.D. research are presented below:

- Demonstrate the hybrid mode of combined temperature and vacuum swing regeneration and identify suitable sorbents for the SARC concept.
- Develop and commission a lab scale standalone reactor for a continuous SARC operation.
- Demonstrate the SARC concept by completing continuous cycles and achieving 90% CO_2 capture. Another important objective of the demonstration study was to confirm the assumptions made in the SARC reactor model [1] with dedicated experiments.
- Estimate the CO_2 avoidance cost for the SARC integration to the cement plant.

1.5 SARC concept

The Swing Adsorption Reactor Cluster (SARC) concept combines temperature and vacuum swings for sorbent regeneration. It is an alternative configuration to interconnected fluidized bed reactors and employs transient standalone reactors. To achieve steady-state CO_2 capture, SARC reactors are operated in a cluster as shown in *Figure **1-2a***. To reduce the energy penalty, a heat pump is used

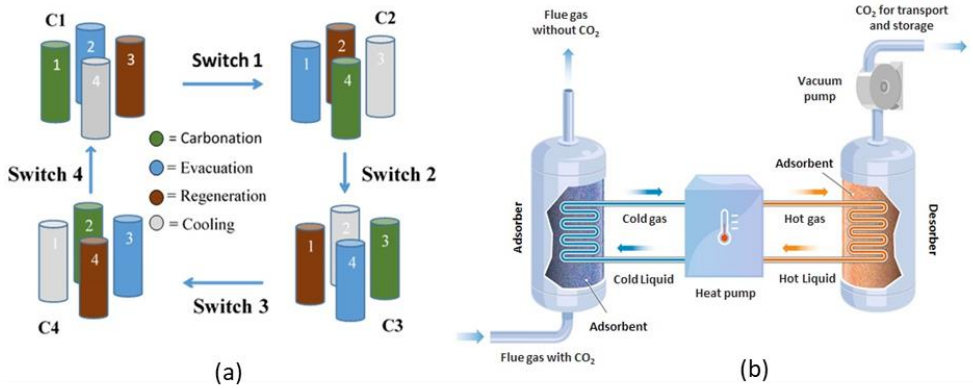

*Figure **1-2**: A conceptual design of SARC: (a) a SARC cluster composed of four reactors for steady operation; (b) a heat pump transferring heat between two SARC reactors in the cluster; one under carbonation and the other under regeneration.*

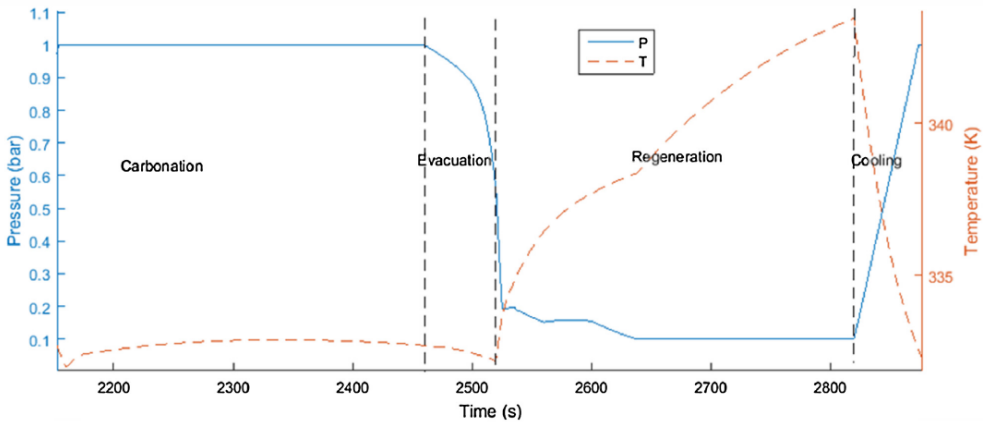

*Figure **1-3**: A typical SARC reactor cycle as simulated using a CSTR model developed in Zaabout et al.[1] where a PEI-based sorbent was used.*

for transferring heat from the exothermic carbonation reaction to the endothermic regeneration reaction as shown in *Figure **1-2b***. Sorbent regeneration under vacuum allows for a small temperature difference between carbonation and regeneration, leading to a high heat pump efficiency, thereby minimizing the resulting energy penalty of CO_2 capture.

Each reactor in the cluster completes the SARC cycle illustrated in *Figure **1-3***, consisting of 1) carbonation (adsorption), 2) evacuation, 3) regeneration and 4) cooling to deliver a concentrated CO_2 stream for utilization or storage. The sorbent adsorbs CO_2 from the flue gas at atmospheric pressure (1 bar) and low temperatures during the carbonation step. To ensure high CO_2 purity, some of the N_2 accumulated in the reactor from the carbonation step is evacuated and vented to the atmosphere in the evacuation step, reducing the pressure to a moderate level (500-700 mbar). In the regeneration step, a temperature swing is applied in combination with a stronger vacuum (compared to the evacuation step) to recover the CO_2 adsorbed in the carbonation step. The last step, cooling, is applied to repressurize the reactor and cool it for starting the next SARC cycle [1]. Application of a 0.1 bar vacuum can allow sorbent regeneration at very low temperature swing, implying a high heat pump efficiency ($COP \approx 0.65\, T_{cold}/(T_{hot} - T_{cold}) = 12$ in the example *Figure **1-3***). Efficient heat transfer via the heat pump requires a fluidized bed reactor, but axial mixing in the reactor must also be restricted to achieve high CO_2 capture rates in the carbonator. The presence of heat transfer tubes will already restrict axial mixing, although good plug flow behaviour can be achieved by strategically placed baffles or a multistage reactor configuration.

1.6 Methodology

The research work combines the experimental approach to demonstrate the technical feasibility of the concept and modelling work to evaluate the economics of the SARC concept.

1.6.1 Experimental approach

The experimental demonstration was completed with two reactor setups; a bench scale and a lab-scale reactor. The bench-scale reactor was designed and constructed to understand the system and screen different sorbents to identify an efficient sorbent for the SARC process. The process flow

diagram of the bench-scale setup is presented in *Figure **1-4***. The setup comprises of a 2 cm diameter and 100 cm length with a porous plate placed at the bottom to hold the particles and uniformly distribute the gas to the reactor. The reactor was placed in a jacketed shell, wherein cooling water can be circulated, or electrical heating can be supplied. The reactor was heated up to the operating

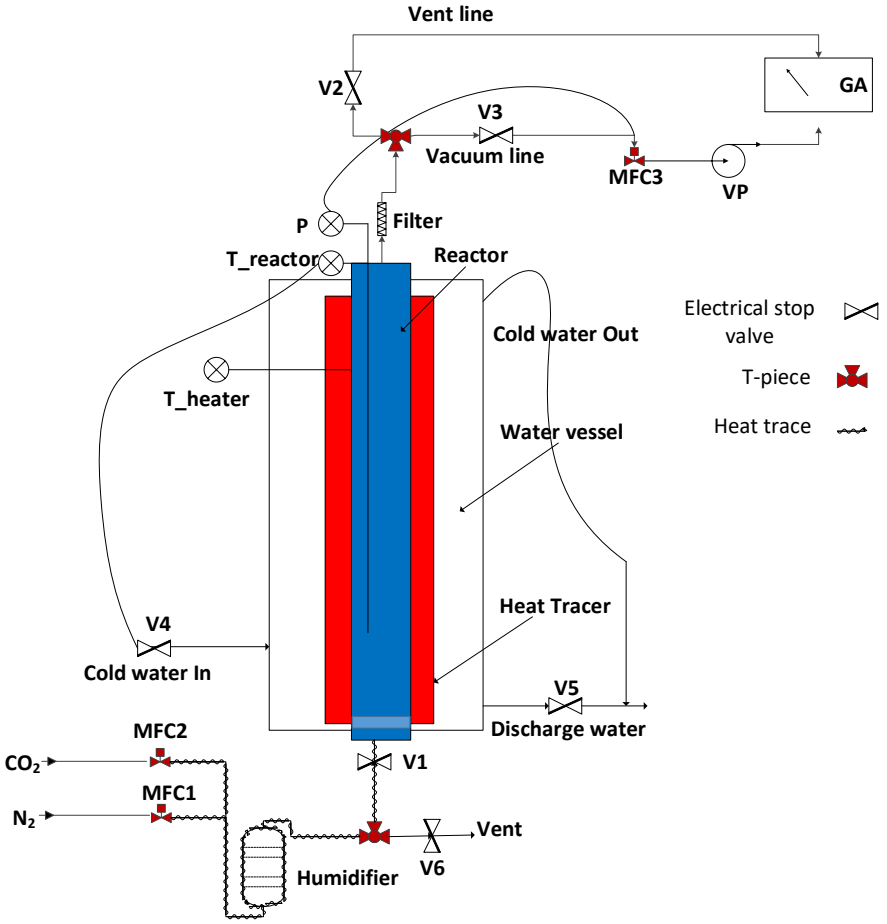

GA	MFC1	MFC2	MF3	P	T_heater	T_reactor	V1	V2	V3	V4	V5	V6	VP
Online gas analyzer	Mass flowmeter for N_2	Mass flowmeter for CO_2	Mass flowmeter to control pressure inside reactor	Pressure transmitter	Thermocouple measuring heater temperature (outside)	Thermocouple measuring adsorbent temperature (inside)	Valve on feed inlet line to reactor	Valve on atmospheric vent line	Valve on vacuum line	Valve on water inlet line	Valve on water discharge line	Valve in humidifier outlet line	Vacuum pump

*Figure **1-4**: Bench scale experimental set up.*

temperature using an external electrical heater surrounding the bottom half part of the reactor body and was monitored using a thermocouple inserted into the bed from the top of the reactor. Vacuum was established inside the reactor using a vacuum pump, while the pressure was controlled using a mass flow controller (MFC3) that was placed on the reactor outlet just before the vacuum pump. A pressure sensor measuring the pressure inside the reactor was then controlled by MFC3 to establish the target pressure. Gas feeds into the reactor were controlled using two mass flow controllers; MFC1 and MFC2. The experimental setup is equipped with an online syngas analyzer (ETG MCA 100 Syn Biogas Multigas Analyzer) sampling gases at the outlet of the atmospheric and vacuum vents to measure the gas composition at 1 Hz frequency.

Based on the learning from the bench-scale reactor, a lab scale multistage reactor setup was designed with the inbuilt heat exchangers which is presented in *Figure **1-5***. The main components of the experimental setup are the multistage fluidized bed reactor with built-in heat transfer surfaces, the oil and water circuits controlling the heat exchange, a vacuum pump, various mass flow controllers, thermocouples and pressure sensors for controlling and monitoring the setup operation.

One standalone reactor (*Figure **1-6a***) was built with a dimension of 15 cm x 12 cm x 250 cm (L x D x H) that can accommodate up to four stages on top of each other, separated by perforated metallic plates (*Figure **1-6b***) when needed, otherwise, it can also be used as one single stage fluidized bed. The separating perforated plates used were selected to have enough space for individual sorbent particles to pass through without any blockage while it creates the multistage effect envisioned for the SARC concept by restricting axial particle mixing. It has circular openings with 1.1 mm diameter and a density of 27 holes/cm^2.

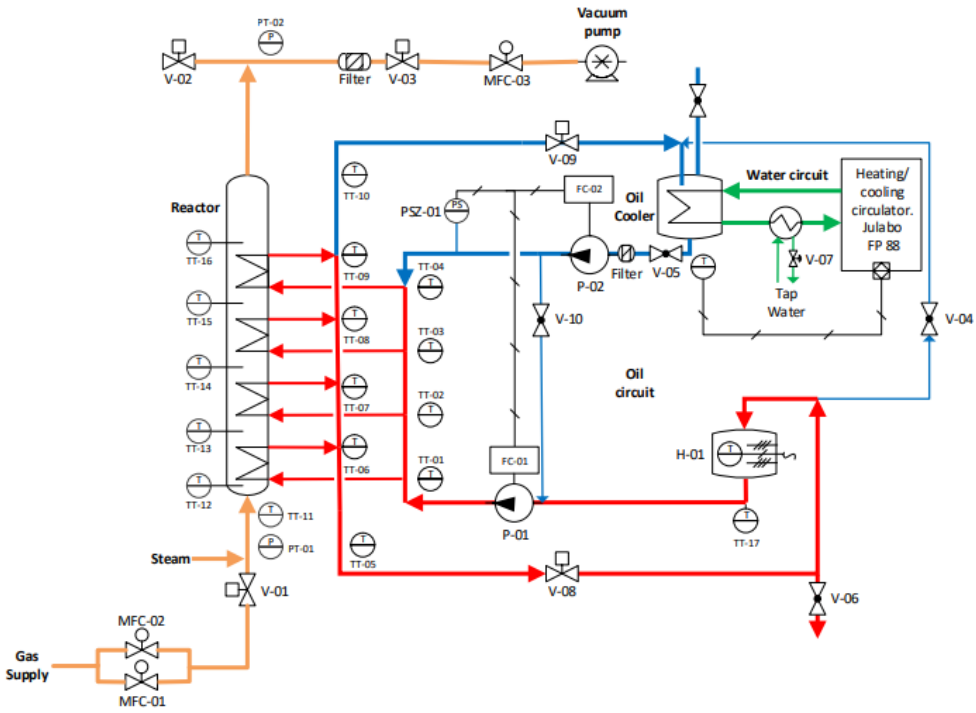

H-01	MFC1	MFC2	MF3	PT-01 & 02	P-01 & 02	PSZ-01	TT-01 - 04	TT-06 - 09	TT-12 - 16	V-04, 05, 07, 08, 10	V-08	V-09
Electric heating tank for oil	Mass flowmeter for N_2	Mass flowmeter for CO_2	Mass flowmeter to control pressure inside reactor	Pressure transmitter	Oil pumps for low and high temp. oil circuits	Pressure safety switch	Thermocouple measuring heat exchanger inlet oil temp.	Thermocouple measuring heat exchanger outlet oil temp.	Thermocouples measuring adsorbent temp. (inside the bed)	Manual and needle valves placed on different points of the circuits for different purposes	Valve on high temp. oil circuit	Valve on low temp. oil circuit

*Figure **1-5**: A process flow scheme of the SARC lab scale experimental setup.*

The heat exchanger (*Figure **1-6c***) used in the lab scale SARC reactor is made of aluminum flat sheets (1 m x 0.1 m) with a U shaped arrangement to provide a good heat exhange area of 3.16 m^2 in the reactor. The heat transfer areas of the internal heat exchanger are equally distributed between the different stages where oil is circulated through for heat addition/recovery depending on the reaction taking place. The experimental setup is equipped with an online syngas analyzer (ETG MCA 100 Syn Biogas Multigas Analyzer) at the outlet of the atmospheric and vacuum vents to measure the gas composition at 1 Hz frequency.

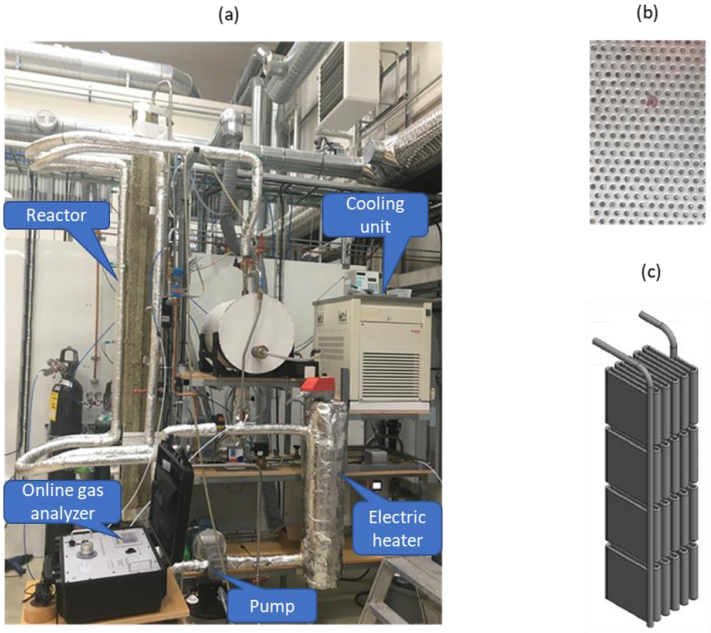

*Figure **1-6**: **a**) Image of SARC lab scale experimental set up; **b**) Metallic plate; **c**) Heat exchanger built in reactor.*

Oil is circulated through separate high and low-temperature circuits to emulate the functionality of the heat pump (recovering heat from the exothermic carbonation for supplying the endothermic regeneration). The oil in the high-temperature circuit (red lines in *Figure **1-5***) is heated by the electric heater, while the oil in the low-temperature circuit (blue lines in *Figure **1-5***) is controlled by the cooling unit (manufactured by Julabo). Oil from the low-temperature circuit is used to recover the heat released in the carbonation step and to cool the reactor, while oil from the high-temperature circuit is used to supply heat during regeneration. This circuit is also used during startup for heating the bed to the targeted operating temperature. The oil from both circuits is pumped into the heat exchanger (P-01 and P-02), where the desired flowrate can be set. A water circuit is also provided to assist in removing the excess heat from the low-temperature oil before it is sent to the reactor for recovering heat from the carbonation.

Each stage of the reactor is equipped with three thermocouples: one that records the bed temperature (inside the reactor) and two more on the heat exchanger to measure the inlet and outlet temperatures of the oil. The information from these thermocouples is used for calculating the heat transfer coefficient between the bed and the oil. The reactor is also equipped with two pressure sensors (bottom and top) for pressure monitoring and recording. Gas feeds are controlled using two mass flow controllers: MFC1 and MFC2 in *Figure **1-5***. The outlet gases pass through a particle filter before being vented or sent to the vacuum pump. A vacuum is established inside the reactor using a vacuum pump, while the pressure is controlled using MFC3 that is placed on the reactor outlet just before the vacuum pump. The reactor and both oil circuits are insulated by a 6 cm thick insulation layer. The feed line is heated with a heat tracer to maintain the temperature of the feed gas entering the reactor. The experimental setup is equipped with an online syngas analyzer (ETG MCA 100 Syn Biogas Multigas Analyzer) sampling gases at the outlet of the atmospheric and vacuum vents to measure the gas composition at a 1 Hz frequency. Given the maximum measurable CO_2 concentration (60%), provision is made to feed a controlled flow of N_2 (not shown in *Figure **1-5***) after MFC3, which is also used as a basis for quantification of the molar flow of CO_2 exiting the reactor during the regeneration step (in combination with the gas composition measured by the gas analyzer). In summary, the experimental demonstration was flexiable enough that different process parameters were studied and evaluated under realistic SARC operating conditions.

1.6.2 Process modelling

Two process models for SARC integration to a cement plant were evaluated in this study. The process models were implemented in Aspen plus and the Peng-Robinson property method was used to estimate the properties of the streams. The process scheme comprises of a heat pump circuit integration to SARC reactors, CO_2 vacuum pumps, and a CO_2 compression section. The results

from the industrial reactor model were used as input to the process models to estimate the energy requirement of the process (blowers, vacuum pump, compressors, auxiliary pumps, etc.). This input was then used in a subsequent economic assessment.

1.7 Contribution

The main contributions of the thesis are summarized below:

- This thesis reports the successful demonstration of the hybrid regeneration (combined temperature and vacuum swing) approach. Additionally, serval sorbents were screened, and polyethyleneimine (PEI) was identified as a suitable sorbent for the SARC concept.
- A multistage standalone fluidized bed reactor with inbuilt heat exchangers for continuous SARC operation was designed and successfully commissioned.
- The first experimental demonstration of SARC using a multistage fluidized bed reactor with inbuilt heat exchangers was completed. The result of the demonstration showed that SARC could achieve 90% CO_2 capture. The multistage effect and the kinetic limitations presented by the PEI sorbent were investigated. The study also reports the heat transfer coefficient measured during the adsorption and regeneration steps.
- Two process models for the integration of SARC concept to cement plant were completed to estimate the techno-economic performance.
- The research activity done for the completion of this project has been reported in five international journal articles (three already published and two submitted) and presented in five international conferences.

1.8 List of articles

Five journal articles (Articles I – V) have been included in this thesis and I am the first author for all. Three of the articles (I, II, IV) have been published already while two (III, & V) have been submitted for publication in international journals. My specific contribution and percentage of efforts in these articles is presented in *Table **1-2***.

*Table **1-2**: My specific contribution in the articles.*

Articles	**Efforts (%)**	**Contribution in paper**
I	80	• Commissioning of small bench scale reactor • Experimentations in bench scale fluidized bed reactor (Proof of concepts- 4 studies) • Data analysis • Manuscript preparation
II	50	• Modification in small bench scale reactor • Experimentations in bench scale fluidized bed reactor (Reactor experiments- 4 studies) • Data analysis • Manuscript preparation
III	60	• Compilation of open literature • Data analysis • Manuscript preparation
IV	80	• Design and commissioning of lab scale fluidized bed reactor • Experimentations in a lab scale fluidized bed reactor (Demonstration- 4 studies) • Data analysis • Manuscript preparation
V	40	• Experimentation in lab scale fluidized bed reactor • Data analysis • Built 2 Process models for SARC integration • Manuscript preparation (experimentation and process modeling)

In all the articles, I was responsible for the experimental demonstration, analysis of the results, discussions, and preparation of the manuscript. Abdelghafour Zaabout participated in the planning, running of the experiments, result analysis, discussion, and preparation of the manuscript in all the studies. Schalk Cloete was involved in result analysis, reactor modelling, isotherm fitting, economics and manuscript preparation for articles I to V. Shreenath Krishnamurthy contributed to the breakthrough experiments in article II and Richard Blom were responsible for isotherm measurements. Hwimin Seo, Ignacio Luz, Mustapha Soukri and Yong-ki Park were responsible for

the material selection, chemistry, and preparation. Leyne Demoulin has contributed for measuring heat transfer coefficient in article IV. The entire study was supervised by Abdelghafour Zaabout and Shahriar Amini.

Article I present the experimental results from a bench scale fluidized bed reactor with the hybrid regeneration mode (VTSA) as proposed in the SARC concept. This provides the experimental validation that the addition of vacuum reduce the temperature swing, which can reduce the heat pump power consumption of the SARC concept. The screening of different sorbents is presented in the Article II to identify suitable sorbent for SARC process. Article III presents the review on various reactor configuration adopted for the CO_2 capture. The advantages and limitations of various configurations and regeneration modes is also discussed. The final demonstration of SARC concept in a standalone multistage fluidized bed reactor with the identified sorbent (PEI) is reported in the Article IV. The study also reports the results of the experimental campaigns designed to validate the assumptions made in previous modelling wok. The learnings from the experimental results were then used to revise the assumptions and a new economics for the SARC integration to cement plant is presented in the Article V.

Article I

Dhoke, C.; Zaabout, A.; Cloete, S.; Seo, H.; Park, Y.-k.; Blom, R.; Amini, S., *The swing adsorption reactor cluster (SARC) for post combustion CO_2 capture: Experimental proof-of-principle*. Chemical Engineering Journal 2019, 377, 120145.

Article II

Dhoke, C.; Cloete, S.; Krishnamurthy, S.; Seo, H.; Luz, I.; Soukri, M.; Park, Y.-k.; Blom, R.; Amini, S.; Zaabout, A., *Sorbents screening for post-combustion CO_2 capture via combined temperature and pressure swing adsorption*. Chemical Engineering Journal 2019, 122201.

Article III

Dhoke, C.; Zaabout;, A.; Cloete;, S.; Amini;, S., *Review on reactor configurations for adsorption-based CO_2 capture.* Industrial & Engineering Chemistry Research 2021.

Article IV

Dhoke, C.; Zaabout, A.; Cloete, S.; Seo, H.; Park, Y.-k.; Demoulin, L.; Amini, S., *Demonstration of the Novel Swing Adsorption Reactor Cluster Concept in a Multistage Fluidized Bed with Heat-Transfer Surfaces for Postcombustion CO_2 Capture*. Industrial & Engineering Chemistry Research 2020.

Article V

Dhoke, C.; Zaabout;, A.; Cloete;, S.; Amini;, *Study of the cost reductions achievable from the novel SARC CO2 capture concept using a validated reactor model.* Industrial & Engineering Chemistry Research (under review)

2 Review on reactor configurations for adsorption-based CO_2 capture

This chapter has been adapted from **Article III**

Dhoke, C., et al., *Review on reactor configurations for adsorption-based CO_2 capture.* Industrial & Engineering Chemistry Research (2021).

Abstract

Adsorption based CO_2 capture has enjoyed considerable research attention in recent years. Most of research efforts focused on sorbent development to reduce the energy penalty. However, the use of suitable gas-solid contacting systems is key for extracting the full potential from the sorbent to minimize operating and capital costs and accelerate the commercial deployment of the technology. This paper reviews several reactor configurations that were proposed for adsorption-based CO_2 capture. The fundamental behaviour of adsorption in different gas-solid contactors (fixed, fluidized, moving or rotating beds) and regeneration under different modes (pressure, temperature or combined swings) is discussed, highlighting the strengths and limitations of different combinations of gas-solid contactor and regeneration mode. In addition, the estimated energy duties in published studies and current technology readiness level of the different reactor configurations are reported. Other aspects, such as the reactor footprint, the operation strategy, suitability to retrofits and the ability to operate under flexible loads are also discussed. In terms of future work, the key research need is a standardized techno-economic benchmarking study to calculate CO_2 avoidance costs for different adsorption technologies under standardized assumptions. Qualitatively, each technology presents several strengths and weaknesses that make it impossible to identify a clear optimal solution. Such a standardized quantitative comparison is therefore needed to focus future technology development efforts.

Keywords: *Post combustion CO_2 capture; Adsorption; temperature swing, vacuum swing, combined vacuum and temperature swing; fixed bed reactor, moving bed, Fluidized bed, regeneration energy*

2.1 Introduction

The growing global warming threats caused by anthropogenic CO_2 emissions are increasingly dictating the need for a radical shift to a more sustainable energy system and environmentally friendly industrial production practices. In this context, the Paris Climate agreement, with the goal of maintaining the global temperature well below 2 °C, recommended implementation of stringent policy measures to incentivize cutting CO_2 emissions. CO_2 capture and storage (CCS) is considered a vital technology to include in CO_2 emission reduction pathways for cost effective mitigation of global warming threats [5]. Among other CCS technologies, there is a growing interest in low temperature adsorption-based post combustion CO_2 capture due to its combined potential of reducing energy penalty and easy retrofitting with minimal integration with existing plants [14, 15]. More importantly, this technology offers the flexibility of capturing CO_2 from different industrial CO_2 sources owing to its different sorbent regeneration modes (temperature/pressure swings) and reactor types. To date, research in this field has focused mainly on sorbent development to reduce the energy penalty through minimizing the heat of reaction and maximizing the adsorption capacity, but also improving tolerance to impurities such as SOx and NOx [14, 16]. Sorbents could be classified in two categories depending on the heat of CO_2 sorption. The mechanism by which physisorption CO_2 adsorption occurs is driven by Van der Waals forces and/or electrostatic interactions between the CO_2 molecule and adsorbent surface [14, 16, 17]. As for chemisorption, a chemical reaction takes place between CO_2 and the active sites introduced to the sorbent through functional groups that usually include alkaline carbonates or various amine groups [14, 16]. The different adsorption mechanisms taking place in each category makes the physisorption based less sensitive to temperature and associated with low reaction enthalpy, being suitable to high CO_2 partial pressure gas streams, while the chemisorption based is more sensitive to temperature swing and can handle low CO_2 partial pressure gas streams. Recent research on

physisorption focused on metal organic framework (MOF) based sorbents that possess high specific surface area, thus maximizing the absolute adsorption capacity [14, 18-23]. As for the chemisorption-based sorbents, the largest focus is on the polyethyleneimine (PEI) based, given their relatively high adsorption capacity, good kinetics and insensitivity to water [14, 18, 24-26].

On the other hand, the energy penalty was the main driving factor behind the rapidly growing research in this field, where it was commonly stated that adsorption-based CO_2 capture can achieve lower energy penalty due to the lower specific heat capacity of solid sorbents in addition to avoiding evaporation of large amount of water in the regeneration as compared to solvent based technologies. This statement was however argued given the scattered range of the energy penalty data that were reported in the literature [27], creating confusions about adsorption-based CO_2 capture competitiveness with benchmarking technologies. Therefore, there is an urgent need for identifying the many factors (beyond the sorbent) that affect the performance and overall cost of adsorption-based CO_2 capture, and discuss the non-linear interaction between them that affect the technology behaviour, performance and prospects for scale up and ultimate industrial implementation.

Adsorption based CO_2 capture beyond sorbent development

A suitable contacting system is a key factor for efficient utilization of each sorbent category, as it affects both the process efficiency, footprint and overall capture costs [18]. In other words, material development should be tightly linked to the reactor configuration and regeneration mode [14, 16]. To this end, different types of reactors were applied to adsorption-based CO_2 capture, including fixed [28, 29], rotating [30], moving [31-33] and fluidized beds [34, 35]. Substantial research has been conducted on the fixed bed configuration, due to the simplicity of its basic design, testing

hundreds of sorbents under different regeneration modes [28, 29, 36], but the interest to the other reactor configurations has steadily grown in recent years [1, 37, 38].

Other key factors that affect the technology competitiveness are the total footprint, the ease of retrofitting to existing plants (e.g. level of integration with the existing plant and possible need for steam) and operability (some reactor configurations require only two reactors with sorbent circulating between them, while other operate using trains of dozens of reactors requiring advanced operating strategies). Additional aspects such as the potential for flexible operation and performance under partial capture scenarios are becoming increasingly important in a future energy system dominated by renewable energy. In this respect, similar to what was proposed for solvent based CO_2 capture technology [39, 40], adsorption technology can make CO_2 capture cost effective if it can use the excess of cheap renewable electricity in peak periods, combined with partial CO_2 capture when electricity price is high [41].

All these aspects will be discussed in this review paper for the different reactor configurations proposed for low temperature post combustion CO_2 capture by putting together key published research on those systems, discussing their working principles, nature of sorbents suitable for each configuration and suitable regeneration modes. The review will also highlight the pros and cons of each configuration, the energy penalty, the level of technological development, the total footprint, the ease of retrofitting into existing plants, operation strategy, the best suited CO_2 sources (industrial, power, waste, etc.), in addition to their potential for flexible operation and partial capture. This review will also shed light on the recent research trends and discuss the technical challenges and future research needs for further scale up of each configuration.

First, the various reactor configurations and different regeneration modes are discussed. Second, the process integration and the technology readiness level (TRL) of these technologies are

discussed. Finally, a discussion highlighting the role of all other factors affecting the overall competitiveness of adsorption technology and conclusions are presented. It should be noted that other published reviews partially touched on this topic [16, 27], but the focus was to a large extent on the fixed bed configuration, given the large number of studies existing in the literature for this configuration, but also due to the rapid advances made especially on the material development side. These reviews have paid little attention to the various other emerging reactor configurations and their sensitivity to the regeneration modes and other factors affecting their further scale up and commercialization.

2.1.1 Reactor configurations

The different reactor configurations previously proposed for low temperature adsorption-based CO_2 capture are shown in *Figure **2-1***. These configurations are classified into three main categories i.e. Fixed, moving and fluidized bed reactors. In fixed bed reactor, adsorbent particles are stationary, while they are moving in moving and fluidized bed reactor configurations. Each of these three categories are further divided into the different configurations. For fixed bed, it includes conventional fixed bed and structured reactor, for moving bed there is conventional moving bed and rotating bed, while for fluidized bed there is one stage, multistage and transient reactor configuration. The details about these reactors, working principles, their pros and cons are discussed in respective sections.

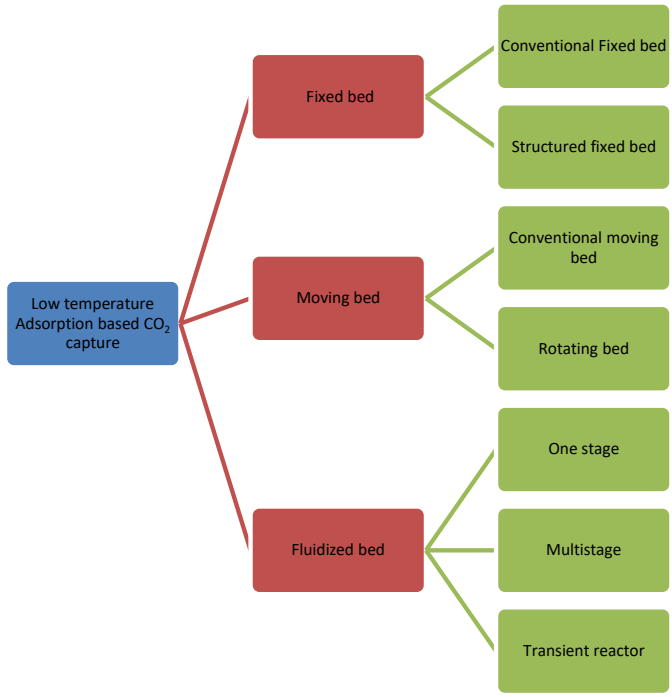

*Figure **2-1**: Reactor configurations used in low temperature adsorption-based CO_2 capture.*

2.1.2 Fixed bed reactor

The fixed bed is the simplest reactor configuration where a flue gas is passed through a fixed bed of sorbents pellets (mm size) or through specially designed structured packings. Structure packings are used to optimize the surface areas and void space for achieving high adsorption rate and low pressure drop. The plug-flow nature in this reactor configuration remains the main advantage, keeping the sorbent towards the end of the reactor in a highly regenerated state to ensure maximum CO_2 capture until almost the entire bed is saturated with CO_2. However, fixed beds are known to impose high pressure drops at even moderate gas flowrates, resulting in very large footprints [42]. Overcoming this key drawback requires the use of large particles or structured packings that greatly reduce the pressure drop, while striving to maintain high adsorption rates to allow for much higher

*Table **2-1:** Physical resistance dominating in bigger pellets of fixed bed reactors.*

Mass transfer	Heat transfer
Mass transfer of CO_2 from gas phase to the surface of the particle (film mass transfer)	Convective heat transfer from the gas phase to the surface of the particle (h_i = 20-50 W/m^{2}K)[43]
Diffusion of CO_2 inside the pores of the particle (k_{LDF} = 0.06 s^{-1}; D_e=5.35 x10^{-5} m^2/s at 301 K and 20% CO_2 in N_2 for 13X Zeolite)[44]	Heat transfer from surface to the inside pores of the adsorbent particle (k_f = 0.259 W/mK for ion exchange resin with a primary benzy sorbent)[45]
	Heat transfer from the heat transfer fluid to the gas phase (applicable in indirect heating cases (hi = ~10 W/m^{2}K)[43]

gas throughput rates [16]. In addition, fixed beds have inherently poor heat transfer properties, making them best suitable to pressure swing adsorption using physical sorbents with low reaction enthalpy and low temperature sensitivity.

2.1.2.1 Conventional fixed bed reactor

Generally, large adsorbent pellets are used in this configuration to minimize the pressure drop. This however comes at the expense of increased mass and heat transfer resistance as specified in *Table **2-1***, undermining the potential of the plug flow regime to maximize the working adsorption capacity. In such cases, these mass and heat transfer limitations create a dispersed reaction front travelling through the reactor. For illustrating this behaviour, typical axial instantaneous plots (along the length of the bed) of the normalized CO_2 concentration in gas phase and normalized vacant site in the solid phase are shown in *Figure **2-2***. Before the adsorption wave, no CO_2 is adsorbed on the solids given that the sorbent is saturated upstream of the wave ($\frac{C}{C_0} = 1 \; and \; \frac{\theta}{\theta_0} = 0$). In the adsorption wave, part of CO_2 adsorbs while the rest slips to the next section $\left(0 < \frac{C}{C_0} < 1\right)$ leading to the formation of a dispersing adsorption wave with a decreasing CO_2 concentration that in turn creates an increasing gradient of vacant sites in the adsorption wave.

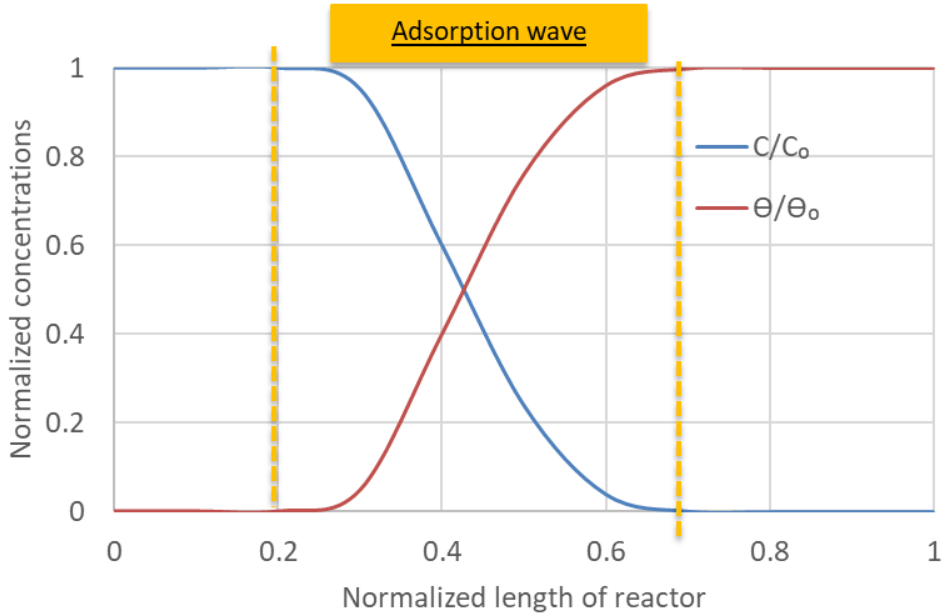

*Figure **2-2**: Concentration profile of CO_2 in gas and normalized vacant sites in solid phase along the length of reactor at particular time.*

A wide adsorption wave will cause CO_2 to break through at the reactor outlet while a large portion of the bed is still not fully saturated [46]. Other parameters that affect the dispersion of the adsorption wave are the sorbent properties (i.e. reaction kinetics, heat of adsorption, specific heat, size of the pellet, porosity, nature of the support) and the initial CO_2 in the flue gas and the process conditions.

One main factor that enhances the creation of the adsorption wave is the heat generation associated with CO_2 adsorption, leading to the creation of a heat front that travels along the bed similarly to the reaction front. Its amplitude depends on the heat of reaction (a range of 25-100 kJ/mole-of-CO_2 were reported for different sorbents), the sorbent specific heat capacity, the sorbent active content, reaction kinetics and the initial CO_2 partial pressure in the flue gas [16, 47, 48]. The resulting

increase in the bed temperature adversely affects the reaction equilibrium, thus decreasing the adsorption capacity. This requires more frequent switching of the inlet and outlet valves as less CO_2 can be captured in each cycle. Such a loss in the adsorption capacity is illustrated in *Figure **2-3*** (using Langmuir isotherm model for zeolite 13X) [49], visualizing the theoretically predicted adsorption capacity L_1 at the target operating temperature and the achieved one L_2 due to the temperature rise caused by the heat generation when CO_2 is adsorbed.

Where:

L_1: CO_2 loading on zeolite 13X sorbent at 25 °C, lower temperature

L_2: CO_2 loading on zeolite 13X sorbent at 60 °C, higher temperature

Various efforts have been made to tackle the heat wave issue encountered in fixed bed reactor configuration using two different approaches namely external and internal thermal management. The first approach is based on the use of smartly designed adsorbent particles that can absorb the

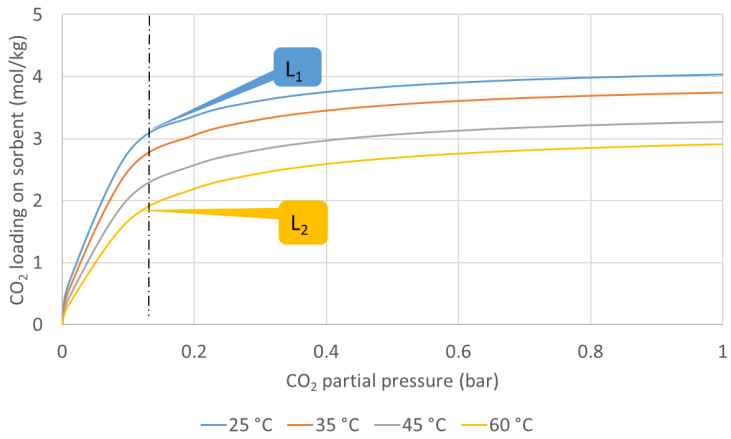

*Figure **2-3**: CO_2 isotherm model prediction for Zeolite 13X [49] illustrating the decrease in the adsorption capacity caused by the increase in temperature from 25 °C to 60 °C.*

released heat with minimal temperature change by embedding phase change materials (PCMs) into the adsorbent particle [50]. The main challenge associated with this approach is the dilution of the active adsorbent material with the PCMs which leads to a decrease in the absolute capacity (moles of CO_2 adsorbed/ m^3 of the reactor). The second approach uses a heat exchanger inserted in the reactor to remove the heat of adsorption, but it suffers from a long heating/cooling time because of the poor heat transfer properties of fixed bed reactors and is therefore not considered a viable option [51]. Both approaches lead to the increase in the volume and cost of the reactor.

2.1.2.2 Structured fixed bed reactor

Structured adsorbent reactors are considered a good alternative to conventional fixed bed. Generally, these systems can accommodate sophisticated packings that can maximize the surface area per volume of sorbent in addition to minimizing gas-particle drag and heat transfer resistance within the packing, thus enabling high gas throughput rates at minimal pressure drop [52] [51-53]. With such advantages, this configuration could theoretically reduce the cycle time and the productivity by orders of magnitude, thus accommodating the use of expensive high adsorption capacity sorbents while maintaining competitive CO_2 capture costs [16]. Tested reactors within this configuration consisted predominately of monolithic structures where the adsorbent material is coated with a thin film on the reactor wall. The thin film coating enables the use of higher flowrates at lower pressure drop thus improving the throughput by 3-10 times as compared to fixed bed configurations [54, 55]. Some of the expected benefits could already be seen, as the pressure drop can be reduced by 50 % as compared to pellet at a superficial velocity of 1 m/s [54]. Such high throughout would require sorbents with fast kinetics to avoid CO_2 slippage. Furthermore, good heat conductivity in the material and reactor wall helps maintaining better control on the temperature. These benefits remain however limited due to the low effective sorbent bulk density

achieved by using thin film (high percentage of the dead volume occupied by the support monolith). On the other hand, a benefit of having a high dead mass is that it acts as a heat sink and avoids the temperature rise in the adsorption step which delays the CO_2 breakthrough resulting in better CO_2 capture efficiency. The different structured packing tested so far [51-54, 56] remain unable to bring the targeted considerable reduction in the footprint of fixed bed reactor configuration given that all of them have less bulk density and use an inert body that occupies a large fraction of the reactor volume. Laminates and foamy structures were also evaluated for CO_2 capture purposes [51, 54, 57, 58].

2.1.3 Moving bed

2.1.3.1 Conventional moving bed reactor

Moving bed reactors are another widely explored reactor type for CO_2 capture as an alternative to fixed bed reactors. Fundamentally, moving beds behave similar to fixed beds, with the primary benefit being that the moving particle bed allows for steady state operation. The plug-flow behaviour of fixed beds is preserved with the additional benefit that the reaction front stays in the same location if the bed moves down at the same rate as the reaction front moves up. This allows for the use of a shorter reactor relative to conventional fixed bed concepts, which helps to reduce the pressure drop. However, the main drawbacks are the complexity of moving relatively large particles between different reactors and the interconnected nature of these reactors that exclude the possibility of a pressure swing. Temperature swing is more complex since mixing in moving beds is much less than in fluidized beds, making indirect heating via heat exchange surfaces relatively inefficient [59].

The first work on this configuration was proposed by Clyde Berg in 1946 and was known as "Hypersorption" process [60] and applied for the refinery off gases to recover propane, ethane and

ethylene. Lately, SRI International and Advanced Technology Materials, Inc. (ATMI) have proposed a new moving bed reactor design with prospects for reducing the energy penalty of post-combustion CO_2 capture technology. The reactor design comprises of a circulating system consisting of falling microbeads of an advanced carbon sorbent (ACS) to make the contact with the rising flue gas in counter-current mode [61, 62]. As shown in *Figure **2-4***, the reactor consists of several sections that the sorbent goes through to complete the CO_2 capture cycle (an adsorber, a transition, a desorber, a dehydrator , a cooler and a lift). The sorbent microbeads enter the reactor from the top starting with the adsorber where the 12.5% CO_2 from the flue gas adsorbs on the sorbent at low temperature (50-60 °C) and atmospheric pressure. While moving downwards it passes by a transition section where a purge of steam is used to preheat the sorbent before entering the desorber for regeneration. In the regenerator, high temperature steam is purged for direct heating at 120 °C. This leads to an additional step in the dehydrator (drying step) followed by a cooling step before the sorbent is lifted to start a new cycle. It should be noted that the used sorbent

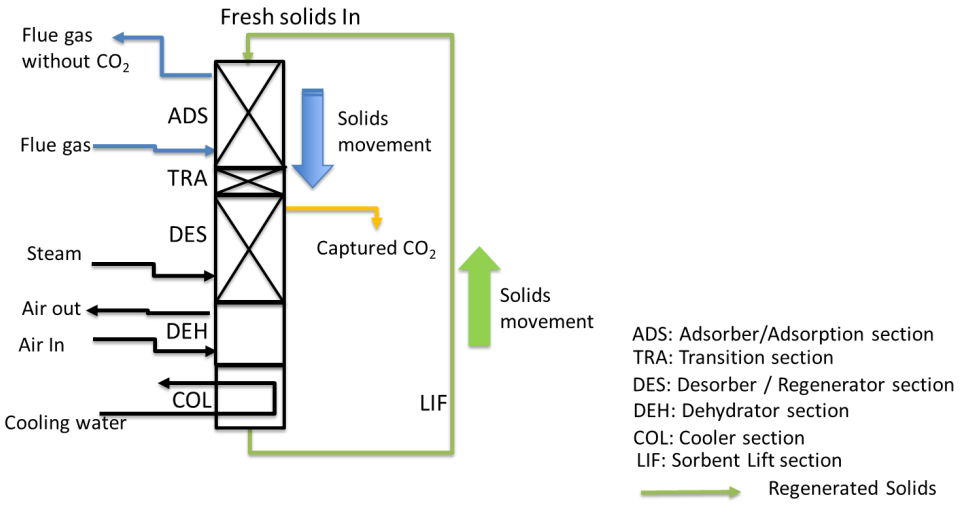

*Figure **2-4**: Moving bed reactor by SRI [63].*

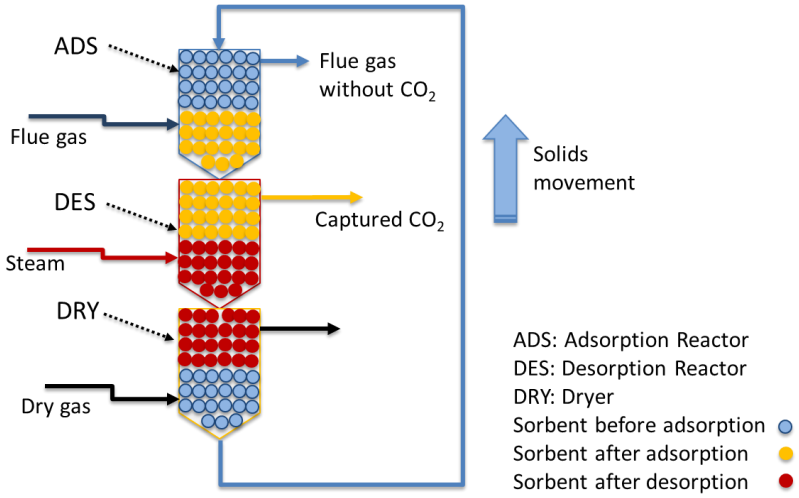

*Figure **2-5**: Moving bed process (KCC process) developed by Kawasaki [32].*

should be insensitive to water in this direct heating by steam while the resulting accumulated water in the CO_2 stream should be removed by condensation before transportation to avoid the corrosion issues caused by water during transportation. Structural packings were embedded in different sections to improve the contact between the rising stream with the falling beads.

Kawasaki has also developed a moving-bed process known as KCC process for CO_2 capture [32]. The process comprises an adsorption reactor, a desorption reactor, and an adsorbent dryer as shown in *Figure **2-5***. The sorbent (porous material impregnated by an amine) material enters the adsorption reactor from top where the exhaust combustion gas is contacted with the fresh sorbent at low temperature (~30 °C) in a counter-current mode. The saturated sorbent with the CO_2 moves then to the desorption reactor where low pressure steam (~ 60 °C) is contacted in counter current mode to desorb the CO_2 from the sorbent. During this step, steam condenses in the sorbent material, and highly concentrated CO_2 is recovered at the outlet of the desorption reactor. To remove the accumulated water and control the water content, the sorbent is fed to the adsorbent dryer, where

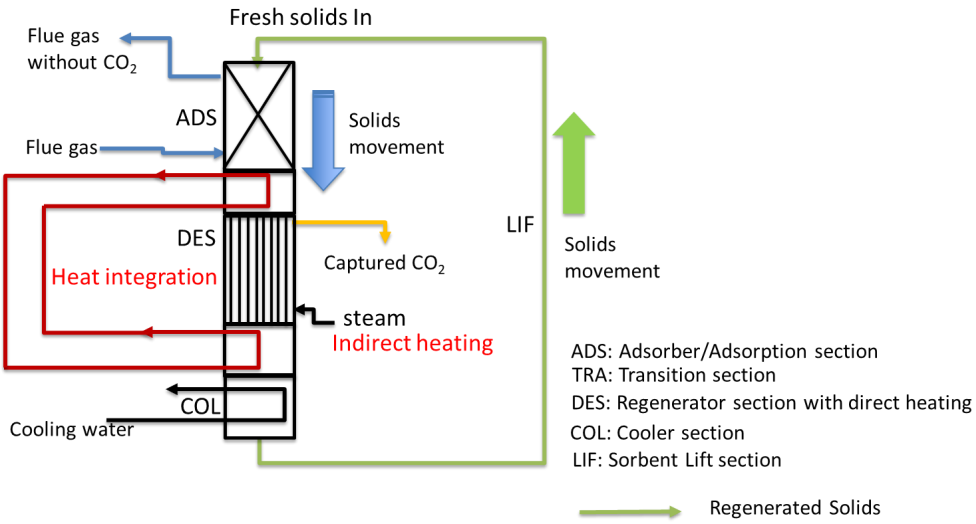

*Figure **2-6**: Moving bed with indirect heating [64].*

dry gas (i.e., warm air) is contacted with the sorbent in counter-current mode. Lastly, sorbent material is discharged from the adsorbent dryer and refed to the top of the adsorption reactor to separate the CO_2 present in the exhaust gas. This process uses low grade steam (< 100 °C) for the regeneration [65]. It is not clear how the temperature of the sorbent is decreased after the dryer to the adsorber inlet temperature.

To avoid the direct steam contact, another version of MBTSA process was proposed by Knaebel in which hot flue gas is used to indirectly heat the adsorbent in the regeneration [66]. A modelling study with such indirect heating in moving bed reactor was recently conducted by Mondino et al. [64], including some heat integration to recover part of the heat from the hot sorbent leaving the desorption section for preheating the powder leaving the adsorption section (*Figure **2-6***). However, the main uncertainty in this version remains the efficiency of heat transfer in the moving bed for the indirect heating and the envisaged heat integration.

2.1.3.2 Rotating bed

As an alternative to traditional moving beds, Svante Inc. (formerly Inventys Inc.) has developed a process using rotating reactor that can efficiently separate CO_2 from industrial flue gas (not much information available in open literature) [67, 68]. A moving bed comprising a rotating bed adsorber (RBA) with combined pressure and temperature swing regeneration mode was proposed and simulated by Gupta et al.[30] The RBA consists of disc-shaped adsorbent sheets with parallel passages that are divided into four sections as shown in *Figure* ***2-7***. At any instant, two of the sections are exposed to flue gas for CO_2 adsorption, while the other two remain in the desorption chamber which consists of a heating section using steam that is maintained under vacuum and a cooling section to cool the adsorbent for next cycle. The separation efficiency and CO_2 purity in this concept depends on the efficiency of the sealing mechanism used to prevent the leakage between the sections operating under different pressures while the solid is rotating. Additionally, long cycle time should be expected in this configuration given that heating and cooling of the sorbent may be slow.

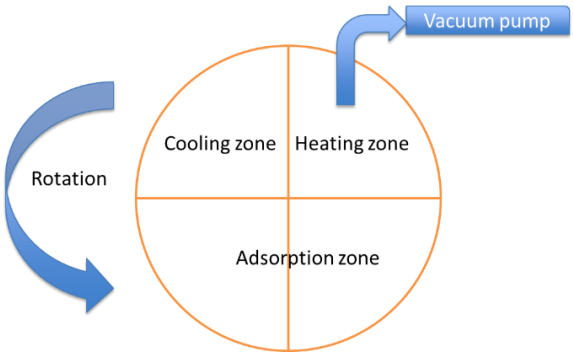

Figure ***2-7****: Rotating bed adsorber [18].*

2.1.4 Fluidized bed

In a fluidized bed, the adsorbent particles behave like a fluid with a high mixing rate resulting in excellent heat transfer within the bed. This inherently removes the heat and adsorption waves drawback encountered in the fixed bed configuration. A better temperature control could though be established using heat transfer surfaces (heat transfer coefficient in the range of h_i = 300-600 $W/m^2 K$) [69, 70] embedded in the bed to recover or add heat, depending on the need, making the fluidized bed configuration particularly attractive for temperature swing adsorption (TSA) applications. However, the good mixing in fluidized beds also presents its primary drawback: the degree of sorbent adsorption happens uniformly within the bed in equilibrium with CO_2 in the flue gas, leading to early breakthrough of CO_2.

Adsorption-based CO_2 capture in fluidized bed reactor predominantly focused on the use of two interconnected reactors [71, 72] (*Figure **2-8***), namely the adsorber and regenerator with the adsorbent particles circulating between them. In early works, the reactors were mainly operated at co-current mode at regimes covering bubbling to fast fluidization running [73, 74], with mainly chemisorption based dry sorbents such as potassium and sodium carbonate. Such a configuration was tested both at lab and pilot scales with the largest being the one by Korea Institute of Energy Research (KIER) and Korea Electric Power Research Institute (KEPRI), using dry sorbents (potassium carbonate) at real flue gas conditions from 2 MW coal fired plant. The adsorption (carbonation) was carried out in the range of 70-90 °C while the regeneration was completed at 160 °C. The average CO_2 removal was however low (~70%) despite the very long riser used in the adsorber [71] as a direct result of the good mixing as discussed above. However, the practicality, scalability and performance of such concept in a bigger scale remain questionable. Recently, chemisorbed sorbents such as monoethanolamine impregnated activated carbon, diethanol amine,

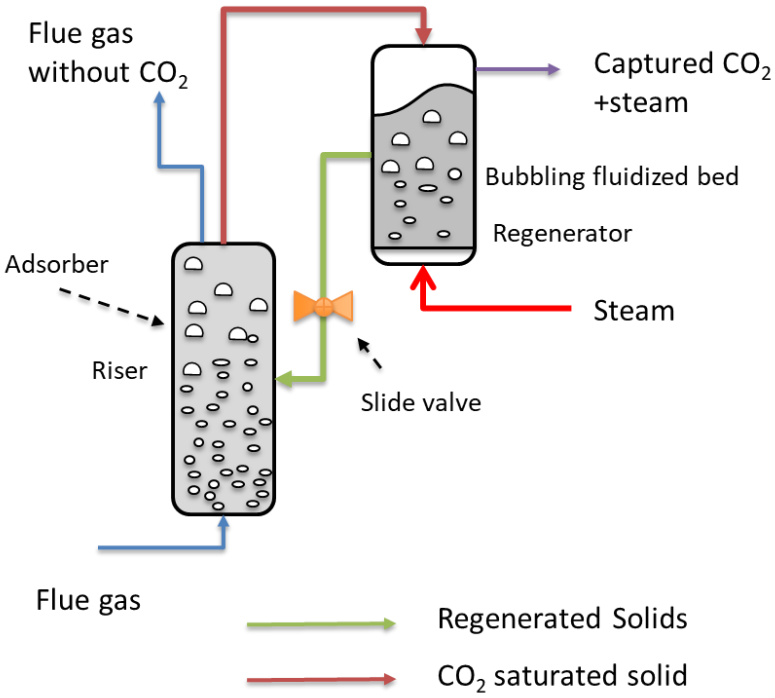

*Figure **2-8**: Interconnected fluidized bed configuration.*

impregnated activated carbon and PEI (Polyethyleneimine) supported on silica (SiO_2) has received major attention for use in this configuration [75] [76].

To minimize the energy penalty in TSA applications with this reactor configuration, an important challenge is the need for a lean/rich heat exchanger (heat exchange between the hot sorbent from the regenerator and the cold sorbent from the adsorber). Such heat exchange becomes particularly important when the sorbent working capacity reduces, requiring a larger sorbent circulation rate. A solid-solid heat exchanger is considerably more complex, bulkier and less efficient than the similar liquid-liquid heat exchanger typically used in absorption processes. In addition, effective solids circulation between reactors needs cyclones for gas-particle separation and loop seals to

prevent gas mixing between the adsorber and regenerator. Fluidized bed adsorption applications will also require mechanically strong particles to minimize attrition.

Another reactor configuration based on fluidized bed is the toroidal fluidized bed also known as vortexing fluidized bed (VFB)[77] with potential for improved gas-particles contact due to the swirling. This is however counteracted by the good mixing that reduces the CO_2 capture rate as emphasized earlier. The major challenges with this configuration remains the high adsorbent attrition rate and the lack of a robust scale up methodology. This design remains however conceptual with no reported experimental demonstration activities to confirm the benefits and identify the drawbacks.

2.1.4.1 Multistage fluidized bed

An important milestone in the use of fluidized bed-based reactor configuration in adsorption-based CO_2 capture was marked by the introduction of the multistage fluidized bed (*Figure **2-9a***) where the solid flows counter-current to the gas, driven by the need to enhancing the working adsorption capacity in these systems. Unlike the single stage fluidized bed reactor, the multistage stage reduces the overall internal back mixing to introduce a degree of plug flow reactor behaviour, bringing the same enhanced CO_2 capture benefit as packed beds.

Staging of a fluidized bed with horizontal screens was initially introduced by Varma and experimentally showed that it reduces the axial mixing of the emulsion and bubble phases in addition to limiting the formation and growth of large bubbles [78]. This promising result prompted several studies combining the multistage fluidized with counter-current adsorber [38, 45, 75, 76, 79-82] where the adsorbent particles move downwards through a series of bubbling fluidized bed stages while the gas is fed at the bottom serving as a fluidizing agent in the stages. Such an arrangement enables contacting fresher adsorbent particles (lower loading of CO_2) flowing

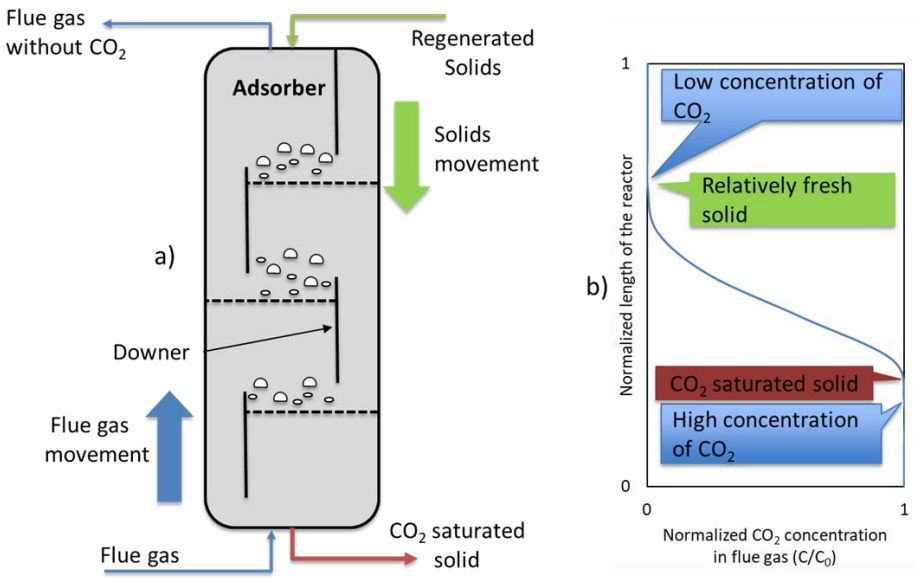

*Figure **2-9**: **a**) Multistage fluidized bed and **b**) Gas phase CO_2 concentration variation across the reactor length.*

downwards with the decreasing CO_2 partial pressure as the gas stream rises through the bed (see the illustration in *Figure **2-9b***), thus creating a high driving force for adsorption and therefore resulting in improved CO_2 capture efficiency at each stage. A thermodynamic study on a such gas-solids contactor with 25 wt.% polyethyleneimine (PEI) and 25 wt.% of 3-aminopropyl (APTES) on a porous silica support has shown that this configuration leads to significant reductions in sorbents recirculation (indication of improved adsorption working capacity) compared to a single stage fluidized bed contactor, thus achieving a higher energy efficiency [83]. Additional higher energy saving (20%) could be achieved in these reactors by providing lean-rich heat exchanger to recover the sensible heat from the hot regenerated rich sorbent and for use to preheat the sorbent from the adsorption reactor [81]. Such solid-solid heat exchange is considerably more complex than the liquid-liquid heat exchange typical in absorption systems though. It should also be noted

that the additional pressure drop caused by the distributor plate in each stage may reduce the energy saving enabled by the reduced circulation rate. Another important component in this counter-current configuration is that each stage has a downcomer to allow the downwards transfer of the adsorbent particles between the stages. Different down comer configurations were explored with the aim of maximizing the achievable solid flux through them [80]. All these additional internal components will increase the cost of the multistage bed relative to a conventional single stage fluidized bed.

The increased complexity of the counter-current multistage fluidized bed in the adsorber makes the hydrodynamics difficult to predict, thus imposing incremental development of such configuration requiring thorough testing for refinement and validation of the preliminary design in a cold flow model before implementation of the reactive case [84]. Such exercise should be repeated each time the design parameters (e.g. sorbent physical size and density) are changed. This may impose large changes to the design in order to control the solid circulation rate, e.g. when adsorbent materials were changed from 180 μm to a 115 μm by Breault, et al. [85]. Additionally, this also brings difficulties in estimating the tube-to-bed heat transfer coefficient when heat addition or removal in the bed is required [86]. Such challenge was encountered in the bench scale unit shown in *Figure **2-10*** designed as a TSA capture system using indirect heating through the tubes inserted in the regenerator. This study concluded that the CO_2 capture performance (especially for high feed concentration of CO_2) of the unit was limited by available heat transfer surfaces [79].

Another multistage based configuration was studied by Veneman , where the solid (supported amine sorbents) concentration in the adsorber is maintained very low (high void fraction > 90%) [87]. The diluted bed allows to operate the reactor at high velocity with a low pressure drop. It is

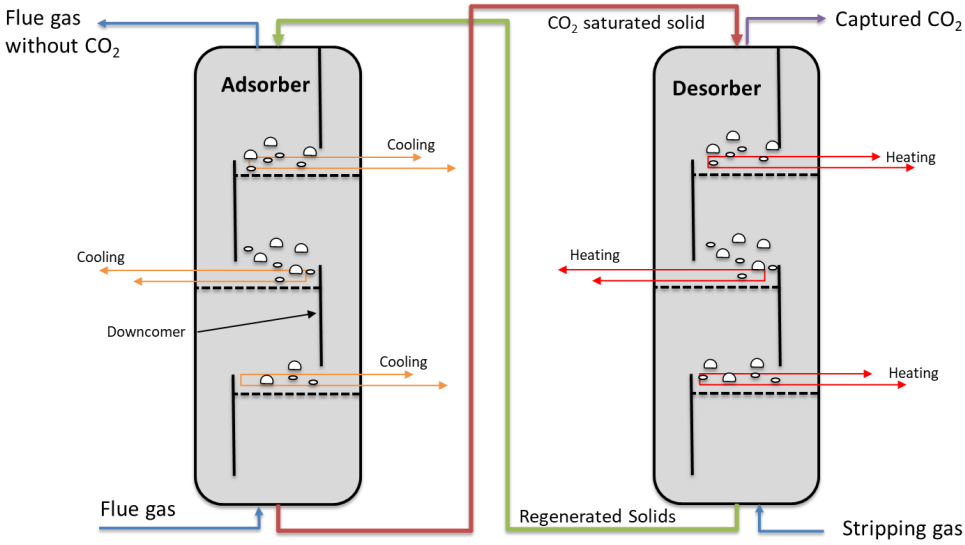

*Figure **2-10**: Multistage fluidized bed with downcomer and heat exchanger.*

also referred as trickle flow reactor where the contact between gas and solid is maintained in counter current mode. This configuration provides the plug flow contacting pattern between both gas and solid phase which is desired in the adsorption process.

Despite the aforementioned challenges, the multistage fluidized bed configuration remains promising for adsorption based CO_2 capture and a number of pilot scale studies have already been completed with such configuration [25, 45, 88].

Another approach to reduce the back mixing uses multiple isolated circulating fluidized bed reactors as proposed by Zanco et al. [89]. The modelling work suggested that this configuration is close to the counter-current multistage adsorption as discussed earlier. However, to achieve the desired separation and minimized energy penalty, multistage counter current reactor configuration with single regenerator is still preferred.

2.1.4.2 Transient fluidized bed

A transient fluidized bed reactor known as the swing adsorption reactor cluster (SARC) concept was proposed by Zaabout et al. [1]. As shown in *Figure **2-11a**,* the SARC concept comprises a cluster of multistage fluidized bed reactors operated in bubbling/turbulent mode, where each reactor is exposed to four different process conditions (i.e. adsorption, evacuation, regeneration and cooling). No solids circulation is involved in this concept enabling to apply a vacuum swing in the regeneration stage. An additional temperature swing is applied using a heat pump transferring heat from the exothermic adsorption (referred as carbonation carried out at 60-80 °C) to the endothermic regeneration (carried out at 80-100 °C) as shown in *Figure **2-11b**.* This is advantageous because the vacuum swing substantially reduces the extent of the temperature swing required, allowing for highly efficient heat transfer via the heat pump.

Such an arrangement brought significant reduction in the energy penalty in comparison to benchmarking technologies, specifically when the reactors were operated under the multistage configuration to reduce the extent of back mixing [90, 91]. This work also provided a quantitative

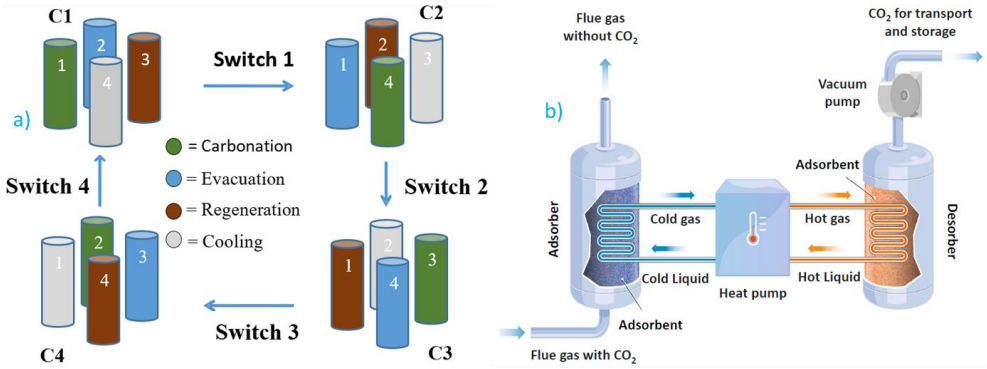

*Figure **2-11**: SARC conceptual design: **a)** a cluster of SARC reactors for continuous gas stream processing; **b)** SARC working principle showing heat transfer from a reactor under adsorption to one under regeneration using a heat pump. Reprinted from Dhoke et al. [92] with permission from Elsevier.*

example of the benefits of a higher degree of plug-flow behaviour on the CO_2 breakthrough curve. As shown in *Figure* ***2-12****,* inserting three perforated plate separators in the fluidized bed greatly delayed the breakthrough of CO_2. Without separators, significant CO_2 concentrations were observed at the outlet after only one minute, but the inclusion of separators delayed this breakthrough to around 8 minutes, allowing a much larger fraction of the CO_2 adsorption capacity to be utilized before excessive CO_2 slippage occurs. As discussed in *Figure* ***2-2****,* this is the result of the reaction front moving through the bed, first loading the bottom sorbent with CO_2, while leaving the top sorbent in a highly regenerated state to ensure complete CO_2 capture. However, in a well mixed fluidized bed, the sorbent is uniformly loaded with CO_2, leading to CO_2 breakthrough as soon as the equilibrium CO_2 partial pressure at this uniform loading rises significantly above zero.

For these reasons, imposing a larger number of stages resulted in greater plug flow behaviour, which improved the CO_2 capture efficiency and sorbent working capacity [93]. It should be noted that the number of stages to adopt should take in consideration the practicality of implementation in industrial scale and the increase in the pressure drop associated with the additional distributor plates in each stage [93]. However, the desired reduced back mixing could be achieved by smart

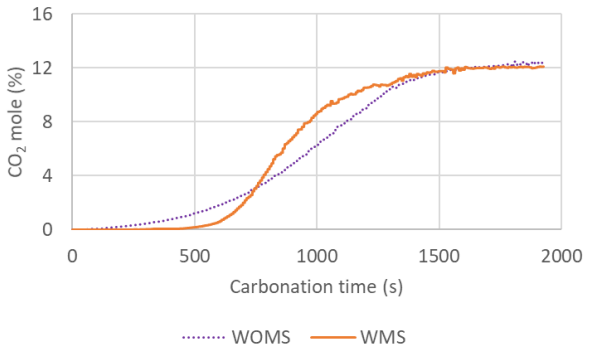

Figure ***2-12****: The CO_2 breakthrough curve in the fluidized bed with separators (WMS) and without separators (WOMS). Reprinted from Dhoke et.al.[69] with permission from American Chemical Society.*

arrangements of the heat transfer surfaces embedded in the bed for the heat pump, without the need for placing additional distributor plates between the stages. The low energy penalty and cost of CO_2 avoidance of this concept [41] and its ease of retrofitting into existing plants, due to the use of heat and vacuum pumps that requires only electricity for operation, makes this concept advantageous over the interconnected configuration with pure TSA reliant on steam for regeneration.

The merits and limitations of the various reactor configurations discussed above for CO_2 adsorption process are summarized in *Table **2-2*** (next page).

*Table **2-2**: Advantages and limitations of the different reactor configurations for adsorption-based CO_2 capture*

Reactors	**Advantages**	**Limitations**
Conventional Fixed Bed	• Simple operation • Inherent plug flow for high sorbent working capacity • No attrition • Easy scale-up	• Mass transfer limitations from large pellets (k_{LDF} = 0.06 s^{-1}; D_e=5.35 x10^{-5} m^2/s for 13X Zeolite)[44] • High pressure drops or large footprint • Low heat transfer coefficient (20-50 W/m^2K)[43, 94] • Transient process operation
Structured Fixed bed	• Same as conventional fixed bed • Better heat transfer • Lower pressure drop (50% reduction as compare to pellets)[54] • Improve gas throughput and productivity (3-10 times)[95]	• Cost of structured packing • Stability of sorbent on support packing • Scale up of the structure production • Expensive sorbents
Moving bed	• Plug flow behaviour for increased working capacity • Steady state operation	• Less severe mass transfer resistance (k_{LDF} for MOF sorbent = 1.56 s^{-1})[96] and pressure drop (~7000Pa/m)[62] than conventional fixed bed • Low heat transfer coefficient (better than conventional fixed bed ~60 W/m^2K)[97] • Sorbent circulation, attrition and solid-solid heat exchanger
Rotary bed	• Steady state operation • Simpler scale-up	• Mixing and dispersion during rotation • Sealing and leakage
Fluidized bed	• High heat transfer coefficient for efficient indirect heating/cooling (300-600 W/m^2K)[69, 70] • Steady state process • Low pressure drop	• Back mixing creates low working capacity or high CO_2 slippage • Attrition of adsorbent particles • Need for solid-solid heat exchanger to reduce TSA energy penalty
Multistage fluidized bed	• Same as conventional fluidized bed • Greater plug flow behaviour for increased working capacity[38]	• Increased complexity creates scale-up challenges and a more costly reactor • Attrition, solids circulation and solid-solid heat exchanger
Transient fluidized bed	• Same as conventional multistage fluidized bed • Possibility of pressure swing • Easier scale-up due to the use of standalone reactors	• Particle attrition • No potential for sensible heat exchange

2.2 Mode of regeneration

Most of the discussion in the previous section was about the behaviour of the different contacting systems in the adsorption. A second important segment that influences the choice of the reactor configuration is the mode of regeneration. In adsorption-based CO_2 capture, the sorbent

regeneration is carried out either by changing the temperature (Temperature Swing; TSA), changing the pressure (Vacuum/Pressure Swing; VSA/PSA), or changing both temperature and pressure resulting in a hybrid regeneration (VTSA/PTSA). The different regeneration modes adopted in published studies are specified in *Figure **2-13***.

It should however be noted that the choice of the regeneration mode depends mainly on the adsorbent material physical properties (specific heat, thermal conductivity, diffusivity in the material) and nature of adsorption (physi- or chemi-sorption based) that determines the shape of CO_2 isotherms returned by the adsorbent and its heat of reaction. Conventional sorbents are generally classified into physisorption based that are better suitable to pressure swing and chemisorption based that are more suitable to temperature swing. In this respect, the CO_2 concentration in feed flue gas from the source is also an influential parameter on the choice of the

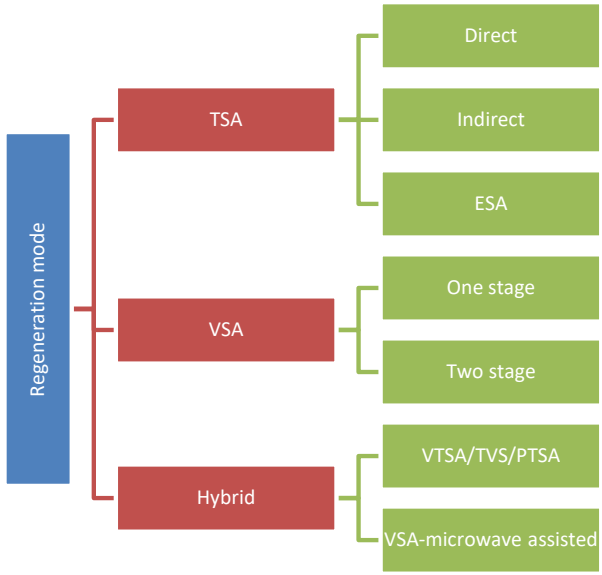

*Figure **2-13**: Various regeneration modes; TSA- temperature swing adsorption, VSA-Vacuum swing adsorption, VTSA/TVS/PTSA- vacuum combine temperature swing, ESA- Electric swing adsorption.*

regeneration mode. CO_2 concentration varies widely over different flue gas sources (4-6% in natural gas power plant, 12-15% in coal power plant and higher in cement and biogas in the range of 20 and 45 % respectively). When a high CO_2 capture rate and maximal working capacity are targeted, the chemisorption-based sorbents (with sharper isotherms) combined with a TSA regeneration mode are more suitable to sources with low CO_2 concentration, while the physisorption-based sorbents combined with a VSA regeneration mode are more suitable to flue gases with high CO_2 concentration [98]. As highlighted earlier, the sorbent physical properties like the specific heat and thermal conductivity can have a big influence on the different regeneration modes; TSA, VTSA and ESA (Electrothermal swing adsorption). The pros and cons of each regeneration mode, their optimal reactor configuration and operating conditions will be presented and discussed in this section.

2.2.1 Temperature swing adsorption (TSA)

TSA is either carried out either in direct mode, where a hot stream (steam, CO_2) is used as purge gas in direct contact with the adsorbent particles, or in indirect mode, where a heat exchanger is used to provide the required heat for regeneration. The regeneration energy requirement in TSA comprises of sensible heat required to heat the adsorbent to the target regeneration temperature, reaction heat to drive the endothermic desorption reaction, and latent heat of vaporization if the sorbent has adsorbed water as well [99]. This regeneration mode has been applied in the different reactor configurations with pros and cons as will be discussed below. The various research works has focused on reducing the overall heat requirement in this TSA mode through sorbent development with improved adsorption capacity, lower specific heat capacity, but more importantly with lower heat of reaction. Others focused on reducing the energy requirement through heat integration in the process [100, 101].

2.2.1.1 Indirect temperature swing adsorption (Indirect TSA)

Indirect TSA is done by heating or cooling of the adsorbent by means of a heat exchanger in the reactor as illustrated in *Figure **2-14***. This heating mode was widely used in early works in fixed bed configuration due to its simplicity and the achieved high CO_2 purity if no purging is applied through the bed [102]. Its major drawback remains the very low tube-to-bed heat transfer coefficient in fixed bed configuration making such heating mode inherently unfeasible in conventional fixed bed. This is well illustrated in *Figure **2-15*** showing the very low heat transfer coefficient in the fixed bed, although some gas purge could improve the convective heat transfer [103, 104], but remains limited though against the values achieved in fluidized bed that could be up to an order of magnitude larger (*Figure **2-15***). This advantage makes fluidized bed favored for indirect TSA, not only for supplying heat in the regeneration, but also for improving the control of temperature in the adsorption to maximize the working adsorption capacity and improve the capture efficiency [1, 64, 79, 81]. Nevertheless, a good example of successful experience of indirect heating in fixed bed was demonstrated in a hollow polymeric fiber that enabled cycling fast TSA in the reactor by pumping hot/cold fluid through the hollow structure [56] discussed earlier. With

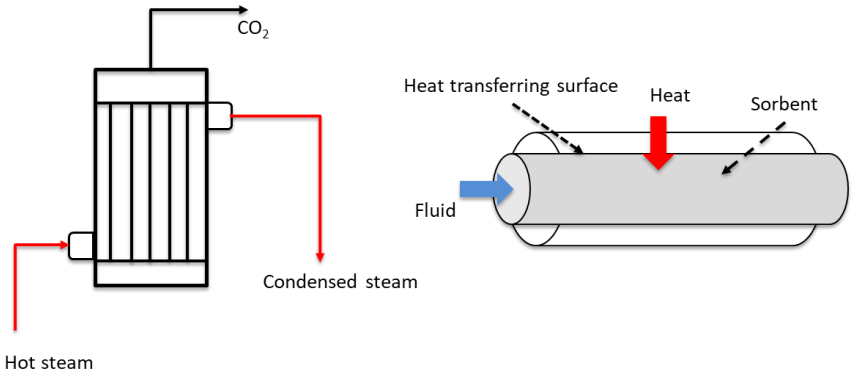

*Figure **2-14**: Indirect TSA.*

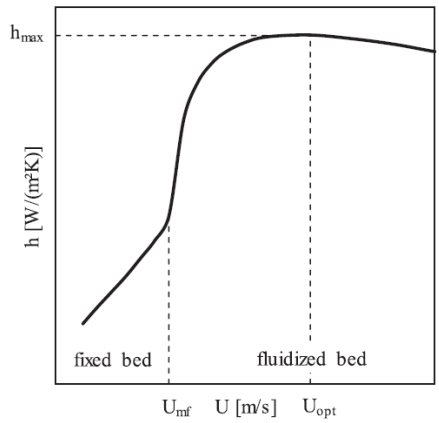

*Figure **2-15**: Heat transfer coefficient with velocity for Geldart Type B particles Reprinted from Hofer et al.[70] with permission from with permission from Elsevier.*

the rapid advances made in 3D printing, making smartly structured bed with embedded heat transfer surfaces could become a feasible and viable option to implement a TSA regeneration mode in fixed bed.

2.2.1.2 Direct temperature swing adsorption (Direct TSA)

Direct TSA is the mode of regeneration where the adsorbent is heated directly by means of a hot gas stream, preferably steam (*Figure **2-16***). This TSA mode has a much better heating rate than the indirect one, thus decreasing the heating time. The main advantage remains the capability of achieving sufficiently high purity of CO_2 with this mode explaining the widespread application of such option to the different reactor configurations discussed in the previous section. The addition of steam reduces the CO_2 concentration which further increases the driving force for desorption, reducing the size of the temperature swing required. However, this also has some drawbacks such as i) the need for an additional unit operation for water removal from the captured CO_2 before being compressed for transportation and storage; ii) the used sorbent should tolerate presence of

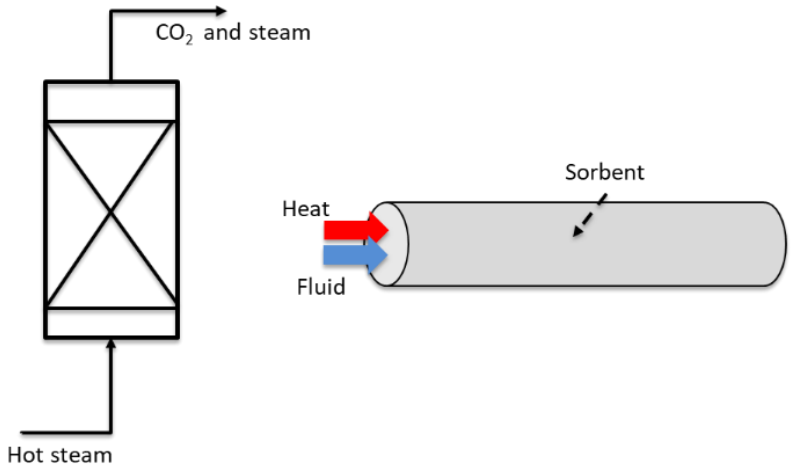

*Figure **2-16**: Direct TSA.*

water and in many cases a drying step is needed before starting a new cycle (this depend on the nature of sorbent and operating conditions in the regeneration step). Such additional steps increase the process complexity, the energy penalty and costs.

To address the aforementioned challenges, direct heating of a fixed bed reactor by a recovered hot CO_2 product gas (purge) was studied by Ntiamoah et al. [103]. The process comprises of a basic three-steps cycle of (i) adsorption, (ii) hot gas purge where the regeneration takes place, and (iii) cooling by N_2/ air. Their study with Zeolite NaUSY adsorbent indicated a specific (thermal) energy consumption as high as 4.5 MJ/kg of CO_2 at a temperature of 250 °C to yield CO_2 purities >91% and CO_2 recoveries of only 83.6%. This purging with hot CO_2 gas removed the need for additional process units associated with the use of steam but it reduced the driving force for desorption, thus imposing the need for higher regeneration temperature and therefore results in higher thermal energy demand. The source of this hot CO_2 stream is also an important consideration.

2.2.1.3 Electro thermal swing adsorption (ESA)

Electro thermal swing adsorption (ESA) is considered as another potential mode to reduce the energy penalty of adsorption-based CO_2 capture. ESA mode is conducted by heating the adsorbent beds by means of Joule heating effect by passing an electric current [105]. This in-situ heating of the particles enables fast heat transfer rate in comparison to conventional TSA mode and also provides better desorption kinetics [106]. The essential feature for the adsorbent to work under ESA mode is its electrical conductivity. Activated carbon fiber was considered as a potential sorbent that work in ESA mode of regeneration [37]. The ESA mode is however applicable only in fixed bed configuration where the long cooling time counteracts the advantage of the in-situ fast heating, thus hindering the prospects of such mode in implementation at industrial scale. From an economic point of view, the main drawback is that electrical energy is many times more costly than the low-grade heat typically used for regeneration in TSA processes.

2.2.2 Vacuum swing adsorption (VSA)

Another widely used regeneration approach is by varying the pressure, commonly known as vacuum swing adsorption (VSA) or pressure swing adsorption (PSA). In post combustion CO_2, only VSA makes sense as the PSA requires pressurizing the incoming large quantities of the flue gas from the source making the process uneconomical. VSA is predominantly applied to fixed bed reactor configuration with physisorption based sorbents such as zeolites or activated carbon [22, 23]. However, as emphasized in the previous section, the VSA regeneration mode can achieve a very short cycle, but a low pressure drop across the bed in adsorption is a prerequisite, thus favoring the structured advanced fixed bed. Additionally, a high CO_2 capture rate requires deep vacuum levels making this regeneration mode suitable only for industrial applications producing flue gases with high CO_2 partial pressure [107, 108].

The first proposal of vacuum swing adsorption (VSA) regeneration mode comprises of four steps: pressurization with feed gas, adsorption, forward blowdown, and reverse evacuation. As shown in *Figure* ***2-17***, the flue gas is fed to the adsorption step where CO_2 is adsorbed close to atmospheric pressure, then the following blowdown step is used to remove the accumulated N_2 from the reactor by using a slight vacuum before starting the following regeneration step at higher vacuum levels. The blowdown step improves the purity of CO_2 but can also reduce its recovery as some of CO_2 can be lost during this step. Finally, the reactor is pressurized again by the flue gas preparing for a new cycle. These basic steps are simple in operations but either suffers from low CO_2 purity or recovery. An experimental study indicated that VSA mode can lead to high purity CO_2 (around 99% purity) but is limited with low CO_2 recovery of 85% [104]. An interesting approach that was proposed to improve the CO_2 recovery was by recycling some of the CO_2 product to the blowdown step (known as heavy reflux or high-pressure rinse) [109]. The presence of the recycled CO_2

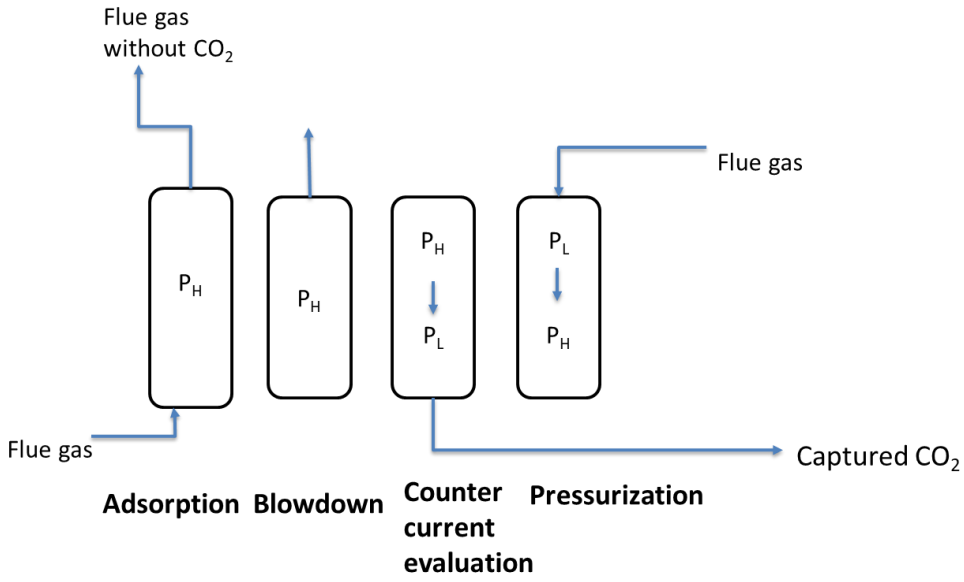

Figure ***2-17****: Basic VSA process (P_H- High pressure; P_L- Low pressure).*

improves the CO_2 purity as it displaces the accumulated nitrogen in the reactor and it also increases the loading of the CO_2 in the column during blowdown. Such an approach has led to higher CO_2 recovery (98.7%) and high purity (98.7%) during the regeneration step. Another improvement in the conventional four-step cycle in terms of CO_2 recovery has been demonstrated in a pilot scale VSA system using Zeochem zeolite 13X [108]. Authors proposed to purge the light product (flue gas without CO_2) for pressurization (LPP) in counter-current direction. This avoids the slippage of CO_2 present in the reactor after the evacuation step. The CO_2 recovery remained below 90 % though.

Another tactic to improve the recovery with high purity is to use a two-stages VPSA process [110]. This is a method to make pressure swing applicable to flue gases with lower CO_2 concentrations where a single step VSA cannot concentrate the CO_2 sufficiently. Wang et al. [55] simulated this two-stages VPSA unit for a coal power plant flue gas and the results indicated that CO_2 purity can be increased to 65% in first stage and then to 96% in the second stage while the achieved CO_2 recovery increases to 93.35 %. Such a two-stages VPSA was experimentally demonstrated at a pilot-scale installed in an existing coal-fired power plant in China by Wang et al. [55]. In addition to the two-steps VPSA process units, a dehumidifying unit was used in the pilot plant to remove the water vapor in the desulfurized flue gas by alumina adsorbent before being fed to the CO_2 capture unit. This study shed light on the issues of existence of water in the flue gas on the VSA CO_2 capture mode given that such a system operates at low temperatures that may result in substantial watering of the sorbent if it is not removed in a pre-processing step. An example of a VSA CO_2 capture process with a water removal pre-processing step is the dual-Adsorbent, four-steps vacuum swing adsorption (VSA) process with silica gel and zeolite 13X packed separately in two beds as illustrated in *Figure **2-18*** [111]. Designing a such system requires careful sizing of each

reactor taking in consideration the isotherms of water and CO_2 adsorption on their respective sorbents. An increase in the energy penalty should be expected due to the additional pressure drop imposed by the additional reactor and the vacuum pump consumption for water removal [112].

Overall, a VSA regeneration looks an attractive option for reducing the cycle time in adsorption-based CO_2 capture to maximize the productivity of the process. The main hurdle remains the high pressure drop encountered in conventional fixed bed making it hard to achieve the low vacuum values required for achieving reasonable CO_2 recovery within sufficiently short cycle times. A design for a Rapid Vacuum Pressure Swing Adsorption (RVPSA) based on conventional fixed bed, was recently proposed to capture CO_2 with 95+% CO_2 purity and 90+% CO_2 recovery from an existing 10 MWth biomass-fueled CHP plant [29]. They considered a two-stage VSA with two

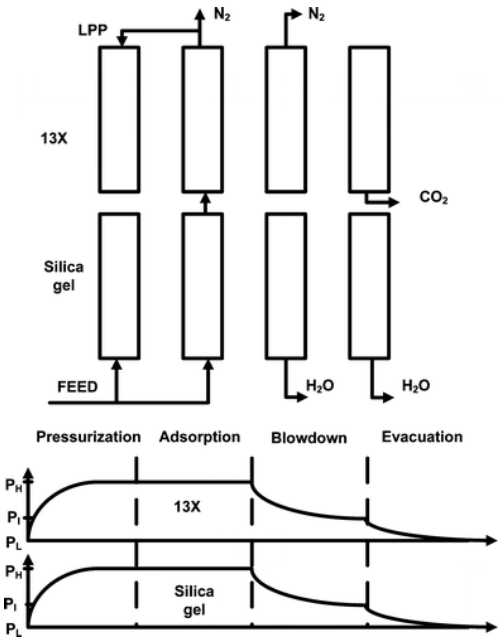

*Figure **2-18**: Dual-Adsorbent, Two-Bed Vacuum Swing Adsorption Process for CO_2 Capture from Wet Flue Gas. Reprinted from Krishnamurthy et al. [111] with permission from American Chemical Society.*

parallel beds in the first VSA stage in order to split the total flue gas feed and reduce the overall pressure drop. Achieving the vacuum pressure of 7.5 kPa in seconds (18 seconds was considered in the entire VSA cycle) will need a specially designed large vacuum pump that could be a practical challenge at industrial scale. Moreover, operation of a VSA based system on large scale CO_2 sources, such as a coal power plant, requires a large number of reactors (73 and 23 for first and second PSA stage, respectively) that have to operate in an automated manner to achieve continuous processing of the flue gas from the plant [42]. Such a case imposes designing a complex operation strategy to automate the different reactors cycling the different process steps.

2.2.3 Hybrid regeneration approaches

Several attempts were made to overcome the shortcoming of the unpracticality of reaching deep vacuums in large scale VSA to achieve the target high CO_2 recovery, by using hybrid regeneration modes such as VTSA and steam aided vacuum swing [113-115]. One of the first successful demonstration of 2000 hours was completed at pilot scale fixed bed reactor by Ishibashi et al. [113] for a two-stage process comprising a first stage PTSA (Pressure and Temperature Swing Adsorption) and a second stage of PSA (Pressure Swing Adsorption). Recently, Wurzbacher et al. [116] evaluated the effect of moisture in humid air on the working capacity of the diamine-functionalized commercial silica gel sorbent when operated under VTSA mode. Their study indicated that under dry conditions, desorption pressures above 100 mbar lead to working capacities below 0.03 mmol g^{-1} while under humid conditions (40% relative humidity) during adsorption working capacities above 0.2 mmol g^{-1} at 150 mbar were achieved. This increase was the result of the dilution effect of steam during the regeneration mode creating larger driving force for desorption of CO_2. Later, Fujiki et al. [117] proposed a low temperature steam-aided vacuum swing adsorption (SA-VSA) process for regeneration of an amine-based solid sorbent. This dilution

with steam under vacuum resulted in similar effect of a direct heating that improved the working capacity. The experimental study was conducted in lab scale set up and it has shown high CO_2 purity (>98%) and recovery rate (>93%) against recovery of 45% with only vacuum (VSA). It should be noted, however, that the improvement in the desorption driving force created by steam does not lead to the expected large saving in the energy penalty because the vacuum pump has to extract a larger amount of gas that increases its electricity consumption [118].

Another nonconventional hybrid VTSA approach used microwave assisted vacuum swing over 13X zeolite by Webley et al. [28]. They showed that a brief exposure to microwave radiation improved the speed of CO_2 and water desorption at reasonably higher achievable vacuum levels. They suggested that this positive effect of microwave could lead to the reduction in overall lower energy penalty. The main challenge with this concept remains the large-scale application and safety consideration with the microwave. The cost of using electrical energy for regeneration is another important challenge.

The Swing Adsorption Reactor Cluster (SARC) that was proposed by Zaabout et al. [1] is another VTSA based hybrid system that has a high potential to bring substantial energy saving. This concept implements heat integration between adsorption (referred as carbonation) and regeneration reactors by means of a heat pump. This is also combined with a practically achievable vacuum swing to minimize the temperature difference between the adsorption and regeneration, thus maximizing the coefficient of performance of the heat pump and reducing the overall energy penalty. Such a configuration achieved competitive energy penalties against benchmarking technologies, both for coal power plants and cement [90, 91] targeting CO_2 recovery of 90% and CO_2 purity of 96%. Experimental demonstration tests using polyethyleneimine sorbent have

proved the feasibility of achieving small temperature difference between adsorption and regeneration at a moderate vacuum of 100 mbar [114].

Several other VTSA hybrid studies have followed. A heat-integrated vacuum and temperature swing adsorption process in a multibed reactor for low temperature adsorption process was studied by Plaza et al. to capture at least 85% of the CO_2 [119]. Waste heat from power plant will be used for regeneration of the sorbent, but the fixed bed configuration used may impose serious heat transfer limitations as discussed earlier. Zhao et al. also evaluated a monolith reactor using a hybrid process of electrical swing adsorption (ESA) combined with vacuum swing adsorption (VESA). They reported that the total specific energy with this approach can be lower than ESA alone, but still higher than VSA [37].

The advantages and limitations of various regenerations modes are summarized in *Table **2-3*** (next page).

*Table **2-3**: Advantages and limitations of the different regeneration modes for adsorption-based CO_2 capture.*

Modes of Regeneration	**Advantages**	**Limitations**
Direct TSA	• High heating rate • Increase in desorption driving force when steam is used • High CO_2 purity	• A post processing step is needed to recover water before compression • Integration with power plant steam cycle or dedicated boiler • A water tolerant sorbent is needed if steam is the heating agent
Indirect TSA	• No need of a post-processing step for water separation • Sorbents sensitive to water could still be used as they won't be in contact with water • It can be combined with direct TSA when applicable	• Lower heat transfer rate, particularly for fixed beds • Need for heat exchange surfaces in the reactor • Integration with power plant steam cycle or dedicated boiler
ESA	• High heating rate • No steam integration, CO_2 recycling or heat exchange surfaces • Uses electric energy only, allowing easy retrofits	• High cost of electrical energy • Long cooling time if implemented in fixed beds • Limited material suitability • Scalability challenges
VSA/PSA	• Fast cycles could be achieved if the pressure drop is minimized • No steam integration needed • Uses electric energy only, allowing easy retrofits	• Single stage VSA is only feasible for high CO_2 concentration flue gases • More complex two-stage VPSA is needed for most flue gases
VTSA / TVS	• Good performance in a single stage with reasonable vacuum • Synergistic combination of vacuum pump and heat pump can further reduce energy consumption • Easy retrofit if no steam is needed	• Increased capital costs from heat transfer surfaces (indirect heating) or steam production and larger vacuum pump (direct heating)

2.3 Reactor operation strategies

The combination of reactor configuration and regeneration mode selected for the adsorption-based CO_2 capture technology determines the operation strategy of the adsorption plant. The following operation strategies could be foreseen for the different reactor configurations. The relative complexity of the operation strategies of different configurations is illustrated in *Figure **2-19**.*

*Figure **2-19**: A simplistic illustration of the extent of complexity of the operating strategy of the different reactor configurations and operating mode.*

2.3.1 Fixed bed

A cluster of reactors is needed for continuous gas processing using the fixed bed reactor configuration, regardless of the nature of the regeneration mode adopted. The number of reactors in the cluster depends on the number of steps in the cycle and the time of the steps. If a PSA regeneration mode is adopted, achieving high CO_2 recovery with most flue gases requires a second processing stage, thus increasing the number of reactors in the plant. *Figure **2-20*** shows an example of an operating strategy for continuous feed processing using a two-stage PSA fixed bed

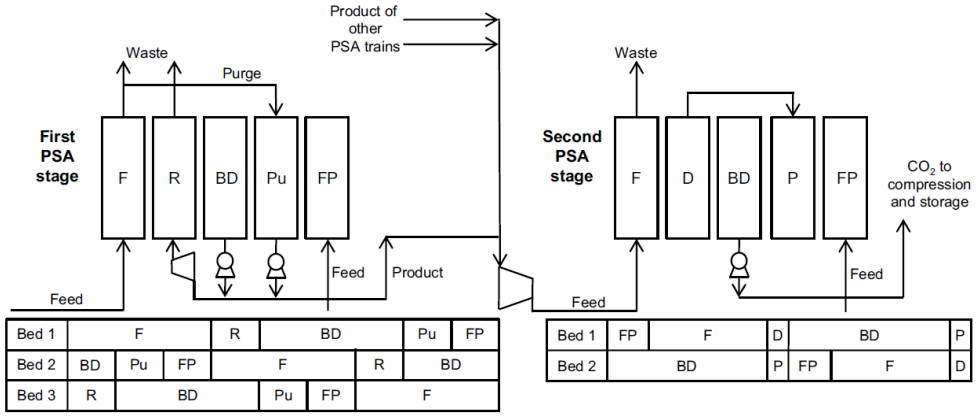

*Figure **2-20:** Two-stage PSA process for post-combustion CO_2 capture from a coal plant and the representation of the sequence of steps undergone by a single column in the first and second PSA stage. Feed (F), Rinse (R), Depressurization (D), Blowdown (BD), Purge (Pu), Pressurization (P), Null (N) where the column is left idle, Feed Pressurization (FP). Reprinted from Riboldi et al.[42] with permission from Elsevier.*

configuration). 96 reactors were needed for continuous flue gas processing from a coal-based power plant using a two-stages PSA system [42]. This complicates the operation strategy, involving hundreds of valves and complex piping to accomplish the different process steps needed to complete the CO_2 capture cycle.

2.3.2 Rotary bed

This reactor configuration can also have a simple operation strategy given that only the speed of rotation and the areas of the different process steps must be specified correctly (these two parameters are mainly affected by sorbent isotherms, physical properties and reaction kinetics). TSA could be the simplest regeneration mode to adopt although the cooling and heating times would be long, imposing a large reactor footprint. Implementing additional steps to improve the separation efficiency in this reactor configuration brings additional complexities to the operation strategy. When a VTSA regeneration mode is adopted as proposed in [30], the operation strategy will not be affected given that the only difference is that, in the regeneration zone, a vacuum will be applied in addition to the temperature swing. If an efficient sealing system is implemented to minimize the gas leakage between the zones operating at different pressures, applying a vacuum in addition to the temperature swing could be beneficial for the process as it will reduce the heating and cooling times due to the reduced temperature swing. However, the extent of complexity in the operation strategy in this case will depend on the level of complexity involved in the sealing solution used for improving the separation efficiency.

2.3.3 Interconnected fluidized bed reactors and moving Bed

The only reported regeneration mode for these two configurations is TSA (*Figure **2-8***) because a pressure swing would create substantial operational challenges in such an interconnected system.

Such a system operates like conventional absorption-based CO_2 capture technologies, continuously feeding the flue gas to the adsorber operating at low temperature while the regeneration occurs in a second reactor operating at higher temperature with continuous solids sorbent circulation between the two reactors [35, 72, 120]. Indirect heating using an inbuilt heat exchanger can be efficient in circulating fluidized bed reactors, given the high tube-to-bed heat transfer coefficient [70]. This option can also ensure efficient use of waste heat that could be available in the host plant, thus further minimizing the energy penalty of CO_2 capture. As for the moving bed (*Figure **2-4***), the direct heating with steam or CO_2 seems to be the most efficient option due to the low tube-to-bed heat transfer [32, 63].

2.3.4 Dense fluidized bed using the switching concept

Similar to fixed bed, a cluster of reactors are needed for continuous flue gas processing. A study on SARC concept with PEI sorbent involved the use of 24 reactors for continuous flue gas processing, although this number could be reduced by increasing the reactor size. This is substantially lower than the fixed bed two-stage VSA case and requires no integration with a second processing stage, but it would still require dozens of valves and complex piping to complete the different steps [1]. Additional complexity should be expected when the heat pump is used for transferring heat from the reactors under adsorption to those under the regeneration and when heat is exchanged between the reactors under cooling and the others under evacuation/heating. The heat pump working fluid will have to be continuously redirected between different reactors cycling through the transient operating strategy. Applying an additional vacuum in the regeneration (jointly with the temperature swing) is not expected to add any complexities to the operation strategy.

2.4 Process integration and energy requirement

One of the most important aspects in any CO_2 capture technology is the energy penalty involved. Various efforts have been made to reduce this energy penalty, mainly by sorbent development, but also via more efficient process integration. Process integration options include the use of solar heat in PTSA systems [121], the combination of high and low temperature sorbents where heat released from the adsorption of the high temperature sorbent regenerates the low temperature sorbent [122, 123], the use of a heat pump to transfer heat from adsorption to regeneration [1, 124], and close heat integration between three moving bed reactors [33]. Others considered combining a single stage VSA with a CO_2 membrane system to reduce the energy penalty [115].

A summary of the thermal energy requirement for sorbent regeneration of various concepts is presented in *Table **2-4***. To allow for reasonable comparisons between different regeneration modes, electrical energy consumption is multiplied by a factor of 5 to account for the fact that low-grade heat would normally be used for sorbent regeneration. This heat is usually supplied by extracting low pressure steam from the steam cycle that would otherwise only be able to produce power at about 20% efficiency. In other words, if a VSA process used 0.5 MJ/kg of electrical energy for sorbent regeneration, a TSA process would be able to use about 2.5 MJ/kg of low grade heat extracted from the power cycle, resulting in the same 0.5 MJ/kg loss in electricity output. In addition, power consumption for CO_2 compression and flue gas blowers are subtracted where necessary to focus only on the energy requirement for capturing CO_2 (mainly regeneration enthalpy and sensible heat). It is worth noted that the comparison in *Table **2-4*** is rather for illustration from published data of the different reactor configurations and a more reliable comparison requires carrying out a standardized techno-economic assessment study.

*Table **2-4**: Energy requirement for various modes of regeneration and reactor configuration (*20% electric efficiency assumed in the conversion of electrical energy to thermal energy for regeneration, excluding electricity required for compression and pressure drop); [a]experimental measurement, [b]Model prediction*

Regeneration mode	**Feed CO_2 (mole %)**	**Reactor type**	**CO_2 purity (%)**	**CO_2 recovery (%)**	**Energy (MJ/kg)**	**Prod. (kg/m^3 ads. h)**
2 stage VSA (Coal) [55]	16.5	Fixed	95.6	90.2	2.44[a]	65.2[a]
2 Stage VSA[23]	15	Fixed	96.5	93.4	2.64[*,b]	20.9[b]
TSA-Direct- CO_2 [103]	15	Fixed	91.0	83.6	4.50[b]	32.9[b]
TSA- heat integration [125]	15	Simulated Moving			2.53[b]	--
VPSA [43]	15	Fixed	85	79	2.37[a]	83.7[a]
TSA-indirect [94]	12	Fixed	0.97	0.77	4.07[b]	46.5[b]
TSA- Indirect (steam purge) [95]	14	Fixed-monolith	95.6	85.4	3.59[b]	228.4[b]
TSA-Steam +CO_2 (Coal) [126]	13.8	Circulating Bubbling fluidized	-	-	2.49[b]	42[b]
TSA-Indirect with vacuum (heat pump) [1, 69]	13.4	Multistage fluidized	96.0	90.0	2.8[*,b]	68.3[a]
TSA (coal) [123]	13.2	Fast Fluidized	-	85.0	1.73[b]	-
VSA+membrane [115]	12.6	Fixed bed + membrane	95.0		4.1[a]	10.8[a]
TSA-Indirect [104]	12.5	Fixed	99.0	79.0	-	
VPSA-2 Stage [22]	10	Fixed	95.3	74.4	3.61[*,b]	26.8[b]
TSA-Indirect with purge- optimized [127]	10	Fixed	95.0	81.0	3.23[b]	43.1[b]
TSA-indirect (Without heat integration) [64]	5.15	Moving	95.1	96.0	2.21[b]	-
TSA-indirect (With heat integration) [64]	5.15	Moving	95.1	96.0	1.46[b]	-
TSA-Steam +CO_2 Heat integration (Natural gas) [126]	4.1	Circulating bubbling fluidized	-	-	2.54[b]	42[b]

Two values below 2 MJ/kg are observed. For the thermally coupled process [123], considerable savings are achieved by cascading the heat down three different adsorption processes operating at

different temperatures. However, the heat must be introduced into the process at a higher temperature, requiring the extraction of higher-grade heat from the power plant. For this reason, the energy penalty of this concept was 9.5-11.5 %-points, which is comparable to MEA. The moving bed TSA with heat integration [64] has a low thermal energy requirement, but includes a considerable additional energy penalty for water removal from the flue gas, resulting in an energy penalty similar to that of an MEA benchmark. The heat integration in the moving bed is also likely to be expensive, given the relatively low heat transfer coefficient.

Another important key performance indicator for benchmarking the different reactor configurations is the productivity that measures the amount of captured CO_2 per unit of sorbent volume and time. As can be seen in *Table **2-4***, the different studies reported a wide range of values with the best performance achieved by the monolithic reactor configuration [95]. This resulted from the short cycle time enabled by this configuration combined with the fast reaction kinetics of the chosen sorbent and the low mass transfer resistance. The TSA-Indirect with vacuum and heat pump- CO_2 configuration has the potential to maximize the productivity despite the low value of 68.3 kg-CO_2/m^3.h found in the experimental study [69]. It was shown in this study that increasing the flow rate to achieve the 1 m/s superficial gas velocity used in the techno-economic study [1] (against 0.19 m/s in experiment) was restricted by the experimental setup (elutriation of particles), not by the kinetics of the reactions nor by the mass transfer. This implies that a productivity of ~360 kg-CO_2/m^3.h could be achieved by such reactor configuration.

Finally, it should be noted that VSA and heat pump processes will appear considerably more attractive in industrial processes where an abundance of low-grade heat is not available. In this case, the conversion to thermal energy should be done assuming typical thermal power plant performance (40-60%), roughly halving the converted thermal requirements of these processes

reported in *Table **2-4***. For example, the SARC process showed only marginal gains over typical MEA energy penalties in CO_2 capture from a coal power plant [1, 91], but strongly outperformed MEA in a cement plant where heat for the MEA process had to be generated in a dedicated boiler [90]. In such industrial applications, CO_2 capture concepts relying on electric energy show the largest potential relative to conventional TSA benchmarks.

2.5 Demonstration status of research

ADA has been working on developing solid sorbents and fluidized bed technology to efficiently capture CO_2 from power plant flue gas for over a decade. Sorbent screened was completed at 1 kWe scale to demonstrate the ADA's solid sorbent CO_2 capture process [128]. Later they designed and completed the construction of a first-of-its-kind in-the-world, 1 MWe scale, CO_2 capture pilot facility in 2014 [129]. The reactor configuration comprises of three-stage fluidized-bed adsorber integrated with a single-stage fluidized-bed regenerator. A recent pilot plant study by ADA indicated 90 % CO_2 capture with TSA mode of regeneration and reported two main operational challenges with the pilot plant: first associated with handling of the sorbent at operating high temperature and second associated with the preloading of the sorbent in the transport line between the regenerator and adsorber that reduced the working capacity [130].

A brief summary about the other low temperature adsorption concept and demonstrated at various scales in past are presented in below *Table **2-5***. Few of the concepts have been demonstrated at pilot scale while the majority of the studies were conducted at lab scale. Capturing CO_2 from coal power plants remains the dominant sector that was targeted by the demonstration studies showing a clear need for extension to other CO_2 intensive sectors such as cement, metal industry and biofuel.

*Table **2-5**: Demonstration status of various concepts.*

Reactor	**Regeneration Mode**	**Scale**	**Adsorbent**	**Sector**
Fluidized [131]	TSA	Pilot- 200 t/d	Dry sorbent (K or Na)	Coal
Moving bed (KCC) [65]	TSA	Pilot- 3.5 t/d	Amine functionalized	Coal
Fixed[55]	VSA(2 stage)	Pilot - 1.6 t/d	Zeolite 13X & Activated carbon	Coal
Moving bed (SRI) [62]	TSA	Pilot- 0.56 t/d	Carbon	Coal
Fluidized bed (RTI) [25]	TSA	Pilot-0.15 t/d	PEI	Cement
Fixed [108]	VSA - LPP	Pilot	Zeochem zeolite 13X	Coal
Multistage fluidized [79]	TSA-N_2	Lab-35 kg/d	PEI/SiO_2	Gas
Multistage Fluidized[69]	VTSA	Lab-24 kg/d	PEI/SiO_2	Coal
Fixed + membrane[115]	VSA-membrane	Lab	Zeolite molecular sieve 13X Grace	Coal
Sound assisted fluidized[132]	-	Lab	Activated carbon	Gas/coal
Fluidized bed[130]	TSA	Pilot	Amine based	Coal

2.6 Discussion

The different sections presented above highlighted the clear fundamental difference in the behaviour of the different reactor configurations in the adsorption that affect the performance in terms of CO_2 recovery efficiency and purity in addition to the overall footprint. Another important factor that affects the choice of the reactor configuration is the regeneration mode that is in general dictated by the nature of the sorbent selected and the initial CO_2 partial pressure in the flue gas. The combination of reactor configuration and regeneration mode are the key elements that impact the footprint, operation strategy, the flexibility for part load operation when needed and the overall energy penalty imposed for CO_2 capture. All these factors along with the maintenance and replacement of sorbent particles will influence the techno-economic attractiveness of the different configurations for different applications. The scattered energy/heat duty values reported in the

limited existing number of studies on techno-economic assessment of adsorption-based CO_2 capture (*Table **2-4***) are far from being systematic to provide any firm conclusions on the link of the reactor configuration and regeneration mode to the overall performance of the technology. It can also be observed that there is a big lack of economic assessment studies with this technology giving clear estimates on the cost of CO_2 avoidance imposed by such technology.

Retrofitting to existing plants is also an important factor when considering the costs of CO_2 capture technology. In principle, regeneration modes that require only electricity are best suited to retrofitting (e.g. VSA, ESA, microwave assisted and SARC using a combination of a heat and vacuum pumps), while the others that require heat for TSA (both direct and indirect) impose constraints to retrofitting, dictating sourcing heat from the plant through complex integration or involving building boilers and associated infrastructure. The interaction of the different factors and their impact on the different reactor configurations are qualitatively discussed and evaluated in *Table **2-6*** (next page).

*Table **2-6**: A qualitative evaluation of the different factors impacting the choice of the reactor configuration for adsorption-based CO_2 capture.*
+ (advantage), o (neutral) and – (drawback) are used to describe the overall performance of each reactor configuration against the different factors

	Adsorption	**Regeneration**	**CO_2 recovery and purity**	**Operation strategy**	**Footprint**	**Flexible load operation**
Conventional fixed bed	(-) The high pressure drop results in a high energy penalty or footprint. Heat and reaction fronts limit the working adsorption capacity and apply thermal stresses on the sorbent.	(o) VSA is the most suited because low heat transfer rates make TSA impractical. However, the high pressure drop imposes a long regeneration time.	(-) Complex two-stage VPSA configurations are required for good CO_2 recovery and purity from most flue gases.	(-) Complex control of multiple transiently operated reactors, particularly when a two-stage process is involved.	(-) High pressure drop both in adsorption and regeneration limit gas velocities, increasing the footprint.	(+) Possible due to the standalone reactors. Beds could also be regenerated faster when electricity is cheap and carbonated later for greater flexibility.
Structured bed	(+) Smartly engineered structures can reduce heat and mass transfer limitations and pressure drop. Sorbents with fast kinetics should be used though.	(+) Similar VSA suitability to fixed beds, but indirect TSA is also possible if the structure enables flowing a fluid through the bores for heat addition or removal.	(-) Similar to the conventional fixed bed.	(o) Indirect TSA could result in simpler one-stage operation strategy, but given that the cluster would still be needed, the operation strategy will be relatively complex.	(o) A lower pressure drop can allow for substantially faster gas flows and thus smaller footprints than fixed beds.	(o) Similar to fixed bed, although the higher cost of the structure could make storing beds of regenerated sorbent during low electricity prices uneconomical.
Moving bed	(o) Counter-current operation maximizes the working adsorption capacity, but this is counteracted by the low heat transfer coefficient that may lead to heat build-up in the adsorption.	(o) Direct heating with steam or CO_2 remains the most feasible mode due to the low tube-to-bed heat transfer coefficient. A drying step should be foreseen when steam is used as a heating agent.	(+) High if leakage between the chambers can be minimized.	(+) Simple steady state operation strategy involving solids circulation to the different chambers of the reactor	(-) Counter-current operation involves a large footprint due to the limitation on the gas velocity to avoid fluidization of the falling solid sorbent.	(o) Varying the feed rate to the reactor could enable flexible load operation. This will however be affected by the mechanism used for solids circulation.

Rotary bed	(-) Similar drawbacks as fixed bed, although smartly engineered structed beds can reduce these challenges. Cooling the rotating system in TSA is complex.	(o) Direct heating with steam or CO_2 is the best option, but this would involve a drying step. VSA requires a sophisticated sealing system.	(-) Acceptable CO_2 recovery and purity require implementing purge zones between the adsorption and regeneration feeding substantial amounts of steam. Complex sealing in VSA mode.	(+) A relatively simple steady state operation strategy if the rotation speed and the zone of the different steps of the capture cycle are designed properly	(o) If smartly engineered structures are used to remove the heat and mass transfer limitation, a reasonable footprint could be achieved	(o) Flexible load operation is possible by varying the feed rate to the reactor and adjusting the rotational speed.
Circulating fluidized bed	(-) The high mixing results in fast CO_2 breakthrough and low working adsorption capacity, requiring large sorbent recirculation rates.	(+) Both direct and indirect heating are possible. Indirect heating is ideal when low-grade heat is available (e.g. from a power plant).	(-) The high mixing requires very long risers in the adsorption and involves larger circulation rate to achieve acceptable CO_2 recovery.	(+) A simple steady state operation strategy due to the use of only two reactors with the sorbent circulating between them.	(+) Small footprint due to the high flue gas velocities permitted by fluidized bed risers.	(-) The range of flue gas feed rates over which stable sorbent circulation can be maintained will be limited.
Counter-current multistage circulating fluidized bed	(+) Counter-current behaviour maximizes the working adsorption capacity. The advantage of good heat transfer of fluidized bed is maintained for effective TSA operation.	(+) Similar to conventional circulating fluidized bed.	(+) High CO_2 recovery and purity could be achieved with this configuration if gas leakage between reactors is effectively minimized.	(+) Similar to conventional circulating fluidized bed.	(o) Counter-current operation will increase the adsorber footprint relative to conventional circulating fluidized beds to maintain down-flowing sorbent.	(-) Similar to conventional circulating fluidized bed.
Multistage dense fluidized bed (switching)	(o) Similar to counter-current multistage circulating fluidized bed, but the transient reaction front will move through the stages over time, requiring a taller reactor.	(+) High heat transfer rates from fluidization and practical vacuum swing from standalone reactors allow for easy VTSA operation, synergistically combining heat and vacuum pumps.	(+) Good CO_2 recovery and purity can be achieved by implementing an evacuation step directly after the adsorption step.	(-) A cluster of transient reactors is needed for continuous flue gas processing and heat pump working fluid must be continuously redirected between different reactors.	(o) Moderately large footprint to avoid elutriation of particles, but sufficient gas velocities can be achieved as particles are allowed to fluidize.	(o) The fluidization velocity could be varied over an order of magnitude while maintaining the dense regime (bubbling and turbulent regime).

Future research needs

From the above discussion, it can be clearly concluded that there is an urgent need for studies that standardize the assumptions for thermodynamic and economic assessments of the different configurations combined with the different regeneration modes. Such studies will bring clear and accurate comparisons of the cost of CO_2 avoidance involved with the different combinations. It can however be speculated that for a specific initial CO_2 partial pressure in the feed flue gas, the different reactor configurations and regeneration modes will perform differently with the different families of sorbents. Therefore, identifying the best combinations of reactor configuration, regeneration mode and sorbent families with taking into consideration the CO_2 source (CO_2 partial pressure in the flue gas) would bring breakthrough insights to the adsorption-based CO_2 capture community to set up clear roadmaps and directions for development and scale up of the most promising combinations for the different industrial sectors. Such an approach was partially followed for screening sorbents based on key performance indicators such CO_2 recovery, purity and avoidance costs, but it was limited to a fixed bed configuration using a PVSA regeneration mode [133]. Future studies should also investigate the technical and economic aspects of flexible load operation and partial capture of the different combinations of reactor configuration and regeneration modes. As observed in *Table **2-4***, most of technoeconomic assessment studies were completed for capturing CO_2 from coal power plants, so there is a clear need for extending them to other CO_2 sources covering power generation (natural gas and waste-to-energy plants), cement, metal production and biofuel.

As for the technical aspect, thorough experimental testing and validation at lab and pre-pilot scale should be dedicated to promising reactor configurations, such as the multistage fluidized bed and the structured reactors. For this latter, the focus should be on investigating the feasibility of integrating the designed regeneration modes and confirmation of achieving

sufficiently high separation performance and sufficiently short cycle time. Measuring the extent of heat recovery and addition in the appropriate configurations and determining its limitations is also of high importance for heat integration purposes. Several recent studies have already touched on this for specific reactor configurations, but the studied designs and achieved performance remain far below expectations [79, 114, 134, 135].

2.7 Summary and conclusion

This paper provides a detailed overview on the different reactor configurations proposed for adsorption-based CO_2 capture. Various gas-solid contacting systems and sorbent regeneration modes are identified and discussed in terms of strengths and limitations. In addition, the suitability of the different combinations of contacting systems and regeneration modes are discussed.

The fundamental behaviour of the conventional fixed and fluidized bed during adsorption is inadequate for extracting the full potential of the technology. Fixed beds exhibit high pressure drop, formation of heat waves in addition to mass and heat transfer limitation issues. The good mixing in fluidized beds results in early CO_2 breakthrough that in turn, results in poor CO_2 recovery or low sorbent utilization.

To overcome the challenges associated with these two reactor configurations, recent research trends focused on structured packings for the fixed bed and counter-current multistage for fluidized bed. Smartly designed structures can minimize the pressure drop, while maintaining a high gas-solids contacting area, thus maximizing the flue gas throughput rate and minimizing the reactor size and footprint. As for fluidized bed, the multistage configuration can minimize the negative effect of the mixing on the CO_2 recovery and working capacity, while maintaining the benefits of the good heat transfer characteristics for heat integration purposes. Both these

configurations pose considerable scale-up challenges due to their increased complexity, but they appear to hold the greatest promise for the future of adsorption-based CO_2 capture.

Alternative configurations include rotating beds, with similar properties to structured fixed beds, and moving beds, with similar properties to multistage fluidized beds. Relative to fixed beds, rotating beds offer steady state process operation, but impose challenges with sealing when a vacuum need to be drawn. Moving beds can further increase sorbent working capacity relative to multistage fluidized beds, but impose challenges regarding heat transfer rate, mass transfer resistance on the larger particles and pressure drop. Another noteworthy alternative is the swing adsorption reactor cluster that synergistically combines vacuum swing and temperature swing using a heat pump.

A range of energy duties has been reported for different adsorption-based CO_2 capture technologies, although the variance in flue gas composition, CO_2 recovery and purity, and process modelling assumptions makes it difficult to compare between different studies. However, several studies find that the sorbent-based processes outperform MEA benchmarks. In addition, VSA and heat pump concepts that consume only electrical energy show great promise for industrial processes without large amounts of low-grade heat that can be used for TSA. In general, there is a clear need for studies using standardized assumptions for comparing the different reactor configurations and benchmarking them using key performance indicators, particularly the cost of CO_2 avoidance that combines both energy efficiency and capital cost into a single metric. It is likely that different sorbent-reactor combinations work best for different flue gas streams and desired CO_2 avoidance rates. Such a standardized benchmarking study therefore needs to be completed for several key future applications of post-combustion CO_2 capture.

Other aspects such as the complexity of the operation strategy of the selected combinations, ease of retrofitting, and the ability to operate under flexible load should also be considered in

this comparison. Following such a standardized study, research efforts can be focused on development and scale-up of the most promising sorbent-reactor combinations to accelerate the commercial deployment of adsorption-based post-combustion CO_2 capture.

3 The Swing Adsorption Reactor Cluster (SARC) for post combustion CO_2 capture: Experimental Proof-of Principle

This chapter has been adapted from **Article I**

Dhoke, C., et al., *The Swing Adsorption Reactor Cluster (SARC) for Post Combustion CO_2 Capture: Experimental Proof-of-Principle*. Chemical Engineering Journal, 2018.

Abstract

This paper presents the first experimental demonstration of the novel swing adsorption reactor cluster (SARC) for post combustion CO_2 capture. The SARC concept combines a temperature and vacuum swing for sorbent regeneration. A heat pump is used for transferring heat from the exothermic carbonation reaction to the endothermic regeneration reaction. Sorbent regeneration under vacuum allows for a small temperature difference between carbonation and regeneration, leading to a high heat pump efficiency. This key principle behind the SARC concept was demonstrated through bench-scale experiments comparing combined vacuum and temperature swing adsorption (VTSA) to pure temperature swing adsorption (TSA), showing that a 50 mbar vacuum can reduce the required temperature swing by 30-40 °C. A complete SARC cycle comprising of carbonation, evacuation, regeneration and cooling steps was also demonstrated. The cycle performed largely as expected, although care had to be taken to avoid particle elutriation under vacuum and the CO_2 release rate was relatively slow. The SARC principle has therefore been successfully proven and further scale-up efforts are strongly recommended.

Keywords: *Post combustion CO_2 capture; Adsorption; Combined vacuum and temperature swing; Fluidized bed*

3.1 Introduction

This paper presents an experimental proof of the SARC principle using a small bench scale reactor designed and constructed for this purpose (*Figure **1-4***).

3.2 Methodology

3.2.1 Sorbent material

A Polyethyleneimine based (PEI) sorbent was used in this study. In general, PEI based sorbents have low regeneration enthalpies and high adsorption capacity, in addition to high selectivity to CO_2 [24]. This sorbent was developed at the Korean Research Institute of Chemical Technology (KRICT) and extensively tested in a pilot scale circulating reactor configuration at KRICT [136]. The sorbent was made following impregnation of PEI on spherical commercial silica spheres [136]. The sorbent properties are depicted in *Table **3-1***. CO_2 isotherms for this sorbent were recorded on a volumetric Belsorp Max instrument in the temperature interval of 313 to 383 K, for pressures from vacuum up to 100 kPa (CO_2).

*Table **3-1**: Physical, chemical and thermochemical properties of sorbent.*

Sorbent composition	BET surface area (m^2/g)	Average Pore diameter (Å)	Density Skeletal (g/ml)	Density Particle (g/ml)	Adsorption enthalpy (GJ/tone CO_2)	Average Heat capacity (40-120 °C) (J/g.K)
PEI (45 wt. %) + SiO_2 (55 wt.%)	42.09	383.1	1.53	1.36	1.47	1.5

A model was fit to the experimental measurements according to the Toth isotherm (*Equation **3-1*** to *Equation **3-4***). The model parameters providing the best fit are given in *Table **3-2*** and the quality of the the resulting fit is illustrated in *Figure **3-1***.

$$q = \frac{n_s b p_{CO_2}}{\left(1 - \left(b p_{CO_2}\right)^t\right)^{\frac{1}{t}}} \qquad \textit{Equation } \textbf{3-1}$$

$$b = b_0 \exp\left(\frac{dH}{RT_0}\left(\frac{T_0}{T} - 1\right)\right)$$ *Equation* ***3-2***

$$n_s = n_{s,0} \exp\left(X\left(1 - \frac{T}{T_0}\right)\right)$$ *Equation* ***3-3***

$$t = t_0 + \alpha\left(1 - \frac{T_0}{T}\right)$$ *Equation* ***3-4***

Table ***3-2****: Toth isotherm parameters for the fit in Figure* ***3-1.***

b_0	69.72 kPa^{-1}
dH	118.6 kJ/mol
T_0	303 K
$n_{s,0}$	2.135
X	0
t_0	0.3648
α	2.242

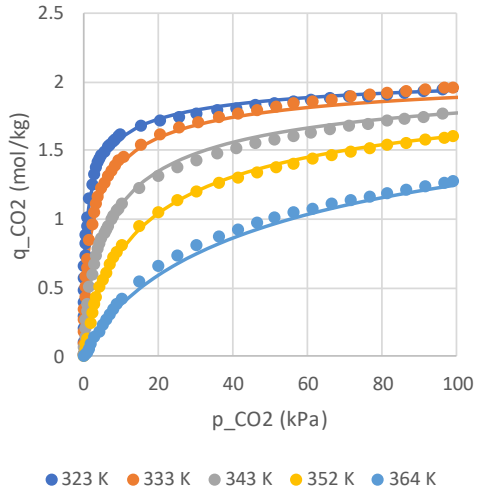

Figure ***3-1****: Illustration of the isotherm fit (Table* ***3-2****)against experimental measurements at five different temperatures.*

3.2.2 Reactor experiments

This study was structured in four experimental campaigns, summarized in *Table **3-3***, completed on 60 g of sorbent placed initially in the reactor (*Figure **1-4**)*.

The first campaign consisted of pure TSA cycles applied on fresh sorbent to investigate the possible need for sorbent activation. This study was conducted over ten successive cycles at atmospheric pressure (1000 mbar) with carbonation at 60 °C and regeneration at 120 °C . The gas composition was sampled continuously at the reactor outlet to estimate the working capacity from carbonation under conditions which is defined as in *Equation **3-5***;

$$Working\ capacity = \frac{(moles\ of\ CO_2\ desorbed - moles\ of\ CO_2\ adsorbed)\ during\ regeneration}{kg\ of\ adsorbent}$$

*Equation **3-5***

The third study investigated the effect of regeneration temperature and pressure over three levels in the ranges indicated *Table **3-3***. Each experiment was repeated three times to quantify the experimental measurement uncertainty. The quantified working capacities from each case were compared with the isotherm model.

The last study was performed to explicitly show how the SARC process would work in practice by completing the whole SARC cycle under the VTSA mode. The sorbent was exposed to the four SARC steps in sequential manner: carbonation, evacuation, regeneration and cooling (as illustrated in *Figure **3-5***). In the carbonation step, the sorbent was exposed to 12.5 mole % of CO_2 in N_2 at 60 °C and 1000 mbar, followed by the evacuation step, wherein, 100 mbar vacuum was established at 60 °C. Subsequently, the sorbent was heated to 80 °C while maintaining the vacuum of 100 mbar for the combined vacuum-temperature swing regeneration step. Finally, the sorbent was cooled back to 60 °C while repressurizing the reactor to 1000 mbar. Gas analysis was carried out continuously and the corresponding working capacity was measured.

*Table **3-3**: Regeneration conditions over the four experimental campaigns. All experiments were completed on a bed with 60 g of sorbent, with carbonation carried out at atmospheric pressure and 60 °C using a 2 Nl/min feed of 12.5% CO_2 in N_2.*

Expt. set	Objective	Mode	Regeneration Temperature	Regeneration pressure	Purge gas in regeneration
1	Equilibrating sorbent	TSA	120 °C	1000 mbar	N_2=0.5 LPM
2	Comparative study TSA vs. VTSA	TSA	60-120 °C	1000 mbar	CO_2=0.5 LPM
		VTSA	60-80 °C	50 mbar	NA
3	Parametric study	VTSA	60-80	50-150 mbar	NA
4	SARC complete cycle	VTSA	80 °C	100 mbar	NA

3.3 Results and Discussion

3.3.1 Sorbent working capacity and stability

The maximum working capacity over 10 cycles was measured and the results are shown in *Figure **3-2***. An average working capacity of 1.2 mol/kg of sorbent was measured for 10 consecutive cycles with a small standard deviation of 0.02 mol/kg. This result confirms the stability of the sorbent and the repeatability of the experimental procedure. As suggested by

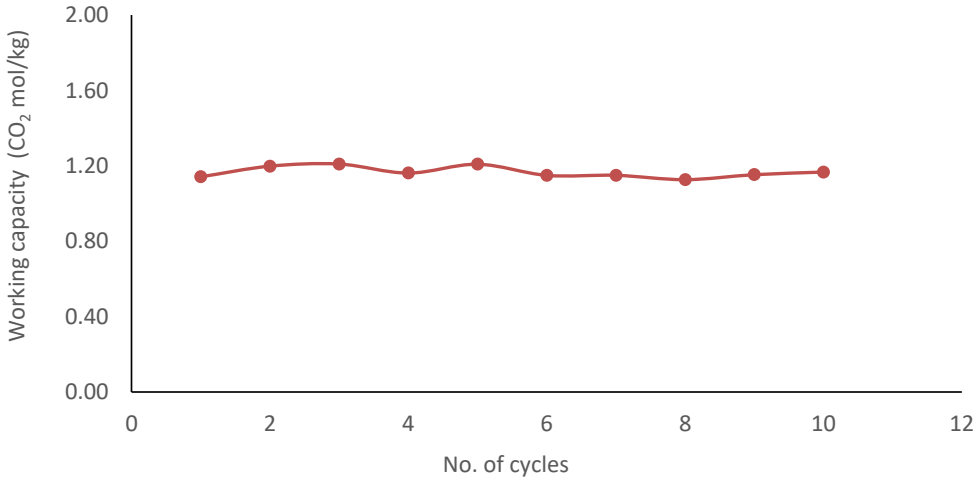

*Figure **3-2**: Sorbent working capacity over 10 consecutive cycles for the first experimental campaign in Table **3-3**.*

*Figure **3-1***, the maximum sorbent working capacity is about 2 mol/kg. However, this is not achievable in practice when completing the carbonation at 60 °C and only 12.5% CO_2 because the sorbent cannot reach its maximum loading under these conditions. The 1.2 mol/kg found in this experiment is thus a good indication of the maximum sorbent working capacity under realistic operating conditions.

3.3.1 Comparative study of TSA and VTSA

As seen in *Figure **3-3***, working capacity increases with increase in the regeneration temperature for both TSA and VTSA operating modes. This is expected as increase in temperature favors the desorption of CO_2. As expected, the presence of a vacuum greatly increased the achievable working capacity at a given temperature relative to pure TSA.

Another interesting result from *Figure **3-3*** is the negative working capacity for TSA at temperatures below 80 °C . In the TSA experiments, regeneration was conducted in the presence of 100% CO_2 showing that the effect of partial pressure is more dominating than the temperature (the increase in partial pressure from 12.5% to 100% of CO_2 lead to more adsorption than desorption even when the temperature was raised from 60 °C to 80 °C). At temperatures beyond 80 °C, a positive TSA working capacity indicates that temperature is dominating compared to partial pressure of CO_2.

In VTSA mode, regeneration was carried out in a vacuum of 50 mbar. In general, the results indicate that this vacuum swing can reduce the required temperature swing by 30-40 °C relative to TSA for achieving a given working capacity. This substantial reduction in temperature swing will have a large positive effect on heat pump efficiency.

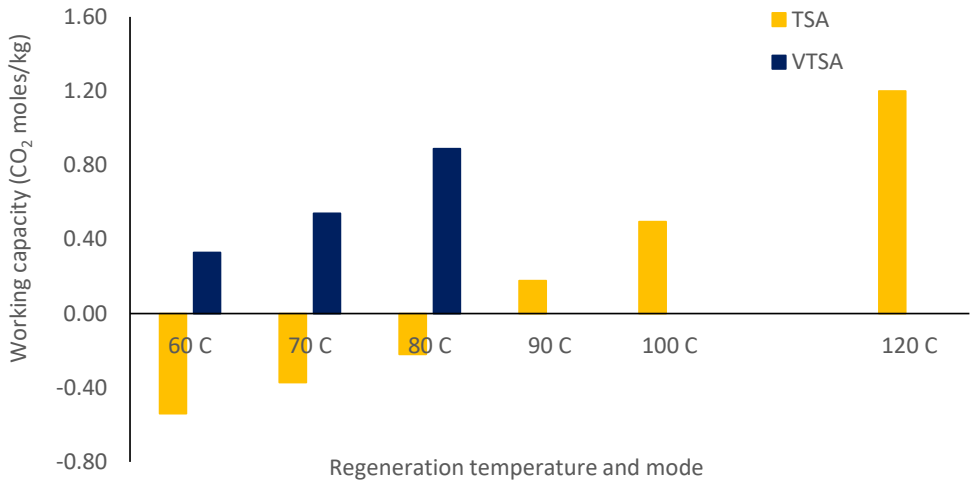

*Figure **3-3**: Comparison of TSA and VTSA following the second experimental campaign in Table **3-3**.*

3.3.2 Parametric study with VTSA

As shown in *Figure **3-4***, the working capacity measured experimentally is consistent with the prediction from the isotherm model illustrated in *Figure **3-1***. Some minor deviations are observed in some cases, but this may be due to variability in the experiments as indicated by the standard deviation bars. As expected, the working capacity increases with increasing vacuum level and regeneration temperature. Within the ranges investigated in this study, the temperature has a larger effect than the vacuum.

It should be noted that a pure vacuum of 50 mbar may not be practical or economical in a large-scale reactor due to sealing requirements and the size of the required vacuum pump. For sorbents that adsorb and desorb water vapor, however, a partial pressure close to 50 mbar can be achievable at a physical pressure of 100 mbar due to the release of water vapor under regeneration. In this way, the adsorption of water vapor may benefit the SARC concept despite the additional heat requirement for water vapor desorption.

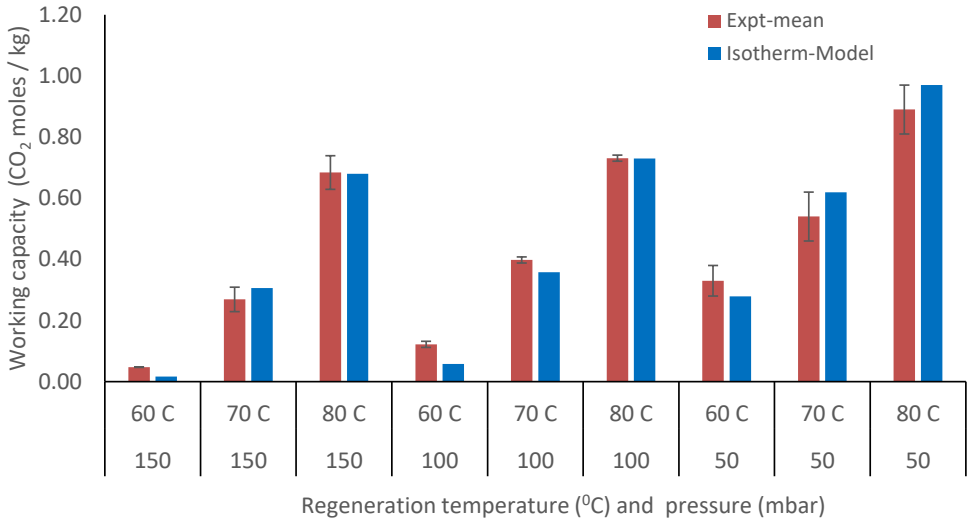

*Figure **3-4**: Parametric study on regeneration temperature and pressure following to the third experimental campaign in Table **3-3**.*

3.3.3 Complete SARC cycle

In this section, the entire SARC cycle consisting of four steps was completed by applying a temperature swing of 20 °C and a pressure swing of 900 mbar when regenerating the sorbent. As mentioned in section 3.2.2, evacuation and cooling steps were applied between the carbonation and regeneration steps. The carbonation time was set to capture 86.3 % of the CO_2 across the step while the regeneration time was manipulated to recover the maximum moles of CO_2 at 100 mbar and 80 °C. This was determined during the experiment by monitoring the gas analyzer signal and the regeneration step ended when the mole percentage of CO_2 approached 0 % in gas analyzer.

*Figure **3-5*** shows the process conditions for SARC cycle, where in the temperature and pressure are plotted against time for one complete SARC cycle. A slight rise in temperature (4 ˚C) was observed in the carbonation step due to the exothermic adsorption of CO_2 on the sorbent. Indeed, during the carbonation step, the CO_2 molar flowrate exiting the reactor is nearly zero for first 4.5 mins (*Figure **3-6***), indicating 100 % capture of CO_2. Towards the end of the

carbonation step, the CO_2 slippage increases substantially as the (*Figure* ***3-6***). In the regeneration step, the molar flow of CO_2 increased significantly when the temperature was increased from 60 to 80 °C (*Figure* ***3-5*** & *Figure* ***3-6***). A slight increase in reactor pressure was observed during regeneration due to the desorption of CO_2 as a result of the increase in temperature while maintaining the 100 mbar vacuum (*Figure* ***3-5***). When the target regeneration temperature was reached, the CO_2 release continued, indicating kinetic limitations in sorbent

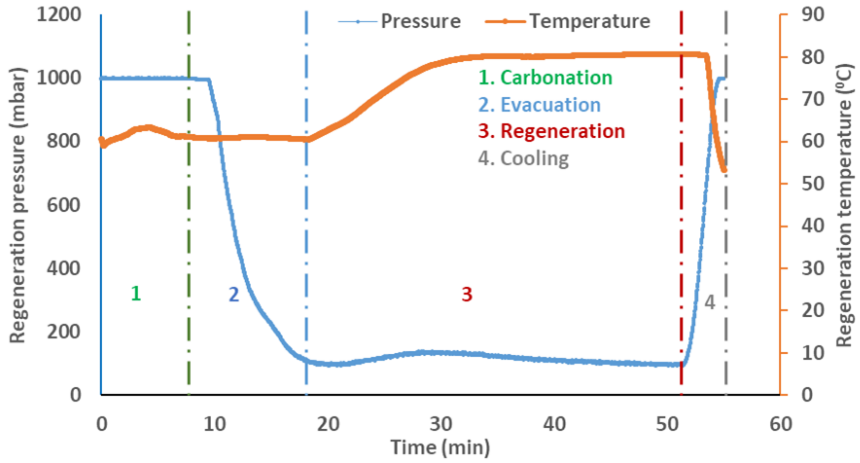

Figure ***3-5****: Pressure and temperature measurements over the SARC cycle.*

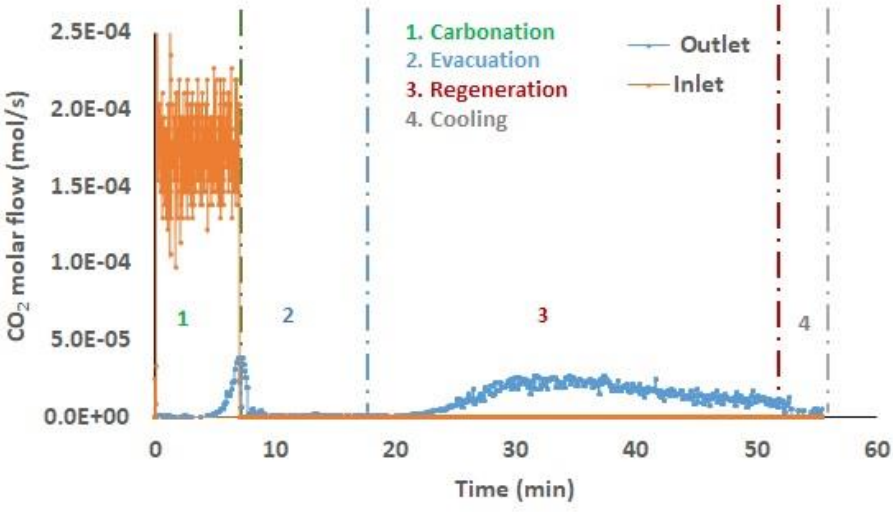

Figure ***3-6****: Molar flow of CO_2 over the SARC cycle.*

regeneration at this temperature (the sorbent required about 20 minutes to reach equilibrium). Finally, the reactor was re-pressurized to 1000 mbar and the temperature lowered to 60 °C.

It can also be pointed out that the evacuation and regeneration steps had to be carried out carefully to avoid the elutriation of particles. The vacuum conditions imposed a high flow velocity at a low mass flow rate and the flow velocity varied significantly over time. Controlling these steps to maximize the rate of regeneration, while avoiding excessive particle elutriation will be an important operating challenge for the SARC concept.

The results indicated that a working capacity of 0.55 mol/kg could be achieved with the capture of more than 85% of CO_2 when a combined VTSA (20 °C and 900 mbar) was applied compared to 1.2 mol/kg when a pure TSA of 60 °C was applied. In other words, the combination of a vacuum swing to 100 mbar and a 20 °C temperature swing could utilize almost half of the practically achievable sorbent working capacity quantified in *Figure **3-2***. This lower sorbent utilization is partly because the sorbent cannot be completely regenerated at 100 mbar and 80 °C, and partly because the carbonation step had to be stopped well before the CO_2 partial pressure reached 125 mbar to avoid excessive CO_2 release. The latter effect is minimized by the large aspect ratio of the test reactor, which will restrict axial mixing, leading to more plug flow behaviour during carbonation. This behaviour must be replicated in larger reactor designs through baffles or a multistage reactor design.

3.4 Summary and conclusion

The SARC concept is a promising new post combustion CO_2 capture solution. Given that it operates only on electricity, SARC is ideally suited to retrofits into industrial applications where large quantities of steam is not available for sorbent regeneration. This concept has thus far only been investigated theoretically, and this study is the first to prove the SARC principle experimentally.

Experiments were carried out in a small bench-scale reactor over a PEI-based sorbent. The sorbent had a maximum working capacity of 2 mol/kg, but this maximum working capacity reduced to 1.2 mol/kg when considering that carbonation will take place at 60 °C with a flue gas containing only 12.5% CO_2.

The sorbent working capacity between carbonation in a stream of 12.5% CO_2 and regeneration at different levels of temperature and pressure clearly illustrated how increased vacuum swing can be traded for decreased temperature swing. In general, a vacuum swing to 50 mbar could reduce the temperature swing required for a given sorbent working capacity by 30-40 °C. This is critical to the SARC concept, which uses a heat pump for achieving the temperature swing, because a decreased temperature swing substantially increases heat pump efficiency.

A full SARC cycle of carbonation, evacuation, regeneration and cooling was demonstrated. The cycle behaved largely as expected, although care had to be taken to control the flow rate during evacuation and regeneration to prevent particle elutriation. Regeneration also appeared relatively slow, which could result in longer regeneration times and a larger reactor footprint. Overall, an acceptable sorbent working capacity of 0.55 mol/kg was achieved over the SARC cycle.

The principle behind the SARC concept has therefore been successfully demonstrated experimentally and further scale-up efforts can be strongly recommended.

4 Sorbents screening for post-combustion CO_2 capture via combined temperature and pressure swing adsorption

This chapter has been adapted from **Article II**

Dhoke, C., et al., *Sorbents screening for post-combustion CO_2 capture via combined temperature and pressure swing adsorption.* Chemical Engineering Journal, 2019: p. 122201.

Abstract

Adsorption-based post-combustion CO_2 capture is enjoying significant research attention due to its potential for significant reductions in energy penalty, cost and environmental impact. Recent sorbent development work has focused on polyethyleneimine (PEI) and dry sorbents that exhibit attractively low regeneration energy requirements. The main objective of this study is to identify best suitable sorbent for the recently published swing adsorption reactor cluster (SARC) concept. The screening results of four sorbents indicated two PEI sorbents to be good candidates for SARC application: a PEI sorbent functionalized with 1,2-epoxybutane supported on silica (referred to as EB-PEI in the rest of the document) and a PEI sorbent supported on mesoporous silica containing confined metal organic framework nanocrystals (referred to as PEI-MOF in the rest of the document). High resolution single-component isotherms revealed substantial differences in adsorption capacity and optimal operating temperatures for the two PEI sorbents, and CO_2 and H_2O isotherm models were derived from this data. Subsequently, breakthrough experiments and bench-scale reactor tests showed that co-feeding of CO_2 and H_2O had no significant effect, allowing the single-component isotherm models to be safely used in large-scale reactor simulations. Such a reactor model was then employed to illustrate the effect of the sorbent adsorption characteristics on the efficiency of the novel swing adsorption reactor cluster, which combines pressure and temperature swings. The EB-PEI and PEI-MOF sorbents were compared to a previously published PEI sorbent with distinctly different adsorption behaviour and recommendations for future sorbent development work were made.

Keywords: *adsorption; post-combustion CO_2 capture; polyethyleneimine; sorbent screening; swing adsorption fluidized bed reactor cluster.*

4.1 Introduction

This study further screens potential sorbents for identifying suitable ones for operation of the SARC concept. Four sorbents (two PEI-based, one potassium and one sodium based) were screened first in a 60 grams reactor scale under real SARC conditions. Then isotherms were measured and fitted for the two best performing sorbents, which were subsequently used in SARC reactor simulations. The energetic performance of SARC with the two sorbents was evaluated using correlations for electricity consumption of the heat and vacuum pumps.

4.2 Methodology

4.2.1 Reactor tests

Experiments completed in this section were structured in two sets as summarized in *Table **4-1***, using four sorbents, two PEI-based; EB-PEI supplied by KRICT [137] and a PEI-MOF also supported on mesoporous silica containing confined metal organic framework nanocrystal [138, 139] developed by RTI and two dry sorbents K/ZrO_2 and Na/ZrO_2 made by KRICT by spray-drying of the slurry that consists of 30 wt.% alkali metal carbonate and 70% of ZrO_2. Other types of sorbents like activated carbon and zeolites were not considered because they typically have low regeneration enthalpies and therefore a low sensitivity to temperature swing. As discussed in a previous work [91], low regeneration enthalpies strongly increase the SARC energy penalty because a low temperature sensitivity requires a large temperature swing, which reduces the efficiency of the heat pump. The experiments were completed in a bench scale experimental setup that was built for demonstrating the working principle of SARC concept (*Figure **1-4**)*.

Each run of these experimental sets comprises of three steps: an adsorption step followed by a VTSA regeneration step and then a total regeneration step. All steps were long enough to ensure that equilibrium is reached. The last step of total regeneration was carried out by feeding 0.5

*Table **4-1**: Regeneration and carbonation conditions over the two experimental sets. All experiments were completed by conducting carbonation at atmospheric pressure in pressure of 12.5% CO_2 (dry basis) in N_2.*

Exp. Set	Objective	Sorbent	Adsorption temperature (K)	VTSA- regeneration		Steam (%)
				Temperature swing (K)	Regeneration pressure (kPa)	
1	Sorbents screening	EB-PEI	333	0-20 K	5-15	NA
		PEI-MOF	363	0-20	5-15	NA
		K/ZrO_2	353	20-60	5-15	6.5
		Na/ZrO_2	333	20-60	5-15	6.5%
2	Effect of steam on 2 PEI sorbents	EB-PEI	333	20	10	5%
		PEI-MOF	363	20	10	5%

Nl/min of N_2 at 393-403 K for the PEI sorbents while, for K/ZrO_2 and Na/ZrO_2, it was carried out at higher temperatures, in the range of 463-546 K. The reason for regenerating the sorbent completely is to enable quantification of the adsorption capacity using *Equation **4-1*** (the actual SARC concept will not include this last step of total regeneration).

The experimental sets were designed to investigate two main objectives. The first experimental set was designed to identify suitable sorbents with a high working capacity under SARC operating conditions. This was done by screening the sorbents at various levels of regeneration pressure and temperature swings. The gas composition was sampled continuously at the reactor outlet to estimate the adsorption and working capacity which is defined as follows:

$$Adsorption\ capacity = \frac{moles\ of\ CO_2\ adsorbed\ in\ carbonation}{kg\ of\ adsorbent} \qquad \textit{Equation } \textbf{4-1}$$

$$Working\ capacity = \frac{moles\ of\ CO_2\ desorbed\ in\ VTSA\ step}{kg\ of\ adsorbent} \qquad \textit{Equation } \textbf{4-2}$$

More specifically, the adsorption capacity is the maximum amount of CO_2 that can be adsorbed on the sorbent from a simulated flue gas stream with 12.5% CO_2. In order to quantify this using *Equation **4-1***, the sorbent must be completely regenerated at the start of the carbonation step,

hence the need for the total regeneration step mentioned earlier. On the other hand, the working capacity considers that the sorbent will not be fully regenerated by the VTSA in the SARC process. Specifically, the working capacity quantifies the maximum amount of additional CO_2 that can be adsorbed from the simulated flue gas on top of the CO_2 that remains on the sorbent after a VTSA regeneration step that is long enough to reach equilibrium.

The second experimental set was designed to study the effect of steam in the feed on the two PEI sorbents. To simulate real flue gas composition, a gas composition of 12.5% CO_2 and 87.5% N_2 (dry basis) was used for the carbonation. The effect of water vapor was studied by passing a mixed gas of CO_2 and N_2 through a temperature-controlled humidifier. The feed line was also heated to same temperature to avoid H_2O condensation. The concentration of H_2O was maintained by controlling the temperature of the humidifier and feed line. The content of water vapor in the simulated gas stream was calculated from the relative humidity and temperature measured at the inlet of the reactor.

For this campaign, the regeneration was carried out in a VTSA step followed by total regeneration step as described earlier. The VTSA step was carried out by applying the temperature swing with vacuum as specified in *Table **4-1***, while the total regeneration step was conducted by purging 0.5 Nl/min of N_2 in the temperature range of 393-403 K without vacuum. In this experiment, the total regeneration step also served to ensure that no adsorbed water remains on the sorbent when transitioning from an experiment with steam addition to an experiment without steam addition.

4.2.2 Single component isotherms

Pure component CO_2 and H_2O isotherms were measured using a commercial volumetric apparatus from BEL inc. The volumetric apparatus has a reference cell which contains a known volume of gas and the sample in the sample cell. During experiments, gas flows from the

reference cell to the sample cell and the amount adsorbed at equilibrium can be obtained from the difference in the pressure before and after adsorption in the reference cell.

78 milligrams of EB-PEI and 114 mg of PEI-MOF were packed in a sample cell and regenerated under vacuum overnight at 383 K. Once regeneration was complete, the samples were weighed again to record the dry weight and mounted on to the apparatus to proceed with the isotherm measurements. The isotherm measurement comprises of two steps: measurement of sample cell volume by helium followed by actual adsorption isotherm measurements.

For CO_2 the adsorption isotherms were measured from 333-403 K in 10 K increments from 0.1 kPa to 100 kPa. In case of H_2O the maximum temperature was set to 373 K and the isotherms were measured up to 4 kPa due to limitations of the instrument. In this study, the final dry weights of the EB-PEI and PEI-MOF samples were 71 mg and 106 mg respectively.

4.2.3 Breakthrough experiments

The two samples were further characterized by dynamic column breakthrough (DCB) experiments. In this setup, a known mass of the sample is saturated with the adsorbate (CO_2/H_2O) in a carrier gas, nitrogen. The adsorbed gas was then desorbed by switching the flow to the pure carrier gas. The exit concentration profile is continuously monitored by the detector. The information on adsorption equilibrium can be obtained by performing a mass balance on the concentration response curve.

The breakthrough set-up used in this study is shown in *Figure **4-1***. It consists of an adsorption column housed inside an oven. The length and diameter of the adsorption column are 12 cm and 0.77 cm respectively. The flow rates of CO_2 and N_2 were controlled by mass flow controllers and water vapor was introduced by bubbling the CO_2 and N_2 mixture through a saturator. About 2 g of the sample was packed in the column and regenerated overnight at 383

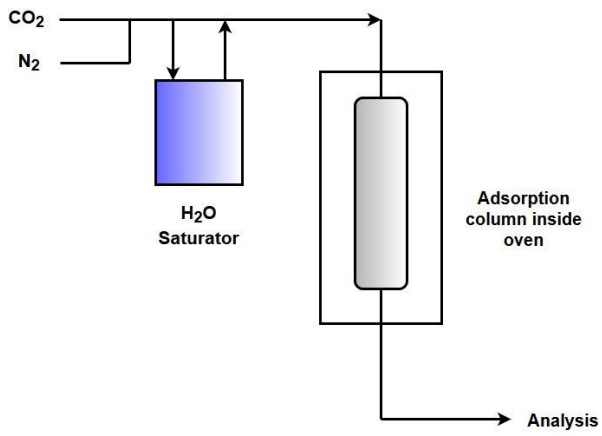

*Figure **4-1**: Schematic drawing of the breakthrough set-up.*

K under a helium purge before each experiment. The breakthrough apparatus was used to study the adsorption equilibrium under dry and wet conditions with N_2 gas as a carrier. Two gas compositions were studied: 1) 22% CO_2 and 78% N_2 and 2) 22% CO_2, 2% H_2O and 76% N_2.

4.2.4 Reactor simulations

This study employs the reactor model developed for the swing adsorption reactor cluster (SARC) in an earlier work [1]. A single SARC reactor is modelled as four continuously stirred tank reactors (CSTRs) in series using MATLAB. This assumption ensures that the behaviour of the SARC reactor falls between that of a complete CSTR and a complete plug flow reactor (PFR), as would be the case in a fluidized bed with many internal obstructions to limit back-mixing. As shown in Zaabout, et al. [1], a greater number of CSTRs in series shifts the model behaviour increasingly towards that of a PFR, leading to better CO_2 capture rates. However, it was argued that four CSTRs in series represents a good compromise between CO_2 capture performance and practicality. Future experimental work will be required to better quantify the degree to which back-mixing can be restricted in a single-stage SARC reactor to achieve PFR-like behaviour, particularly whether the heat transfer tubes in the reactor are sufficient or whether additional flow obstructions are required.

The transient reactor model simulates the four steps in the SARC cycle as graphically illustrated in *Figure **4-2***:

1. Carbonation: The flue gas is fed at close to atmospheric pressure to a regenerated sorbent bed and most of the CO_2 is adsorbed. The heat pump continuously extracts the heat from the exothermic carbonation reaction to keep the reactor temperature close to constant.
2. Evacuation: In this short step, the evacuation pump extracts a portion of the N_2-rich gases in the reactor and vents these gases to the atmosphere to ensure a sufficiently high CO_2 purity from the subsequent regeneration step. No gas is fed to the reactor in this step.
3. Regeneration: The main vacuum pump draws a strong vacuum while the heat pump continuously adds heat into the reactor. The resulting combined pressure and temperature swing causes the sorbent to release CO_2, which is extracted by the vacuum pump and sent to the downstream CO_2 compression train. The CO_2 release may be enough to fluidize the bed, but prior process simulations have assumed that 10% of the extracted CO_2 is recycled to ensure good fluidization (see Figure 3 in Cloete, et al. [90]).
4. Cooling: Before the next carbonation step, the reactor must be cooled by the heat pump to ensure a sufficiently high CO_2 capture ratio at the start of the subsequent carbonation step. Flue gas is fed at 10% of the fluidization velocity used in the carbonation step.

Since the evacuation and cooling steps require much less time than the carbonation and regeneration steps, a large cluster of 25 reactors is required to achieve a steady state process unit [90]. The SARC reactor model repeats this transient cycle of four steps multiple times, each time adjusting the condensation temperature of the heat pump (to achieve 90% CO_2 capture by changing the amount of temperature swing) and the evacuation pump extraction rate (to achieve 96% CO_2 purity by changing the amount of N_2-rich gases extracted in the evacuation

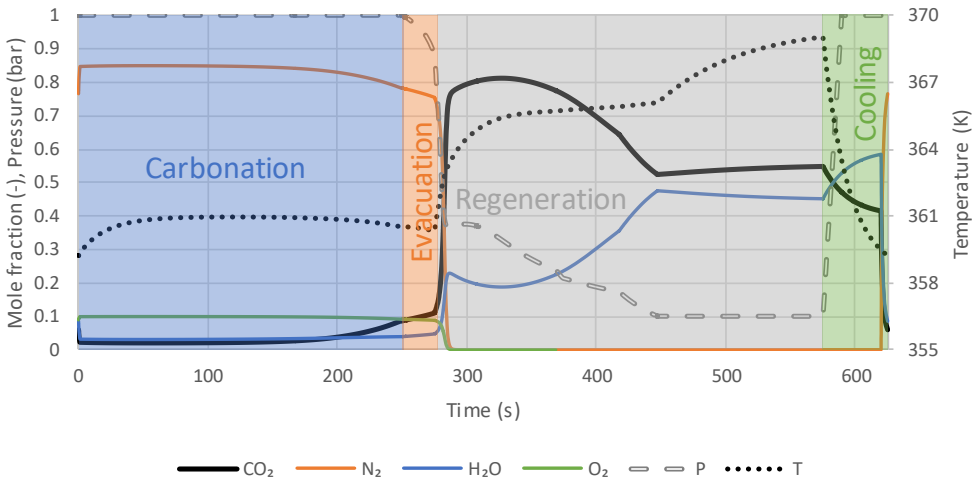

*Figure **4-2**: Typical transient cycle of the SARC reactor.*

$$\frac{E_{HP}}{W_{HP}} = C\,\frac{T_H}{T_H - T_C} \qquad \textit{Equation } \textbf{4-3}$$

step). The final model result is taken only for the final cycle where the objective of 90% CO_2 capture and 96% CO_2 purity is met.

SARC consumes only electrical power, making it attractive for retrofit applications. Four main sources of power consumption are present: CO_2 compression, the vacuum pumps (a large pump for the regeneration step and a small pump for the evacuation step), the heat pump and the flue gas blower required to feed the flue gas through the reactors. This study will focus only on the consumption of the heat pump and main vacuum pump, which will be influenced by the sorbent isotherm. The remaining sources of power consumption will remain constant if the reactor size, flue gas flowrate and regeneration pressure are kept constant.

Heat pump power consumption will be estimated using *Equation **4-3***, where W_{HP} is the heat pump power consumption, E_{HP} is the energy transfer by the heat pump from carbonation to regeneration, $C = 0.72$ is the fraction of theoretical maximum efficiency achieved in Cloete, S.

et al. [90], and T_H and T_C are the hot (condensation) and cold (evaporation) temperatures of the heat pump working fluid.

Vacuum pump power consumption will be scaled proportionately to the gas volume flowrate being extracted through the vacuum pump relative to a gas volume flowrate of 236 m^3/s for a power consumption of 6.44 MW for the central case (0.1 bar vacuum) as presented in Cloete, S. et al. [90]. All other aspects of the simulation are kept constant in the aforementioned study to facilitate a direct investigation into the effect of the change in the isotherm on the SARC reactor performance.

4.3 Results and discussion

Results will be presented and discussed in four sections. First, the adsorbent screening and effect of higher H_2O concentrations will be investigated in a bench-scale reactor. Next, the single component isotherms for CO_2 and H_2O will be presented for the two-best performing sorbents together with the associated model fits. Subsequently, the effect of simultaneous CO_2 and H_2O adsorption will be studied in breakthrough experiments. And finally, the performance of the two sorbent isotherms presented in this work will be evaluated in large-scale reactor simulations for the swing adsorption reactor cluster (SARC) concept.

4.3.1 Reactor experiments

The working capacity (quantified in VTSA step) measured experimentally for four sorbents is presented in *Figure **4-3*** for various VTSA process conditions. As expected, the working capacity increases with increasing vacuum level and regeneration temperature. Overall, PEI sorbents (EB-PEI and PEI-MOF) indicate better working capacity under VTSA operation as compared to dry sorbents (K/ZrO_2 and Na/ZrO_2). Na/ZrO_2 performed reasonably well at the strongest vacuum (5 kPa), but such vacuums may not be practically achievable in large scale SARC applications.

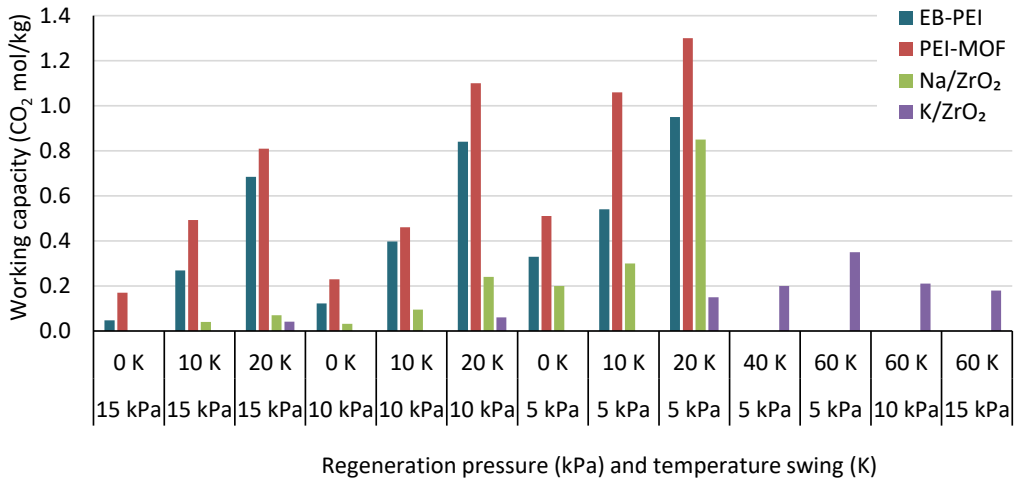

*Figure **4-3**: Working capacity for four sorbents under different combinations of temperature and vacuum swing.*

In general, PEI sorbents work well with a small temperature swing as compared to dry sorbents. This small temperature swing (20 K) is an important parameter in SARC concept as it improves the COP of the heat pump. Between the two PEI sorbents tested, PEI-MOF achieved the highest working capacity which is 37 % more than EB-PEI working capacity. Within the ranges investigated in this study, the temperature has a larger effect than the vacuum pressure.

The effect of water was studied on best performing PEI sorbents. The adsorption capacity with H_2O (5%) and without H_2O in the feed is presented in the *Figure **4-4***. The variability in measured adsorption capacity in the experiments is indicated by the standard deviation bars. The adsorption capacity from single component isotherm models (presented later in *Equation **4-4*** to *Equation **4-7*** and *Table **4-1***) for both PEI sorbents is also plotted for comparison. As seen in the *Figure **4-4***, the experimental adsorption capacity for both sorbents is close to the respective single isotherm model predictions. It was interesting to observe that, even at higher H_2O (5%) concentration, the adsorption capacity remains unchanged for both the sorbents. As predicted

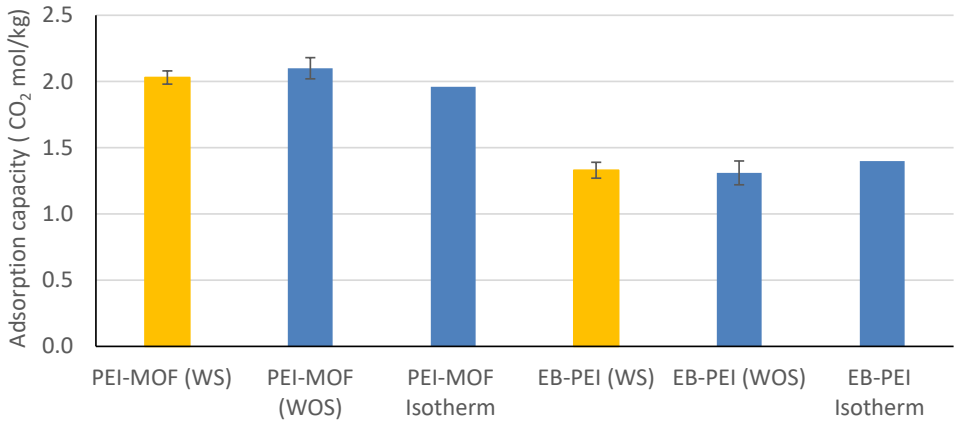

*Figure **4-4**: Adsorption capacity for two PEI sorbents, with and without H_2O; *WOS-Without H_2O; *WS- with 5% H_2O.*

from single component isotherm, PEI-MOF achieves 40% more adsorption capacity as compared to EB-PEI in bench scale experiments.

The working capacity (*Equation **4-2***) at 10 kPa and 20 K of temperature swing is presented in *Figure **4-5*** for two PEI sorbents with and without H_2O. It was interesting to see the increase in the working capacity by the addition of the H_2O for both PEI sorbents. This increase could be related to the dilution of CO_2 because of simultaneous desorption of water. The resulting reduced CO_2 partial pressure increases the driving force for regeneration, which improves the working capacity for both the PEI sorbents.

Another perspective is given by plotting the working capacity with H_2O for both PEI sorbents at 10 kPa next to the working capacity at 5 kPa mbar and temperature swing of 20 K without H_2O in *Figure **4-6***. Interestingly, the working capacity with H_2O at 10 kPa comes close to the case at 5 kPa without H_2O. As discussed in an earlier work [91], this added partial pressure swing facilitated by the release of H_2O during regeneration cancels out the energy penalty of additional heat supply required to release the H_2O and the added gas volume that must be

extracted through the vacuum pump. Co-adsorption of H_2O and CO_2 from the flue gas is therefore not a problem for the SARC concept, although it will increase the energy penalty of pure TSA adsorption processes.

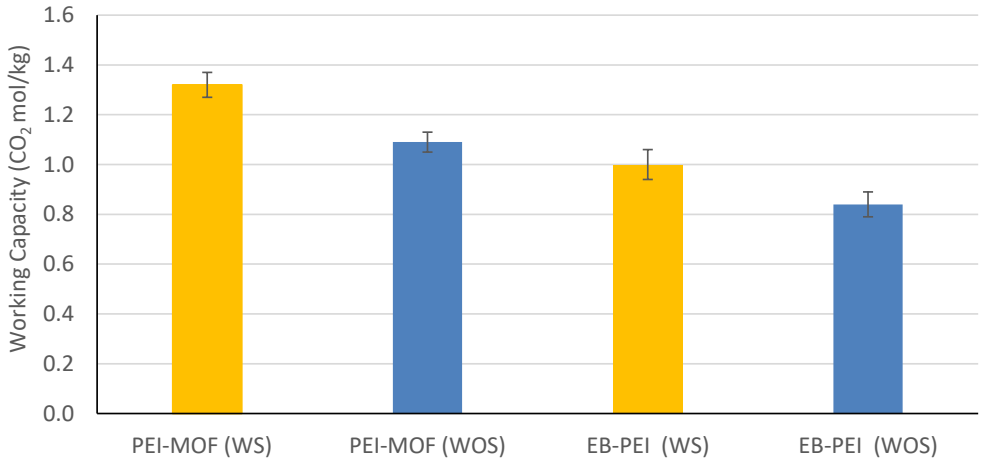

*Figure **4-5**: Effect of H_2O on the working capacity of two PEI sorbents; *WS - With 5% H_2O; *WOS - Without H_2O.*

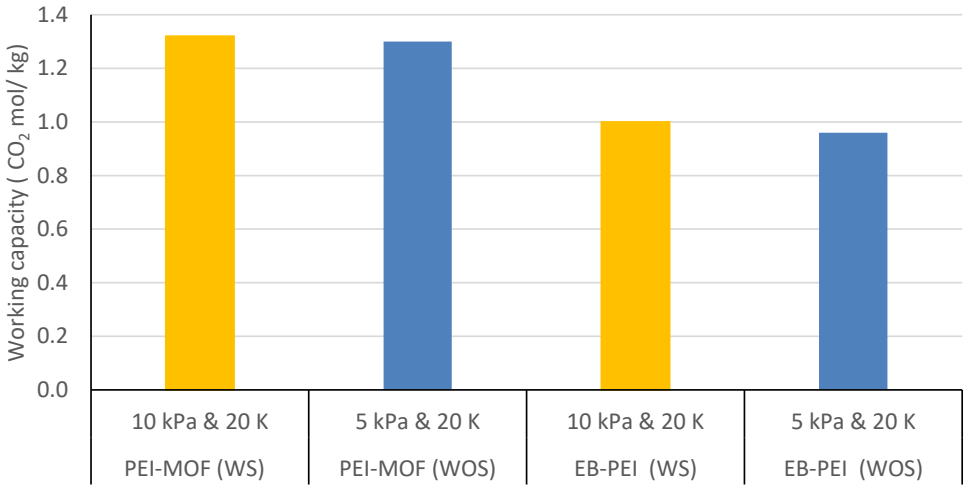

*Figure **4-6**: Working capacity for two PEI sorbents at 10 kPa with steam and 5 kPa without steam; *WS - With 5% H_2O; *WOS - Without H_2O.*

4.3.2 Isotherm fits

Experimentally determined CO_2 isotherms for the two well-performing PEI sorbents are presented in *Figure* ***4-7***. Two key differences are observed between the two sorbents: 1) The adsorption capacity of PEI-MOF is about 40% higher than EB-PEI and 2) PEI-MOF appears to be qualitatively similar to EB-PEI at about 30 K higher temperatures.

The isotherms in *Figure* ***4-7*** were described using the Toth model because a more simplified Langmuir isotherm model could not capture the shape of the isotherms with sufficient accuracy.

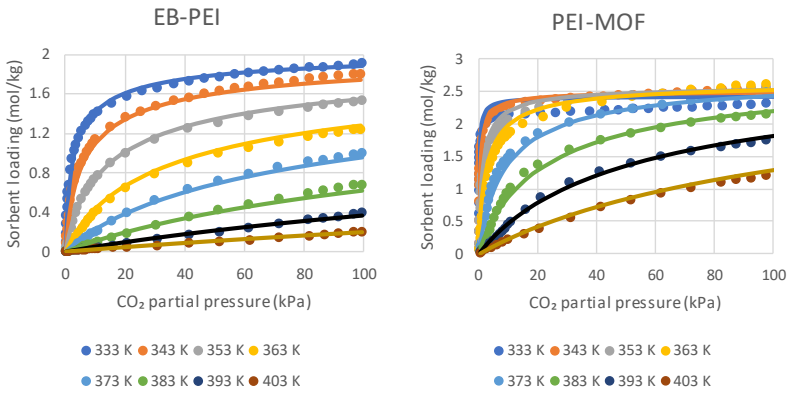

Figure ***4-7****: Experimental CO_2 adsorption isotherms (symbols) and model fits (lines) for the two PEI sorbents.*

$$q_{CO_2} = \frac{n_s b p_{CO_2}}{\left(1 - \left(b p_{CO_2}\right)^t\right)^{\frac{1}{t}}} \qquad \textit{Equation } \textbf{4-4}$$

$$n_s = n_{s,0}\, exp\left(X\left(1 - \frac{T}{T_0}\right)\right) \qquad \textit{Equation } \textbf{4-5}$$

$$b = b_0 \exp\left(\frac{dH}{RT_0}\left(\frac{T_0}{T} - 1\right)\right) \qquad \textit{Equation } \textbf{4-6}$$

$$t = t_0 + \alpha\left(1 - \frac{T_0}{T}\right) \qquad \textit{Equation } \textbf{4-7}$$

$$q_{H_2O,EB\text{-}PEI} = \begin{cases} 5.69\varphi + 0.2528 \\ 37.66\varphi \text{ if } \varphi < 0.0087 \end{cases}$$ *Equation **4-8***

$$q_{H_2O,PEI\text{-}MOF} = \begin{cases} 13.33\varphi + 0.2416 \\ 35.48\varphi \text{ if } \varphi < 0.0109 \end{cases}$$ *Equation **4-9***

Subsequently, the H_2O isotherms were experimentally measured, and model fits were determined as illustrated in *Figure **4-8***. All the data showed a simple linear relationship with the relative humidity, φ. The resulting model is described by *Equation **4-8*** for EB-PEI and *Equation **4-9*** for PEI-MOF.

*Table **4-2**: Model coefficients for use in Equation **4-4** to Equation **4-7** to yield the fit illustrated in Figure **4-7**.*

Coefficient	EB-PEI	PEI-MOF
$n_{s,0}$	2.146	2.200
X	0.317	-0.983
b_0	38.25	657.6
dH	104581	113958
t_0	0.497	0.710
α	1.273	0.714
T_0	303	303

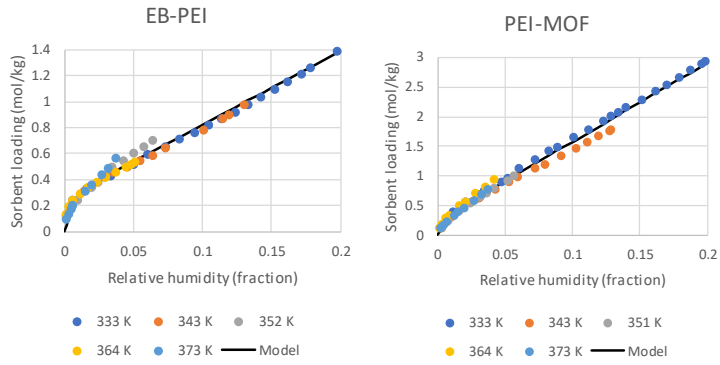

*Figure **4-8**: Experimental H_2O adsorption isotherms (symbols) and model fits (lines) for the two PEI sorbents.*

4.3.3 Breakthrough experiments

The breakthrough profile of CO_2 for EB-PEI is shown in *Figure* ***4-9***. After regeneration, the column was kept under nitrogen flow until the experimental temperature was attained. The sample was then saturated with 22% CO_2 in nitrogen followed by desorption using pure N_2. As seen from the profile, the adsorption profile was sharper. The breakthrough time was 1 min. In case of the desorption, the response was more spread and this was used to obtain the equilibrium information. To account for the dead volume in the system, a similar breakthrough procedure was carried out with an empty column. In both the cases the total flowrates in the adsorption and desorption were 120 and 50 ml/min respectively.

The adsorption equilibrium at 22 kPa, 13 kPa and 7.5 kPa were obtained by subtracting the empty column desorption response from the packed column desorption response at the same concentrations (shown in *Figure* ***4-7***) by doing the following mass balance around the column using *Equation* ***4-10***:

$$q^* = \frac{FC_T}{m_{ads}}\left(\int_o^t \frac{\frac{c(t)}{c_0}}{1-\frac{c(t)}{c_0}y0}\bigg|_{packed} - \int_o^t \frac{\frac{c(t)}{c_0}}{1-\frac{c(t)}{c_0}y0}\bigg|_{blank}\right) \qquad \textit{Equation } \textbf{\textit{4-10}}$$

Where F is the total carrier flowrate during desorption, C_T is the total gas phase concentration, and m_{ads} is the mass of adsorbent. The denominator in the integral is the flow rate correction during desorption.

As the feed concentration is 22% CO_2, integrating the curves from C/C_0=1 from the base line would give the capacity at 22 kPa, while integrating from 0.59 and 0.34 to the baseline will give the capacity at 13 and 7.5 kPa respectively. The isotherms from the breakthrough are compared with the corresponding temperatures at the volumetric study (presented in the previous section). In general, there is a good agreement between the two systems as shown in *Figure* ***4-10***. Experiments were also carried out with 2% water in both the samples. As seen from

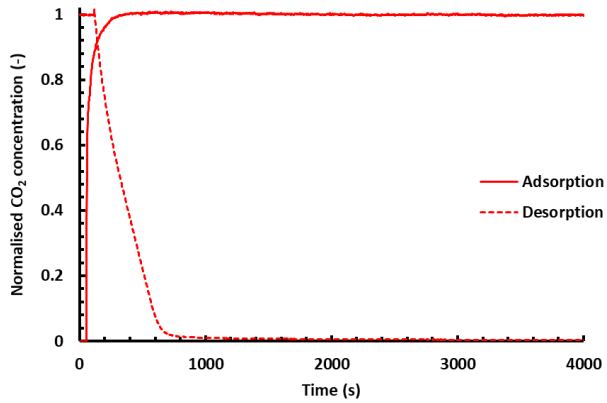

*Figure **4-9**: Adsorption-Desorption profiles for CO_2 breakthrough in EB-PEI. The feed concentration was 22% CO_2 and 78% N_2.*

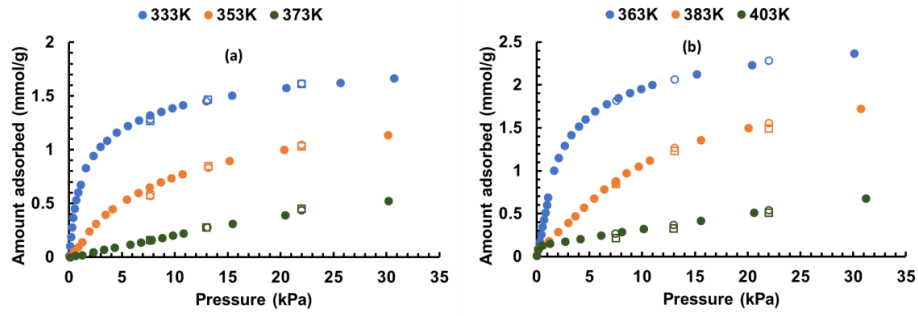

*Figure **4-10**: CO_2 isotherms in (a) EB-PEI and (b) PEI-MOF. Solid symbols denote volumetric experiments, while open circles and squares denote dry and wet breakthrough experiments with 2% H_2O respectively.*

*Figure **4-10***, no change took place when adding H_2O, indicating that both sorbents are tolerant to moisture.

4.3.4 Reactor simulations

Reactor simulations were completed at different carbonation temperatures for three PEI sorbents: the Veneman sorbent presented in [24] used previously to model the SARC performance in a coal [1] and a cement plant [90] and the two sorbents investigated in this study. Changing the carbonation temperature (the flue gas inlet temperature is set equal to the

carbonation temperature) will change average sorbent loading during the SARC cycle, with higher temperatures generally keeping the sorbent in a less carbonated state.

The combined heat and vacuum pump consumptions of the three sorbents at different carbonation temperatures are illustrated in *Figure* ***4-11***, showing a clear optimum for each sorbent. As could be anticipated from the preceding results, PEI-MOF exhibits better working adsorption capacity at temperatures 30 K higher than EB-PEI. From an efficiency point of view, this results in a lower heat pump power consumption (because of a higher T_H in *Equation* ***4-3)*** but a higher vacuum pump power consumption (because of a larger gas volume at higher temperatures). In this case, the negative effect on the vacuum pump consumption outweighs the positive effect on the heat pump consumption, making the total power consumption of PEI-MOF higher than EB-PEI.

The good performance of EB-PEI is surprising in this case because it has a substantially smaller

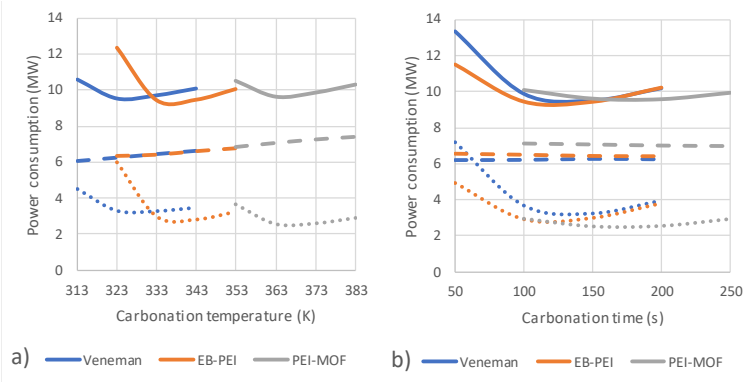

Figure ***4-11****: Heat pump (dotted lines) and vacuum pump (dashed lines) power consumptions for the three sorbents: a) the effect of carbonation temperature at a carbonation time of 150 s and b) the effect of carbonation time at the optimal carbonation temperature of each sorbent. The solid line indicates the combined heat and vacuum pump power consumption.*

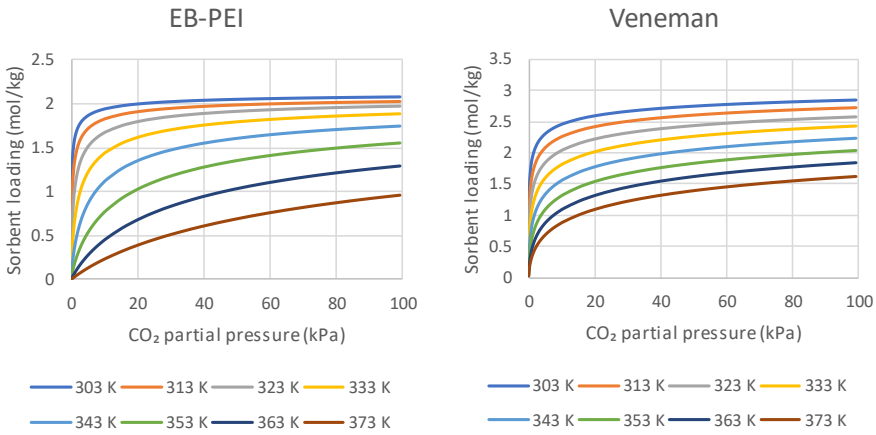

*Figure **4-12**: Comparison between the CO_2 adsorption isotherms of EB-PEI sorbent from the current study (Table **4-2**) and the sorbent presented by Veneman et al. [24].*

maximum CO_2 adsorption capacity than the other two sorbents. A higher CO_2 adsorption capacity is positive for SARC energy efficiency because it allows for more CO_2 to be adsorbed in each SARC cycle where the sorbent needs to be heated and cooled. The sensible heat transfer needed to heat and cool the sorbent therefore yields more CO_2. In this case, this effect is relatively small because of the small temperature swing (about 8 K) and the resulting high efficiency of the heat pump, thus reducing the importance of a high CO_2 adsorption capacity.

*Figure **4-11b*** shows the effect of carbonation time on each sorbent. Longer carbonation times will increase the amount of CO_2 adsorbed in each cycle, requiring a larger temperature swing, which will decrease the heat pump efficiency. On the other hand, the total amount of sensible heat required per unit of CO_2 captured in each cycle will reduce with longer carbonation times, countering the lower heat pump efficiency. Clearly, an optimum is also reached for each sorbent where the trade-off between these two conflicting effects is minimized.

As expected, PEI-MOF performs best at longer carbonation times where its higher adsorption capacity is well utilized. EB-PEI operates best at shorter carbonation times because its lower CO_2 adsorption capacity cannot facilitate much CO_2 uptake in each cycle. Even so, the optimal

power consumption with the EB-PEI sorbent remains lower than that of the PEI-MOF sorbent. This is due to the higher vacuum pump consumption required to extract the hotter gases from the PEI-MOF sorbent. If the PEI-MOF sorbent could operate optimally at a 30 K lower carbonation temperature like the EB-PEI sorbent, it would have had the lowest total power consumption. It should be noted, however, that the longer optimal cycle time of the PEI-MOF sorbent will be beneficial in reducing the frequency of switching of the reactor inlet and outlet valves as well as the valves directing the heat pump working fluid between the different reactors. This will increase valve lifetime and, if there is a significant time delay involved in switching, it can improve the overall process throughput rate.

Interestingly, the Veneman sorbent also operates best at relatively low carbonation times, despite having the highest CO_2 adsorption capacity of all the sorbents (~3 mol/kg). As shown in *Figure* ***4-12***, this is due to the Veneman sorbent having a distinctly different isotherm shape and a lower temperature sensitivity, making less of its high CO_2 adsorption capacity accessible via reasonable temperature and pressure swings. This distinction between absolute CO_2 adsorption capacity and practically accessible CO_2 adsorption capacity is important for judging the attractiveness of different CO_2 capture sorbents.

4.4 Summary and conclusion

This work has evaluated the performance of two new polyethyleneimine (EB-PEI and PEI-MOF) sorbents and two dry sorbents (K/ZrO_2 and Na/ZrO_2) for application in the SARC concept. Their performance was evaluated by performing bench scale experiments in a fluidized bed reactor, where the two PEI sorbents (EB-PEI and PEI-MOF) clearly showed the best performance under SARC operating conditions.

High resolution single-component isotherms for CO_2 and H_2O adsorption by both PEI sorbents showed that the PEI-MOF has a substantially higher CO_2 and H_2O adsorption capacity than

EB-PEI. In addition, the optimal operating temperature for PEI-MOF appears to be around 30 K higher than that of EB-PEI. This has important implications for the application of the sorbents in SARC concept. For example, EB-PEI operates best at a carbonation temperature around 333 K, which is a typical coal power plant flue gas exhaust temperature. Operating PEI-MOF at 363 K instead will reduce the amount of heat recovery from the flue gas stream, leading to some efficiency penalty. Higher temperature flue gases are common in some industrial processes where complete heat recovery is of lesser importance. Such processes, such as cement production, can be more suitable to PEI-MOF.

Breakthrough experiments showed no interaction effects of co-feeding CO_2 and H_2O, leading to the conclusion that the single-component isotherms can safely be used in reactor modelling studies using these sorbents. This result was confirmed via experiments conducted in a bench-scale reactor running the swing adsorption reactor cluster (SARC) cycle. The behaviour of this bench-scale reactor could be accurately predicted using the single component isotherms derived in this study, adding further confidence in reactor modelling studies based on easily derived single-component isotherms.

Finally, large scale reactor simulations using these two sorbents illustrated the effect of the difference in the isotherms on the energy efficiency of the SARC process. PEI-MOF, operating at a higher temperature, achieved lower heat pump power consumption, but also imposed a higher vacuum pump power consumption. Its higher adsorption capacity allowed for optimal operation at longer cycle times, which will reduce the wear on the valves in the SARC process. However, the substantially higher adsorption capacity of PEI-MOF did not result in an efficiency advantage relative to EB-PEI, mainly due to the higher vacuum pump power consumption.

The CO_2 adsorption isotherms of EB-PEI and PEI-MOF were qualitatively similar and were compared via simulation to a published PEI sorbent used in earlier SARC modelling works.

The CO_2 adsorption isotherm of this sorbent showed clear qualitative differences compared to the sorbents investigated in the present work, making a significant portion of its high CO_2 adsorption capacity inaccessible via practically achievable pressure and temperature swings.

In summary, significant differences were observed between two different PEI sorbents developed by different research groups. Generally, it is beneficial to maximize the sorbent working capacity, lower the optimal operating temperature and achieve a CO_2 adsorption isotherm that allows for high degrees of regeneration at practically achievable CO_2 partial pressures. None of the sorbents investigated in this study achieved all three of these criteria, leaving room for future optimization of PEI sorbents for CO_2 capture using the SARC concept.

5 Demonstration of the Novel Swing Adsorption Reactor Cluster (SARC) concept in a multistage fluidized bed for post combustion CO_2 capture

This chapter has been adapted from **Article IV**

Dhoke, C., et a., *Demonstration of the Novel Swing Adsorption Reactor Cluster Concept in a Multistage Fluidized Bed with Heat-Transfer Surfaces for Postcombustion CO_2 Capture,* Industrial engineering and chemistry research (2020)

Abstract

This paper reports the experimental demonstration of the novel swing adsorption reactor cluster (SARC) concept in a multistage fluidized bed reactor with inbuilt heat transfer surfaces for post-combustion CO_2 capture at a capacity up to 24 kg-CO_2/day. SARC employs combined temperature and vacuum swings (VTSA), driven by heat and vacuum pumps, to regenerate the solid sorbent after CO_2 capture. The lab-scale reactor utilized a vacuum pump and a heating oil loop (emulating the heat pump) to demonstrate 90% CO_2 capture from an N_2/CO_2 mixture approximating a coal power plant flue gas fed at 200 Nl/min. In addition, dedicated experiments demonstrated three important features required for the success of the SARC concept: 1) the polyethyleneimine sorbent employed imposes no kinetic limitations in CO_2 adsorption (referred to as carbonation) and only minor non-idealities in regeneration, 2) a high heat transfer coefficient in the range of 307-489 W/m^2 K is achieved on the heat transfer surfaces inside the reactor, and 3) perforated plate separators inserted along the height of the reactor can achieve the plug-flow characteristics required for high CO_2 capture efficiency. Finally, a sensitivity analysis revealed the expected improvements in CO_2 capture efficiency with increased pressure and temperature swings and shorter carbonation times, demonstrating predictable behaviour of the SARC reactor. This study provides a sound basis for further scale-up of the SARC concept.

Keywords: *adsorption; post-combustion CO_2 capture; polyethyleneimine sorbent; swing adsorption reactor cluster; experimental demonstration.*

5.1 Introduction

This study advances the state of the art by demonstrating the SARC concept at a scale of 24 kg-CO_2/day in a four-stage fluidized bed reactor constructed and designed with built-in heat transfer surfaces for heat addition and recovery. Special focus is placed on quantifying the efficiency of the stage separations in limiting axial mixing and the heat transfer coefficients that can be achieved in the reactor.

5.2 Methodology

5.2.1 Sorbent material

Previous screening studies [92, 140] identified a polyethyleneimine-based (EB-PEI) sorbent as a good candidate for use in this demonstration study. The sorbent was prepared from polyethyleneimine functionalized with 1,2-epoxybutane supported on commercial silica spheres [97] (properties are summarized in *Table **5-1***).

*Table **5-1**: Physical, chemical and thermochemical properties of the sorbent.*

Parameters	**Value**	**units**
Composition	EB-PEI (45 wt. %) + SiO_2 (55 wt.%)	(%)
BET surface area	42.09	(m^2/g)
Mean particle size	145	µm
Average pore diameter	383.1	(Å)
Adsorption enthalpy	1.47	(GJ/tonne CO_2)
Average heat capacity (40-120 °C)	1.5	(J/kg K)

5.2.2 Experimental procedures

Four experimental campaigns were completed using the EB-PEI sorbent in a lab scale reactor (*Figure **1-5)***, as summarized in *Table **5-2***. All the experiments were conducted with a synthetic flue gas by mixing 99.9% pure CO_2 and N_2 gases. The gas velocity of the synthetic flue gas was maintained at 0.19 m/s (18 times the minimum fluidization velocity) during carbonation to

establish the bubbling flow regime in all experiments. Heat was removed and added to the reactor by circulating oil at a flowrate of 88.6 - 105 LPM. A standardized startup procedure was developed to attain a steady-state temperature inside the reactor. This procedure was executed before starting any experiment, and it was ensured that the high-temperature oil circuit had reached the required temperature for heating the reactor close to the target carbonation temperature (60 °C). Then the low-temperature oil was circulated in the heat exchanger, and the sorbent was fluidized with 200 LPM of N_2 until a steady-state target temperature was attained.

*Table **5-2**: Process conditions for the four experimental campaigns. Carbonation in all experiments was completed at atmospheric pressure and 60 °C using 12.5% CO_2 in N_2.*

Set	**Objective**	**Separator**	**Carbonation time (mins)**	**Regeneration Pressure (mbar)**	**Regeneration temperature (°C)**
1	Kinetic limitation and heat transfer coefficient estimation	Without	30	100	80
2	Multistage effect	With and without	30	1000	120
3	SARC continuous operation	With	5	100	80
4	Sensitivity study	With	3-6	50-150	80-90

The first experimental campaign was designed to investigate whether the sorbent imposes significant reaction kinetic limitations and to estimate the heat transfer coefficient during the carbonation and regeneration steps at conditions relevant to the SARC concept. The experiments in this set were conducted by varying the weight of fresh sorbent at a constant total flowrate of 201 LPM to provide different residence times of the gas in the bed (τ = 2.6, 5.2, 7.6 sec). A long carbonation step was completed to achieve the maximum achievable adsorption capacity with 12.5% of CO_2 at 60 °C for all the cases, followed by regeneration. The regeneration was carried under VTSA (combined vacuum and temperature swing) mode by drawing the vacuum to 100 mbar and increasing the temperature to 80 °C. The gas composition

was sampled continuously at the reactor outlet to estimate the CO_2 loading on the sorbent using *Equation* ***5-1*** and *Equation* ***5-2***.

$$Q'_{Ad} = \frac{\int_{t=0}^{t=t_c}(\dot{N}_{CO_2}^{in} - \dot{N}_{CO_2}^{out})}{m_{sorb}} \qquad \textit{Equation } \textbf{5-1}$$

$$Q'_{De} = Q'_{Ad,end} - \frac{\int_{t=0}^{t=t_r} \dot{N}_{CO_2}^{out}}{m_{sorb}} \qquad \textit{Equation } \textbf{5-2}$$

Here, Q'_{Ad} and Q'_{De} are the sorbent CO_2 loadings (mol/kg) at times t_c and t_r (times of carbonation and regeneration, respectively). $\dot{N}_{CO_2}^{in}$ and $\dot{N}_{CO_2}^{out}$ are the CO_2 molar flowrates (mol/s) measured at the reactor inlet and outlet, respectively, while m_{sorb} is the mass of the sorbent in the reactor (kg).

The experimentally measured CO_2 loading on the sorbent was then compared to predictions from the Toth Isotherm model previously derived for this sorbent (*Equation* ***4-4*** to *Equation* ***4-7*** and *Table* ***5-3***) [92].

The temperature of the bed and the oil inlet and outlet temperatures from the respective reactor stages were also recorded continuously to estimate the heat transfer coefficients (h_i) for that stage during the carbonation and regeneration steps using *Equation* ***5-3***.

$$h_i = \frac{\dot{m}_{oil} \times C_{p,oil} \times \left(T_{oil}^{out} - T_{oil}^{in}\right)}{A \times \left(T_{bed} - \left(\frac{T_{oil}^{out} + T_{oil}^{in}}{2}\right)\right)} \qquad \textit{Equation } \textbf{5-3}$$

Here, $\dot{m}_{oil}$ is the mass flow rate of oil (kg/s), $C_{p,oil}$ is the oil specific heat capacity $\left(\frac{J}{kg\ K}\right)$, T_{oil}^{in} and T_{oil}^{out} are the oil inlet and outlet temperatures (°C), T_{bed} is the bed temperature (°C), and A is the heat transfer area (m^2).

The average heat transfer coefficient (H_i) inside the reactor was estimated from the heat transfer coefficient and heat transfer rate in each stage using *Equation* ***5-4***.

$$H_i = \frac{\sum(h_i \times q_i)}{\sum q_i}$$ *Equation **5-4***

Here, h_i is the instantaneous heat transfer coefficient calculated from *Equation **5-3*** for i^{th}stage (W/m^2K), q_i is the heat transfer rate for the i^{th}stage (W).

The second experimental campaign was designed to investigate the degree to which the separator can provide the required multistage effect in a fluidized bed reactor. In this set of experiments, the tests were carried out using 11.5 kg of fresh sorbent in the reactor. For comparison, the experiments were conducted with and without separators at the same process conditions. The carbonation step was maintained for 30 minutes to reach the maximum achievable CO_2 loading on the sorbent with 12.5% CO_2 in N_2 at 60 °C, followed by complete regeneration by heating the bed to 120 °C while fluidizing with N_2 at a flowrate of 150 LPM for 60 minutes. It is worth noting that the complete regeneration step is not a part of real SARC operation, and it was only used to investigate the multistage effect in this experimental campaign. The gas composition was sampled continuously at the reactor outlet. Each experiment was repeated three times to have confidence in the experimental data.

The third experimental campaign was performed to demonstrate the SARC process over 6 consecutive cycles under the VTSA regeneration mode, using 11.5 kg of sorbent. In the carbonation step, the sorbent was exposed to 12.5% CO_2 in N_2 at 60 °C and 1000 mbar, while the pressure was reduced to 100 mbar in the evacuation step, still maintaining a constant temperature of 60 °C. Subsequently, the sorbent was heated to 80 °C while maintaining the vacuum of 100 mbar for the combined vacuum-temperature swing in the regeneration step. Finally, the sorbent was cooled back to 60 °C while repressurizing the reactor to 1000 mbar at a smaller gas feed with the same composition used in the carbonation (12.5% CO_2). The gas composition was analyzed continuously, and the corresponding CO_2 capture efficiency was

estimated for each cycle from *Equation* ***5-5*** (averaged over the entire carbonation duration). The instantaneous heat transfer coefficient was calculated for these continuous cycles using *Equation* ***5-3*** for each stage, and then the average heat transfer coefficient was estimated using *Equation* ***5-4***.

The final experimental campaign was a sensitivity study designed to investigate the effect of different process parameters such as regeneration pressure, regeneration temperature and carbonation time (the duration of the carbonation step in the SARC cycle shown in *Figure* ***1-3***) on the CO_2 capture efficiency. The carbonation step was completed with 12.5% CO_2 in N_2 at 60 °C, followed by partial regeneration. The regeneration pressure, regeneration temperature and carbonation time were varied in this study, as indicated in *Table* ***5-2***. Each experiment was repeated four times to quantify the experimental measurement uncertainty. The gas composition was sampled continuously at the reactor outlet and the CO_2 capture efficiency $\left(\eta_{CO_2}\right)$ was calculated using *Equation* ***5-5***.

$$\eta_{CO_2} = \frac{\int_{t=0}^{t=t_c}\left(\dot{N}_{CO_2}^{in} - \dot{N}_{CO_2}^{out}\right)}{\int_{t=0}^{t=t_c}\dot{N}_{CO_2}^{in}} \times 100\% \qquad \textit{Equation } \textbf{5-5}$$

The experimental results are presented and discussed in four parts. The first part details the investigation of the kinetic limitation and heat transfer coefficient in the carbonation and regeneration steps, while the second part focuses on the effect of adding separators between the reactor stages on the axial temperature profile and CO_2 breakthrough. The third part presents the demonstration of the continuous SARC operation over several consecutive cycles, designed to achieve 90% CO_2 capture, while the final part reports results from the sensitivity study.

5.3 Results and discussion

5.3.1 Kinetic limitations and heat transfer coefficient

The results from the kinetic experiments for two different gas residence times (τ = 2.6 s, 5.2 s and 7.6 s) for carbonation and regeneration are presented in *Figure **5-1***. The CO_2 breakthrough curves during these runs are presented in *Figure **5-2***. The CO_2 loading on the sorbent during carbonation and regeneration calculated from *Equation **5-1*** and *Equation **5-2*** is plotted as Q'. For comparison, the equilibrium CO_2 loading on the sorbent during carbonation and regeneration was also estimated from the Isotherm model (*Equation **4-4*** to *Equation **4-7*** and *Table **4-2***) and is presented as Q*.

During carbonation, the CO_2 loading on the sorbent increases with the carbonation time and reaches the maximum achievable loading for 12.5% CO_2 at 60 °C and 1000 mbar. It can also be seen from *Figure **5-1*** that the actual CO_2 loading on the sorbent (Q') is close to the theoretical equilibrium CO_2 loading estimated from the Isotherm, Q*, using the transient pressure and temperature information measured in the reactor, even at the lowest gas residence time (2.6 sec). This match is particularly close during carbonation, indicating that the EB-PEI sorbent attains quickly reaches equilibrium without facing kinetic limitations. This is a favorable feature of the sorbent that can facilitate smaller reactors resulting in lower CAPEX and smaller pressure drops.

As for the regeneration step, CO_2 releases from the sorbent, as evident from the decrease in CO_2 loading over time, following the decrease in pressure and increase in temperature. However, as the pressure plays a large role in the sorbent regeneration, the theoretical prediction from the isotherm is presented for the two different pressure readings at the top and the bottom of the reactor, accounting for the reactor pressure drop, to be compared to the experimental sorbent loading estimated from the CO_2 measured at the reactor outlet. The pressure sensor at

the bottom shows a higher reading than the one at the top, which is a direct result of the hydrostatic pressure gradient in the fluidized bed. Consequently, the measured overall CO_2 loading fell between these two isotherm predictions. In the case with the shortest bed (τ = 2.6 s), where the pressure drop is small, the match between the experimental results and the ideal theoretical performance estimated for both pressure readings is almost exact. As the bed height increases (larger gas residence time), the pressure drop along the bed increases, thus increasing

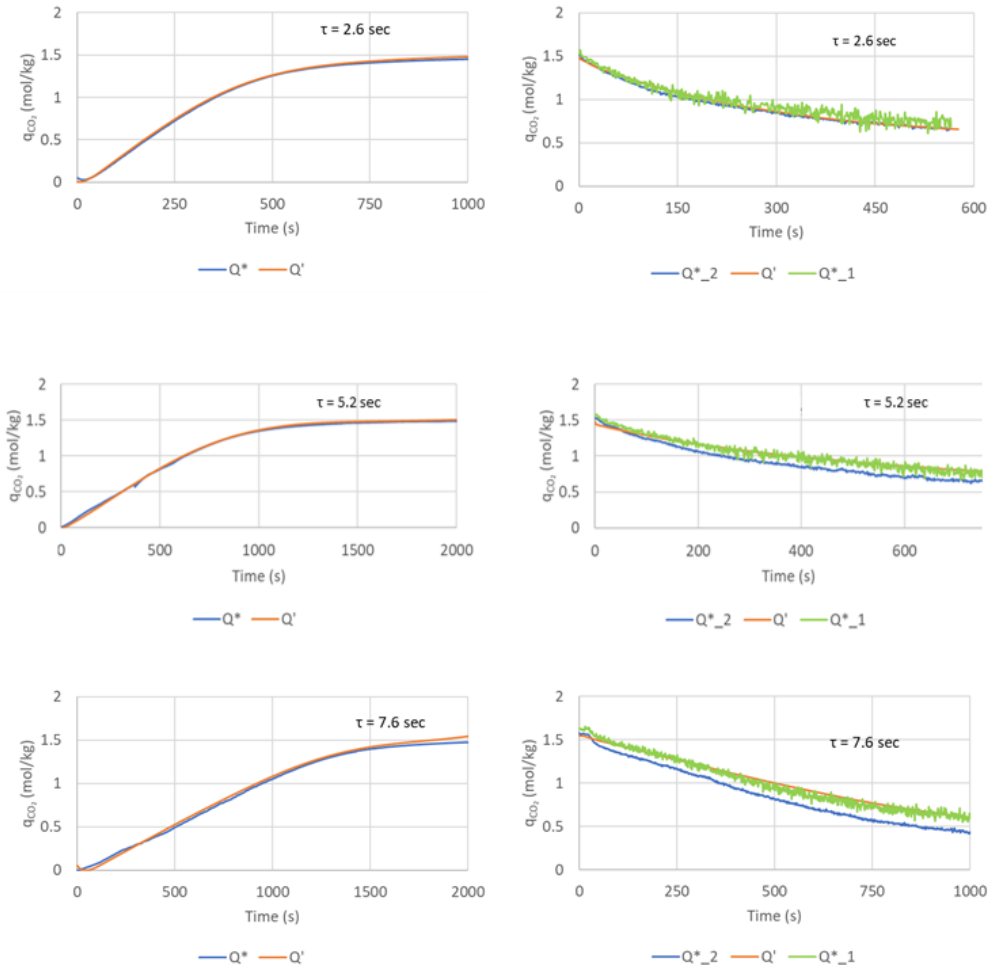

*Figure **5-1**: CO_2 loading on the sorbent during carbonation (left) and regeneration (right) for different contact times; Q*- equilibrium CO_2 loading on the sorbent, Q'- actual CO_2 loading on the sorbent; 1 and 2 – Q* estimated using the bottom and top pressure sensors.*

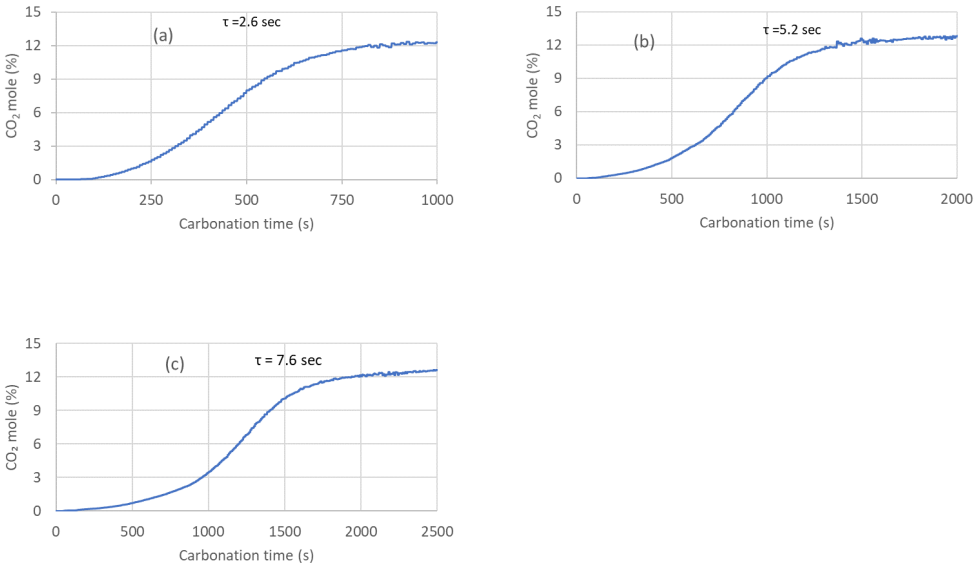

*Figure **5-2**:The CO_2 concentration measured at the outlet of the reactor during the carbonation step for three contact times.*

the gap between the two isotherm predictions. The experimental measurement closely follows the isotherm prediction based on the pressure reading at the bottom. This can be clearly seen in *Figure **5-1*** for $\tau = 5.2$ s and $\tau = 7.6$ s.

To conclude, this experimental campaign confirms that both the carbonation and regeneration steps respond according to the equilibrium predictions from the previously measured isotherm for the EB-PEI sorbent with no kinetic limitation. This implies that greater reactor productivity is possible by reducing the gas-solid contact time via higher gas feed rates or a shorter reactor. Further studies are needed to quantify how much the reactor can be intensified before significant reaction rate limitations are observed.

The heat transfer coefficient was calculated from *Equation **5-3*** for these experimental runs (a short bed) as 487 W/m^2K and 489 W/m^2 K, respectively, for the carbonation and regeneration steps (*Figure **5-3***). These values are quite high and indicate good fluidization during both steps.

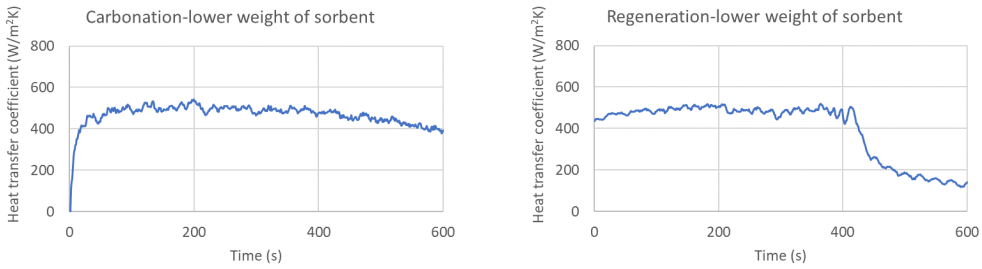

*Figure **5-3**: Heat transfer coefficient calculated during carbonation (left) and regeneration (right) with a low sorbent weight (0.42 m bed height) and without the perforated plates during the kinetics limitation experiments.*

The result suggests that the previously simulated heat transfer coefficient of 300 W/m^{2}K, employed in the SARC reactor modelling, was conservatively low [1]. Thus, the result of this experimental demonstration will have a positive impact on the techno economics and the scale-up of the SARC technology if such high heat transfer coefficients can be maintained in larger-scale systems.

5.3.2 The effect of multistage operation

Perforated plate separators were placed above each heat exchanger to create a four-stage fluidized bed reactor (see the scheme in *Figure **1-5**).* Experiments were then completed with and without those separators for comparative purposes. The carbonation transient temperature profile along the reactor length with and without perforated plate separators between the stages is presented in *Figure **5-4a*** and *Figure **5-4b***, respectively. As soon as the CO_2 is fed to the reactor, the sorbent temperature starts increasing because of the exothermic carbonation reaction. This temperature increase was observed in both cases, but there was a distinct difference in the respective axial temperature profiles. For the case with separators, a maximum temperature rise of 8 °C was observed. This rise of temperature was noticed first in stage 1 before moving upwards to stages 2, 3 and 4. This indicates that the CO_2 initially reacts in the first stage,

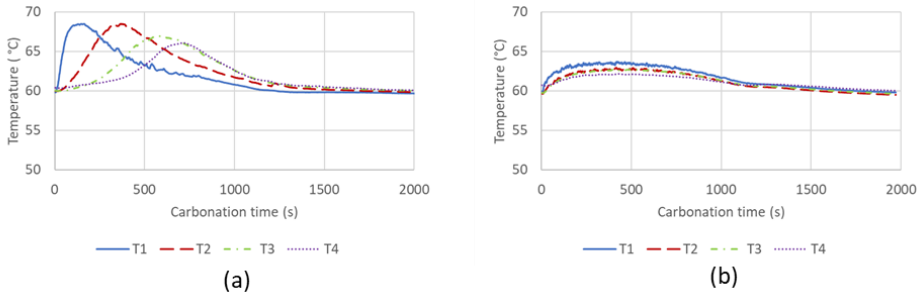

*Figure **5-4**: Transient temperature profiles measured during the carbonation step in the fluidized bed reactor at stages T1-T4, (a) with separators-Left, (b) without separators-Right.*

followed by the second, third and fourth stages, proving that the desired plug-flow behaviour is successfully achieved by inserting the perforated plate separators into the reactor.

In the case without separators, the temperature rise along the axial direction was uniform, indicating a high degree of axial mixing in the reactor. This profile was similar to the conventional fluidized bed, behaving like a continuously stirred tank reactor. The high degree of axial mixing restricts the maximum temperature rise to only 4 °C in this case. The CO_2 molar concentrations measured at the reactor outlet for these two cases (with and without separators) are presented in *Figure **5-5***. As expected, the CO_2 concentration increases asymptotically to the feed concentration (12.5%) as the equilibrium sorbent CO_2 loading is approached. The beneficial effect of the multistage reactor design is clearly visible in *Figure **5-5***

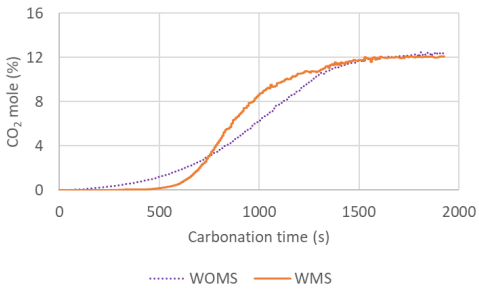

*Figure **5-5**: The CO_2 breakthrough curve in the fluidized bed with separators (WMS) and without separators (WOMS).*

in the form of a delayed CO_2 breakthrough. Significant CO_2 concentrations were measured at the outlet after 5 minutes in the case with separators (WMS) as opposed to only 1 minute for the case without separators (WOMS). The suppression of axial mixing by the separators ensures that the upper reactor regions retain colder sorbent in a highly regenerated state, facilitating a high CO_2 capture rate. This result proves that a multistage fluidized bed with perforated plate separators can achieve the plug-flow characteristics of a fixed bed with the good heat transfer characteristics of a fluidized bed, making it ideally suited to the SARC concept.

5.3.3 SARC continuous operation

In this section, the continuous operation of the multistage fluidized bed SARC concept (with separators) is presented for 5 consecutive SARC cycles. The transient reactor pressure, sorbent temperature in each stage (T1-T4) and the CO_2 mole % for 5 SARC cycles are presented in *Figure* ***5-6***. As shown, the SARC cycle was repeatable, demonstrating the easy control of the process throughout the cycle. The carbonation temperature was maintained close to 60 °C by recovering the heat released from the exothermic carbonation reaction under atmospheric

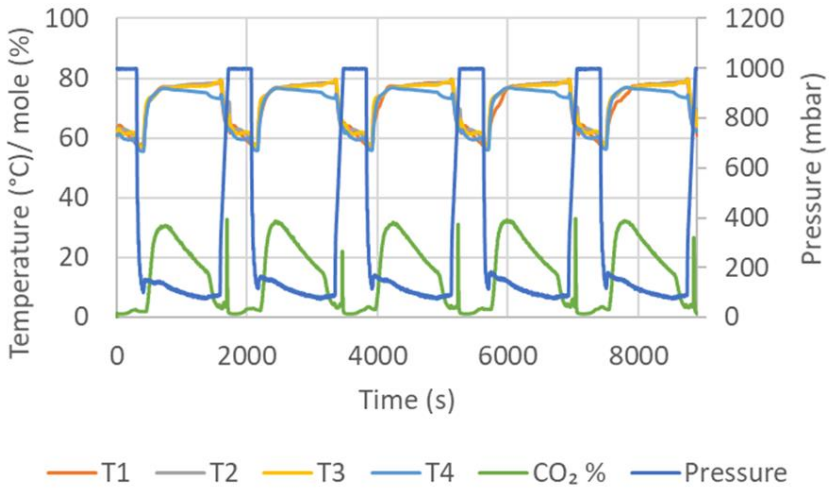

Figure ***5-6****: Process parameters and CO_2 mole % for SARC cycles (continuous operation of 5 SARC cycles).*

pressure. The pressure was later reduced during the evacuation step, followed by a regeneration step where a strong vacuum of 100 mbar was applied, and the temperature was increased to 80 °C. The carbonation time was set to capture 90% of the CO_2 across the step (5 minutes), while the regeneration time was set to the time required to reach equilibrium desorption conditions (28 minutes). For better visibility of the process behaviour throughout the SARC cycle, the transient reactor pressure and the sorbent temperature in each stage (T1-T4) for one SARC cycle consisting of four steps are presented in *Figure* ***5-7***, and the corresponding CO_2 mole % measured at the reactor outlet is presented in *Figure* ***5-8***.

In continuous operation, the sorbent cannot be completely regenerated by the partial vacuum and mild temperature swings required for high heat pump efficiency. Thus, each carbonation step starts with an already partially carbonated sorbent. For this reason, the amount of carbonation taking place is lower and the temperature wave moving along the length of reactor is less pronounced in *Figure* ***5-7*** than in *Figure* ***5-4a***.

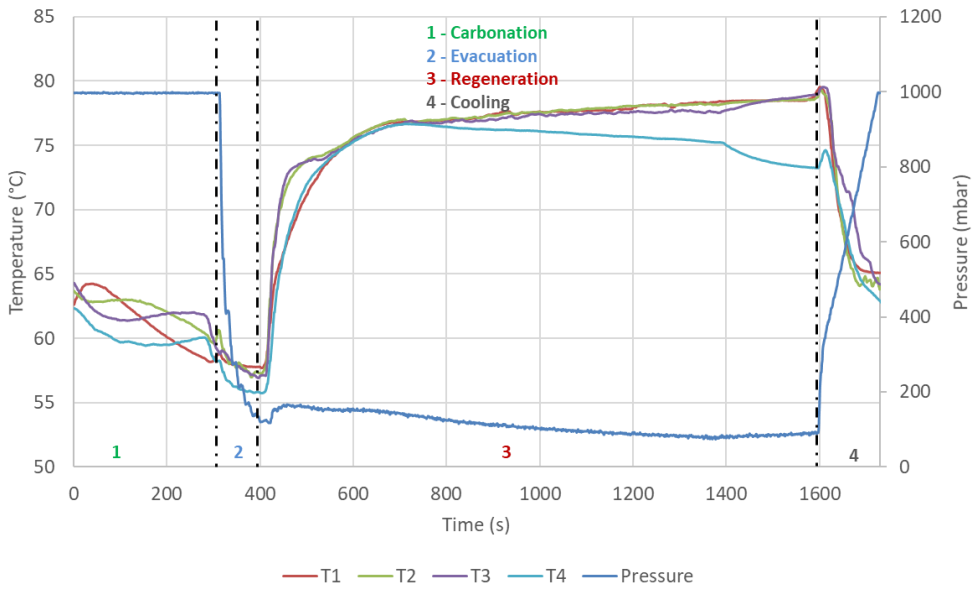

Figure ***5-7****: Process parameters for one SARC cycle.*

During the first part of the regeneration step, a large amount of CO_2 release leads to a slight increase in pressure. The increase in pressure is due to the resistance imposed by the filter placed at the outlet of the reactor before the vacuum pump. This resistance and limitation make the regeneration step longer than it should be given the high pressure-sensitivity of the reaction equilibrium in this pressure range. However, in a large-scale reactor, this problem can be addressed by employing an optimized fines removal system with a small pressure drop, shortening the regeneration step, and reducing the number of reactors in the cluster. In addition, minimizing the pressure drop between the reactor and the vacuum pump is important to minimize the vacuum pump power consumption and cost in large-scale SARC systems.

The mole % of CO_2 measured at the reactor outlet increases from 1.1% to 2.6% during the carbonation step. In this case, some slippage of CO_2 at the start of the carbonation step occurs because the sorbent was only partially regenerated by the vacuum and temperature swings. Despite this slippage, the carbonation time was designed to achieve 90% CO_2 capture efficiency, as mentioned earlier. In the regeneration step, the CO_2 mole % increases initially and then starts to decrease. The CO_2 stream exiting the reactor during regeneration is close to 100% purity, but it was diluted with a constant feed stream of N_2 after the reactor to enable the quantification of the CO_2 flowrate. This CO_2 flowrate was also quantified using the mass flow meter (MFC-03 shown in *Figure **1-5***) during the regeneration step. The slippage of CO_2 (indicated by the sharp peak) in all cycles just after the cooling step (*Figure **5-6***) is caused by the CO_2 remaining in the freeboard space above the sorbent bed in the reactor during the regeneration. Once the reactor is repressurized in the cooling step, this CO_2 exits the reactor as soon as the outlet valve (V-02 in *Figure **1-5**)* is opened, reducing the CO_2 capture efficiency by 0.8-1%. In a large-scale SARC system, this loss will be proportional to the regeneration pressure and the freeboard size, with stronger vacuums and smaller freeboards leaving less CO_2 in the freeboard after regeneration. This loss could be further reduced by an order of magnitude

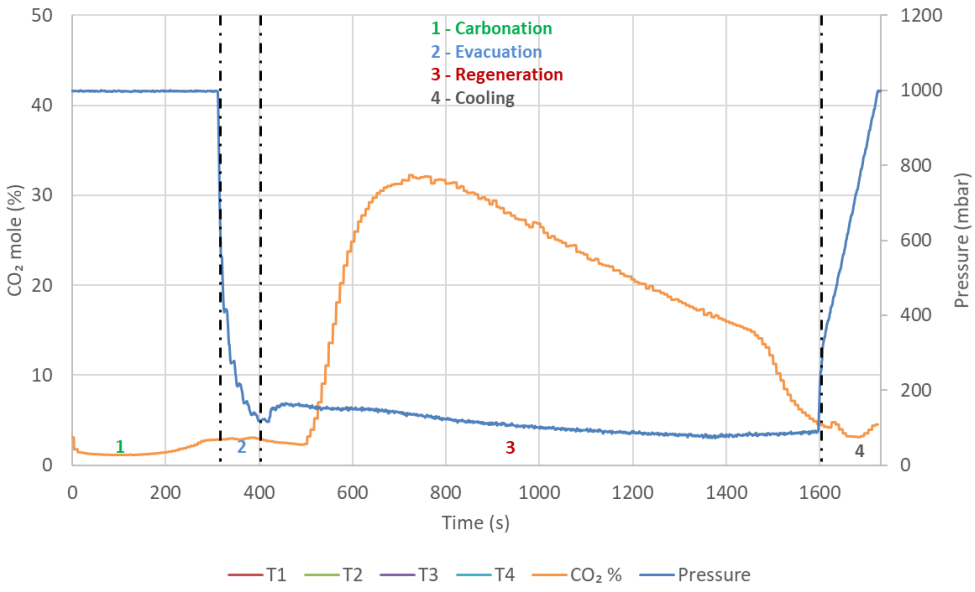

*Figure **5-8**: Transient CO_2 mole % for one SARC cycle (the transient pressure behaviour is also shown for visualizing the steps of the cycle).*

by feeding this peak from the cooling step back into the main flue gas line being fed to the carbonation step.

The average heat transfer coefficient was calculated from *Equation **5-4*** as 487 and 307 W/m^2 K during the carbonation and regeneration steps, respectively. The average heat transfer coefficient during the carbonation step for these continuous cycles was the same as in the kinetic limitation study discussed earlier. However, the heat transfer coefficient calculated in the regeneration step was lower (307 W/m^2 K) than observed in the kinetic limitation study (489 W/m^2 K).

It was interesting to observe the variation of the heat transfer coefficient along the height of the reactor (*Table **5-4***). Low values were obtained in the lowest stage, but the upper stages approached the heat transfer performance of the carbonation step. This suggests that the amount of gas released at the bottom is rather small, resulting in poor fluidization (or a stagnant region),

*Table **5-4**:Heat transfer coefficients and heat transfer rates from each stage calculated in the demonstration experiments with perforated plates and a higher sorbent weight (0.82 m bed height).*

	Heat transfer coefficient (W/m^2 K)		**Heat transfer rate (W)**		**Remark**
	Carbonation	**Regeneration**	**Carbonation**	**Regeneration**	
Stage 1 - First thermocouple	514	122	1413	816	Bottom of the reactor
Stage 1 - second thermocouple	566	167	1621	860	
Stage 2	458	455	1451	1524	
Stage 3	483	420	1300	1253	
Stage 4	309	186	671	770	Top of the reactor

but it increases along the height of the bed (the upper stages see the cumulative CO_2 flux released in all lower stages), leading to full fluidization of the solids (*Table **5-4***).

The greater bed height causes the bottom parts of the bed to see higher pressures than the set vacuum values (due to the pressure drop created by the weight of the sorbent), thus further reducing the quantity of released CO_2 relative to the case for the short bed heights (the results shown in *Figure **5-3**).* This self-strengthening negative effect is further enhanced by the low heat transfer coefficient at the bottom that results from the poor fluidization, limiting the rate at which the sorbent can be heated up to drive off CO_2 to cause fluidization. Thus, it is recommended to recycle part of the captured CO_2 (as proposed in previous techno-economic assessments [1]) into the regeneration step to overcome this issue and prevent defluidization in the lowest reactor regions when taller beds are used.

5.3.4 Sensitivity study

The results of the study on the sensitivity of the CO_2 capture efficiency to different regeneration pressures and temperatures are presented in *Figure **5-9*** and *Figure **5-10***, respectively. *Figure **5-9*** confirms the expected trend that higher regeneration pressures result in lower CO_2 capture

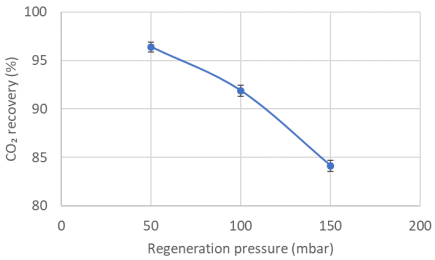

*Figure **5-9**: The effect of regeneration pressure on CO_2 capture efficiency; Carbonation time = 3 mins and regeneration temperature = 80 °C.*

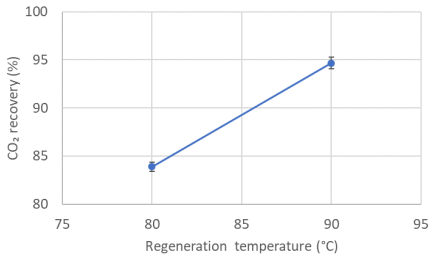

*Figure **5-10**: The effect of regeneration temperature on CO_2 capture efficiency; Regeneration pressure = 150 mbar and carbonation time = 3 mins.*

efficiencies. A larger pressure swing (lower regeneration pressure) allows for more sorbent regeneration, facilitating more CO_2 capture in the subsequent carbonation step. In this case, the CO_2 capture efficiency increased from 84% at 150 mbar to 97% at 50 mbar. However, it should be noted that reaching such a low vacuum (50 mbar) could be challenging in large industrial applications because of sealing and economics.

Another option to improve the capture efficiency is by completing the regeneration step at higher temperatures. This larger temperature swing will have the same positive effect on sorbent regeneration as the larger pressure swing discussed earlier. As seen from *Figure **5-10***, the CO_2 capture efficiency can be improved from 84 % to 95 % by increasing the regeneration temperature from 80 °C to 90 °C at 150 mbar. This improvement in the CO_2 capture efficiency will reduce the heat pump efficiency, thus increasing the electricity consumption of the plant.

The CO_2 capture efficiency at different carbonation times (duration of the carbonation step in the SARC cycle) for constant regeneration conditions is presented in *Figure **5-11***. It can be seen that the CO_2 capture efficiency increases with a decrease in the carbonation time. For example, the 90% CO_2 capture achieved with 5 minutes carbonation time in the previous section can be increased to 92 % for 3 minutes carbonation time. The increase in the CO_2 capture efficiency is the result of less CO_2 slippage taking place in the latter part of the carbonation step when the

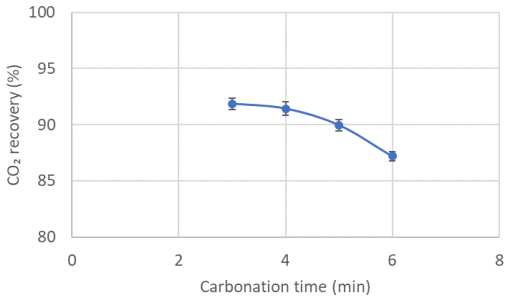

*Figure **5-11**: The effect of carbonation time on CO_2 capture efficiency; Regeneration temperature = 80 °C and regeneration pressure = 100 mbar.*

sorbent becomes more carbonated and the equilibrium CO_2 concentration increases. However, the trade-off for this improvement in CO_2 capture efficiency will be a larger heat pump power consumption to transfer the sensible heat needed to heat and cool the sorbent in each temperature swing. Shorter cycles imply that a smaller quantity of CO_2 is captured with each temperature swing, increasing the heat pump work required per unit of CO_2 captured.

Finally, the error bars in *Figure **5-9*** - *Figure **5-11*** indicate good repeatability between the three SARC cycles completed for each experiment. It should also be mentioned that the employed sorbent produced fines at a rate of about 0.09 %/hour across the experimental campaign, which is too high for commercial viability. Thus, further work on sorbent mechanical strength is recommended.

5.4 Summary and conclusion

This study presents the experimental demonstration of the novel swing adsorption reactor cluster (SARC) concept in a multistage fluidized bed reactor with inbuilt heat transfer surfaces to emulate the functionality of the heat pump. Although the SARC principle was proven in a 2 cm tube reactor in previous work, this study demonstrated the concept at a 100x larger scale in a reactor that includes all the functional elements required for large-scale operation. The study

with EB-PEI sorbent shows the 90% CO_2 capture is feasible with the hybrid regeneration mode (combined vacuum and temperature swing) in this system.

Experimental results indicate that no kinetic limitations are present during carbonation as the reactor achieved equilibrium performance even at a low gas residence time of 2.6 s. Some mild deviations from equilibrium were observed for regeneration in taller beds, although this non-ideality was relatively small. This result validates the equilibrium assumption employed in previous SARC reactor modelling studies [1, 90]. The heat transfer coefficient was measured during the experiments as 487 W/m^2K and 489 W/m^2K for the carbonation and regeneration step, respectively, which is considerably higher than the 300 W/m^2K used in the aforementioned modelling works.

The experimental campaign also demonstrated the ability of perforated plate separators to limit axial mixing of the sorbent and approximate the reaction characteristics of a packed bed. This behaviour involves reaction and temperature waves traveling through the reactor instead of the uniform conversion of all sorbent particles observed in a well-mixed fluidized bed. In equilibrium-limited adsorption applications, this behaviour prevents the early breakthrough of CO_2, thus facilitating a higher sorbent working capacity. Combined with the heat transfer measurements, this experiment shows that simple perforated plates can achieve the CO_2 capture benefits of packed beds while preserving the excellent heat transfer characteristics of fluidized beds.

Finally, a sensitivity study indicated the expected improvements of CO_2 capture efficiency with larger pressure and temperature swings and shorter carbonation times. This further confirmed the predictable operation of the SARC reactor concept and provides a sound basis for further scale-up of this promising post-combustion CO_2 capture technology.

6 Study of the cost reductions achievable from the SARC concept using a validated reactor model

This chapter has been adapted from **Article V**

Dhoke, C., et a., *Study of the cost reductions achievable from the novel SARC CO_2 capture concept using a validated reactor model* (Submitted to Journal of cleaner production)

Abstract

New process concepts, such as the swing adsorption reactor cluster (SARC) CO_2 capture process, are often techno-economically investigated using idealized modelling assumptions. This study quantifies the impact of this practice by updating a previous economic assessment with results from an improved reactor model validated against recently completed SARC lab-scale demonstration experiments. The experimental comparison showed that the assumption of chemical equilibrium was valid, that the previously employed heat transfer coefficient was conservatively low, and that the required reduction of axial mixing could be easily achieved using simple perforated plates in the reactor. However, the assumption of insignificant effects of the hydrostatic pressure gradient need to be revised. In the economic assessment, the negative effect of the hydrostatic pressure gradient was almost cancelled out by deploying the experimentally observed heat transfer coefficients, resulting in a small net increase in CO_2 avoidance costs of 2.8-4.8% relative to the unvalidated model. Further reductions in axial mixing via more perforated plates only brought minor benefits, but a shorter reactor enabled by the fast experimentally observed adsorption kinetics had a larger positive effect: halving the reactor height reduced CO_2 avoidance costs by 13.3%. A new heat integration scheme feeding vacuum pressure steam raised from several low-grade heat sources to the SARC desorption step resulted in similar gains. When all improvements were combined, the optimal CO_2 avoidance cost was 23.7% below the best result from prior works. The main uncertainty that needs to be overcome to realize the great economic potential of the SARC concept is long-term sorbent stability: mechanical stability must be improved substantially and long-term chemical stability under real flue gas conditions must be demonstrated.

Keywords: *CO_2 capture from cement; polyethyleneimine sorbent; swing adsorption fluidized bed reactor cluster; reactor model validation; Techno-economic assessment.*

6.1 Introduction

This study quantifies the impact of the assumptions made in the previous economic assessment using results from an improved reactor model validated against recently completed SARC lab-scale demonstration experiments. Additionally, it evaluates the potential of new heat integration scheme in bringing down CO_2 avoidance costs.

6.2 Methodology

6.2.1 Experimental procedure

The experimental campaign comprised of breakthrough experiments and full SARC cycles using a polyethyleneimine based (EB-PEI) sorbent to capture around 90% of CO_2 in lab scale fluidized bed reactor (*Figure **1-5***.). Adsorption in the breakthrough experiment was carried out with a fully regenerated sorbent while in the SARC cycle it started with a partially regenerated sorbent. In both the experiments, adsorption was completed at 60 °C with 12.5% of CO_2 in N_2 and atmospheric pressure. The heat transfer coefficient from each stage (h_i) was measured for all 4 steps of the SARC concept using *Equation **6-1***.

$$h_i = \frac{\dot{m}_{oil} \times c_{p,oil} \times \left(T_{oil}^{out} - T_{oil}^{in}\right)}{A \times \left(T_{bed} - \left(\frac{T_{oil}^{out} + T_{oil}^{in}}{2}\right)\right)} \qquad \textit{Equation } \textbf{6-1}$$

Here, $\dot{m}_{oil}$ is the mass flow rate of oil (kg/s), $C_{p,oil}$ is the oil specific heat capacity $\left(\frac{J}{kg\,K}\right)$, T_{oil}^{in} and T_{oil}^{out} are the oil inlet and outlet temperatures (°C), T_{bed} is the bed temperature (°C), and A is the heat transfer area (m^2).

The average heat transfer coefficient (H_i) in the different reactor steps (e.g., adsorption or desorption) was then estimated from the instantaneous heat transfer coefficient and the heat transfer rate in each stage using *Equation **6-2***.

$$H_i = \frac{\sum(h_i \times q_i)}{\sum q_i}$$ *Equation* ***6-2***

Here, h_i is the instantaneous heat transfer coefficient calculated from *Equation* ***6-1*** for i^{th} stage (W/m^2K), q_i is the heat transfer rate for the i^{th} stage (W).

More details about the experimental procedure and campaign can be found in the previous publication [69]. The results from these two studies were used to validate the reactor model as described below.

6.2.2 Reactor modelling

The multistage SARC reactor is simulated as a series of continuous stirred tank reactors (CSTRs) using an in-house Matlab code first introduced by Zaabout et al. [1] and subsequently deployed in several follow-up studies [41, 90, 141]. Transient mass and energy balances are solved for each CSTR in series, assuming that thermal and chemical equilibrium is reached in each CSTR. Gas travels from one CSTR to the next, whereas the solids phase remains fixed in each CSTR. Regarding chemical equilibrium, CO_2 and H_2O isotherms for the PEI sorbent were derived in a previous work [140].

In the present study, this CSTR-in-series model will be used for two purposes: 1) validation against the experimental results from the lab-scale SARC unit and 2) large-scale simulations to quantify the change in the energy penalty and CO_2 avoidance cost when implementing the learnings from the validation exercise in the large-scale SARC simulations.

The most important modification to the model made for the present work was the inclusion of the previously neglected hydrostatic pressure gradient in the bed. This will increase the pressure in the lower reactor stages, increasing CO_2 adsorption and inhibiting CO_2 desorption. Due to the shape of the CO_2 adsorption isotherm, the negative effect during desorption will outweigh the positive effect during adsorption, increasing the energy penalty of the SARC concept.

Furthermore, the description of heat transfer differs significantly between the reactor simulations for validation and for large-scale process modelling. In the large-scale cases, heat transfer is modelled as in our previous studies, assuming a heat pump with a working fluid condensing and evaporating at specified constant temperatures when heating and cooling the reactor. Here, *Equation* ***6-3*** shows that the heat transfer is driven by a constant heat transfer coefficient (h), a heat transfer surface area (A), and a varying temperature difference between the condensing or evaporating heat pump working fluid $\left(T_{wf}\right)$ and the bed in each stage of the reactor (T_{bed}).

In the validation cases, however, the heat transfer was carried out using heating oil without phase change. Hence, the oil outlet temperature changed relative to the inlet temperature, depending on the rate of heat transfer, changing the average working fluid temperature. In this case, *Equation* ***6-3*** was modified on the assumption that the working fluid temperature is the average between the inlet and outlet temperatures. *Equation* ***6-4*** shows the resulting equation, accounting for the finite flowrate of the heating oil $(\dot{m}_{oil})$. It is clear that, if the heating oil flowrate approaches infinity, the denominator approaches unity and *Equation* ***6-4*** becomes identical to *Equation* ***6-3*** because the heating oil outlet temperature would be equal to the inlet temperature $\left(T_{oil}^{in}\right)$. However, for a finite heating oil flowrate, the heat transfer rate will reduce because the average heating oil temperature will be closer to the reactor temperature. If the heating oil flowrate approaches zero, so does the heat transfer rate.

$$q_{large} = hA\left(T_{wf} - T_{bed}\right) \qquad \textit{Equation } \textbf{6-3}$$

$$q_{lab} = \frac{hA\left(T_{oil}^{in} - T_{bed}\right)}{1 + \frac{hA}{2\dot{m}_{oil}c_{p,oil}}} \qquad \textit{Equation } \textbf{6-4}$$

The heat transfer coefficient was assumed constant for all reactor stages in all SARC steps for the large-scale simulations. However, dedicated heat transfer coefficients were derived for

different stages and steps to maximize accuracy in the lab-scale simulations. These heat transfer coefficients are specified in the results and discussion section.

6.2.3 Process modelling

For the large-scale process modelling, the reactor model was run to achieve 90% CO_2 capture and 96% CO_2 purity using 2000 m^2 of heat transfer surface area per reactor and 0.1 bar desorption pressure. These conditions are identical to Case 1 in Cloete, et al. [41], which proved to be the most economical case investigated for CO_2 capture from a cement plant.

The reactor model provided the flowrates and compositions of the streams exiting each step in the SARC cycle, the total heat transfer rate through the heat pump, the heat pump evaporation and condensation temperatures, and the evacuation pump pressure. This information was then used in the process model modelled in Aspen plus to calculate the power consumption of the heat pump and the two vacuum pumps (large pump for desorption and small pump for evacuation). The assumptions made in the process modelling are presented in *Table* **6-1**.

Two different process schemes for SARC integration with cement plant were evaluated in this study. The standard scheme introduced first by Cloete et.al [90] for SARC integration to a cement plant is presented in *Figure* ***6-1***. As seen in the *Figure* ***6-1***, the flue gas from the cement plant (stream 1) is fed to the adsorption reactor of SARC process via CO_2 blower. The CO_2 lean flue gas (stream 3) from the adsorption reactor is mixed with the stream from the evcuation reactor and is then sent to the stack. The sorbent regeneration is carried out in a desorption reactor with the help of a heat and vacuum pump. During regeneration, the CO_2 (stream 5) is extracted by the vacuum pump in three intercooled stages and then compressed for storage purpose (stream 7). A small fraction of the extracted CO_2 stream (stream 6) is recycled to ensure good fluidization in the regeneration step. In this study, ammonia is used as a working fluid of the Heat pump, that transfers the heat generated in the adsorption reactor to the regenerator

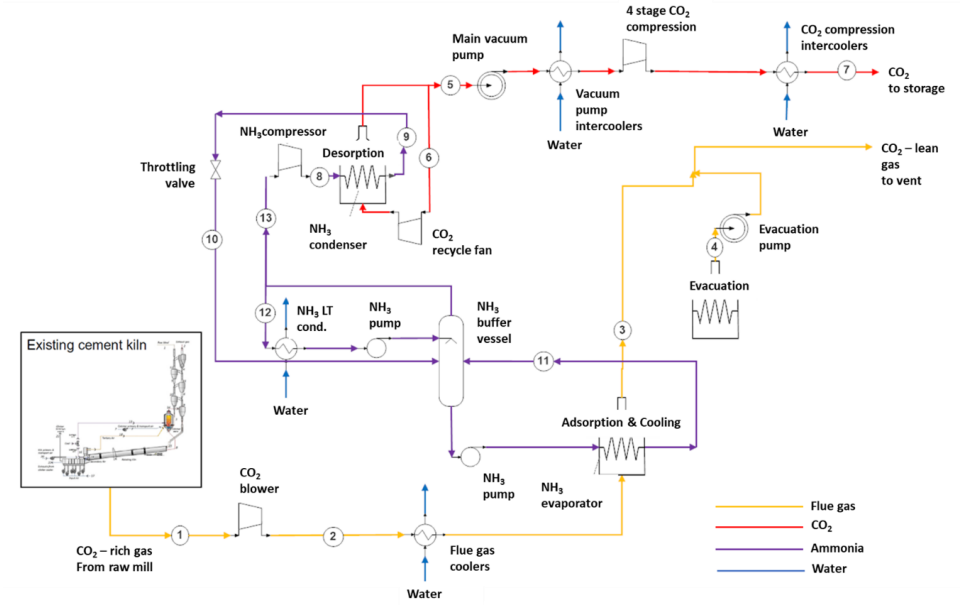

*Figure **6-1**: Standard process scheme for SARC integration [90].*

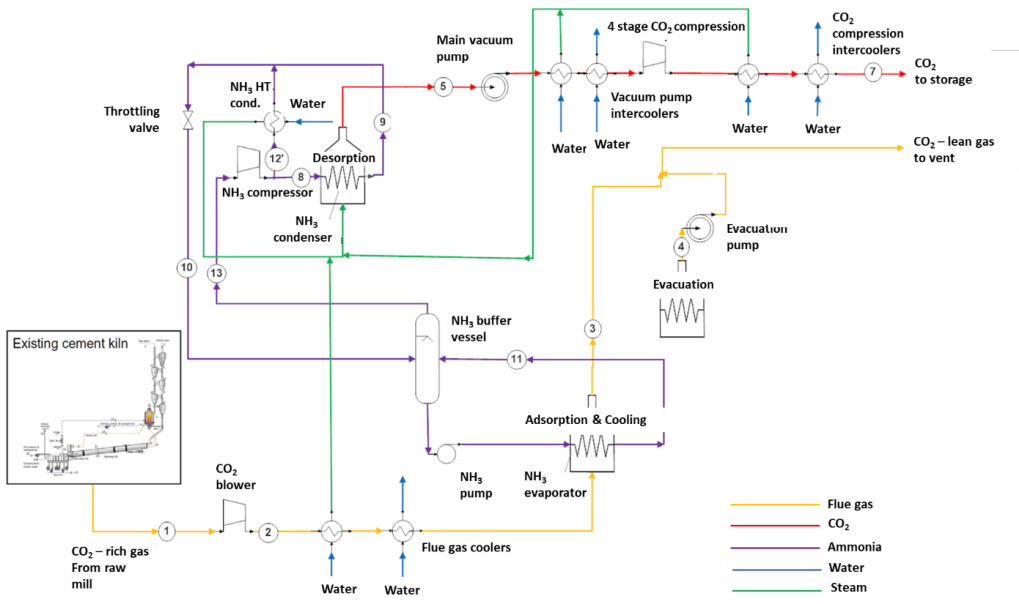

*Figure **6-2**: Modified process scheme with steam injection in SARC desorption step.*

reactor. The ammonia vapor (stream 13) from the buffer vessel is compressed using the heat pump compressor and fed (stream 8) to the desorption reactor, where hot ammonia vapor provides the necessary heat for regeneration and gets condensed to saturated liquid (stream 9).

Condensed ammonia is then throttle and fed back to the buffer tank. The liquid ammonia from the buffer tank is fed to the adsorption reactor to remove heat of adsorption. Excess heat from the heat pump circuit is rejected to the ambient (NH_3 LT cond.) to close the heat balance.

This scheme was modified in this study for improved technoeconomic performance as presented in *Figure **6-2***. It comprises of low-pressure saturated steam production from three different sections of the process. First, low-pressure saturated stream is produced from the surplus heat from the high temperature (NH_3 HT cond.) circuit of the heat pump which was rejected from the low temperature circuit of the heat pump in the original scheme. This slightly increases the heat pump consumption, while providing considerable amount of steam. The second location for steam production is from the intercoolers of the CO_2 compression train and the vacuum pump. A subsequent cooler is still required after each intercooling boiler to minimize the stream temperature and the compressor duty. Third, additional steam is produced from cooling the flue gas stream. The produced steam was then fed to the desorber where it served to reduce the partial pressure of CO_2 (which allowed the desorption pressure to be increased from 0.1 to 0.2 bar) and to suppress H_2O desorption (which reduced the required heat duty to drive the endothermic desorption). The saturated steam was produced 0.2 bar higher than the desorption pressure to overcome the pressure drop in the reactor. The main stream data for these two schemes are presented in *Table **6-2*** (original setup) and *Table **6-3*** (modified and optimized).

These two process models were evaluated for the cases presented in *Table **6-4***. The first 5 cases were studied with the standard process scheme (*Figure **6-1***) while the last two cases were evaluated using the modified process scheme (*Figure **6-2***). From left to right, the cases in *Table* **6-4** can be described as follows: First, the benchmark case from the earlier techno-economic assessment of SARC [41] is simulated with the current process model for consistency.

*Table **6-1**: Assumption used in process model.*

SARC process	
Heat pump compressor isentropic efficiency, %	85
Heat pump compressor electric-mechanical efficiency, %	94
Vacuum pumps isentropic efficiency, %	85
Vacuum pumps electrical-mechanical efficiency, %	95
Vacuum pumps intercooling temperature, °C	35
Regenerator recycle fan isentropic efficiency, %	80
Regenerator recycle fan electrical-mechanical efficiency, %	94
CO_2 compression	
Compressors isentropic efficiency, %	85
Compressor electrical-mechanical efficiency, %	95
Number of compressor stages	4
Intercoolers outlet temperature, °C	35
After-cooler outlet temperature, °C	25
Pump isentropic efficiency, %	80
Pump electrical-mechanical efficiency, %	95
Pressure drop in the intercoolers of compression and vacuum section	1% of the inlet pressure
Minimum Pinch in the intercooler- steam production	5 °C
Low pressure stream produced in modified scheme	Saturated steam
Aspen property method	Peng-Robinson

*Table **6-2**: Properties of the main streams of the standard configuration shown in Figure **6-1**.*

Stream	**T, °C**	**P, bar**	$\dot{m}$**, kg/s**	**Mole fraction**				
				CO_2	**H_2O**	**N_2**	**O_2**	**NH_3**
1	130	1.1	88.4	0.22	0.11	0.6	0.07	0
2	161.9	1.2	88.4	0.22	0.11	0.6	0.07	0
3	60.5	1.1	54.2	0.03	0.03	0.85	0.09	0
4	63.8	0.6	3.1	0.09	0.04	0.78	0.07	0
5	69.1	0.1	31.1	0.66	0.31	0.03	0.01	0
6	69.1	0.1	3.4	0.66	0.31	0.03	0.01	0
7	25	82.5	26.5	0.97	0.02	0.02	0.01	0
8	104.0	38.2	68.8	0	0	0	0	1
9	75.8	38.2	68.8	0	0	0	0	1
10	54.9	23.2	68.8	0	0	0	0	1
11	54.9	23.2	65.6	0	0	0	0	1
12	54.9	23.2	5.05	0	0	0	0	1
13	54.9	23.2	68.8	0	0	0	0	1

Next, the pressure drop is correctly accounted for in the model and the higher experimentally observed heat transfer coefficient is reflected. The third case increases the number of CSTRs in series to investigate the potential benefits of more inhibition of axial mixing, given the experimentally demonstrated simplicity of achieving this with perforated plates. Fourth, a more optimistic heat transfer coefficient (the upper bound of experimentally observed values) is investigated. The fifth case investigates the effect of shortening the reactor to lower the pressure drop and the reactor cost based on experimental observations that the CO_2 adsorption is fast enough to reach equilibrium. Sixth, the effect of injecting additional steam raised in the modified process scheme to the adsorption step is investigated. The final case combines all the potential positive effects together to investigate the ultimate potential of the SARC process.

*Table **6-3**: Properties of the main streams of the modified configuration with steam injection shown in Figure **6-2** (Ideal case).*

Stream	T, °C	P, bar	$\dot{m}$, kg/s	Mole fraction				
				CO_2	H_2O	N_2	O_2	NH_3
1	130	1.014	88.4	0.22	0.11	0.6	0.07	0
2	145.2	1.13	88.4	0.22	0.11	0.6	0.07	0
3	65.5	1.014	56.7	0.03	0.07	0.81	0.09	0
4	69.4	0.6	2.45	0.08	0.11	0.72	0.08	0
5	76.3	0.2	38	0.47	0.51	0.02	0.01	0
7	24	81.4	26.4	0.96	0.01	0.04	0.01	0
8	97.8	35.5	73.9	0	0	0	0	1
9	73.11	35.5	73.9	0	0	0	0	1
10	54.85	22.9	78.9	0	0	0	0	1
11	54.85	22.9	71	0	0	0	0	1
12’	97.8	35.5	5	0	0	0	0	1
13	54.85	23.9	78.92	0	0	0	0	1

*Table **6-4**: Summary of 7 cases considered in this study.*

Case	Original setup	PD & 400 W/m²K	8 CSTRs	500 W/m²K	Half PD	Steam	Ideal
Desorption pressure (bar)	0.1	0.1	0.1	0.1	0.1	0.2	0.2
Heat transfer coefficient (W/m²K)	300	400	400	500	400	400	500
Pressure drop (bar)	0.2	0.2	0.2	0.2	0.1	0.2	0.1
Hydrostatic pressure included in model	No	Yes	Yes	Yes	Yes	Yes	Yes
Number of CSTRs	4	4	8	4	4	4	8
Steam addition in desorption	No	No	No	No	No	Yes	Yes

6.2.4 Process economics

The methodology used in the economic assessment is unchanged from our previous work [41] where the SARC concept was benchmarked under consistent assumptions against several

competing technologies previously assessed in the CEMCAP project [142]. This study applies this established methodology to compare the CO_2 avoidance cost (CAC) resulting from the different cases detailed in *Table **6-4***. The most important economic assumptions are detailed in *Table **6-5***.

*Table **6-5:** Summary of key economic assumptions. Installed costs = base cost of fully installed equipment. Total direct costs = installed costs plus process and plant contingencies. Total plant costs = total direct costs plus project contingency and indirect and owner's costs.*

Plant economic lifetime	25 years
Construction period	3 years
Capacity factor	91.3%
Discount rate	8%
Process contingencies	
Reactors (including heat exchangers)	40% of installed costs
All other equipment	20% of installed costs
Plant contingency (all equipment)	12% of installed costs
Project contingency	15% of total direct costs
Indirect costs	14% of total direct costs
Owner's costs	7% of total direct costs
Maintenance, insurance, and taxes	4.5% of total plant costs per year
Labour costs	3.2% of total plant costs per year
Sorbent cost	15 €/kg
Sorbent lifetime	2 years
Electricity costs	58.1 €/MWh
Indirect CO_2 from electricity consumption	262 kg/MWh

6.3 Results and discussion

The results are presented in two sections. The first section reports the validation of the reactor model with the breakthrough experiments and the full SARC cycle, while the second section disseminates the results from the process and economic model for the 7 cases in *Table **6-4***.

6.3.1 Validation cases

6.3.1.1 Breakthrough experiments

The first validation simulation evaluated the accuracy of the CSTR-in-series assumption. In the experiments, perforated plates are inserted to separate the reactor into four parts. However, the perforations are considerably larger than the particles, allowing for some particle exchange between the four reactor stages. Because of this additional axial mixing between stages, it can be expected that the reactor will not show the ideal behaviour expected from four CSTRs in series.

*Figure **6-3*** illustrates that this is indeed the case. The simulation with four CSTRs overpredicts the time before significant CO_2 breakthrough, which is an overly optimistic result. However, the simulation with three CSTRs achieves a close match to the experimental results. Given the practical simplicity of the solution for creating stages within the reactor, this is a very positive

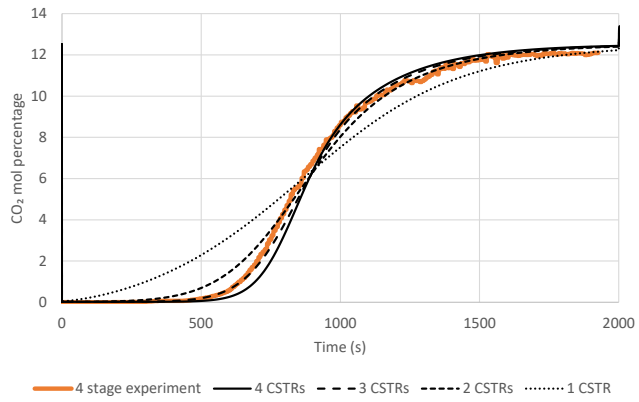

*Figure **6-3**: The effect of the number of CSTRs in series on the simulated breakthrough curve, compared to experimental data with and without stage separators in the reactor.*

result. It should be simple and cheap to insert additional perforated plates in the reactor to further reduce the degree of axial mixing within the reactor, implying that it may be possible to approach the ideal breakthrough curve of a fixed bed while maintaining the high heat transfer coefficients of a fluidized bed.

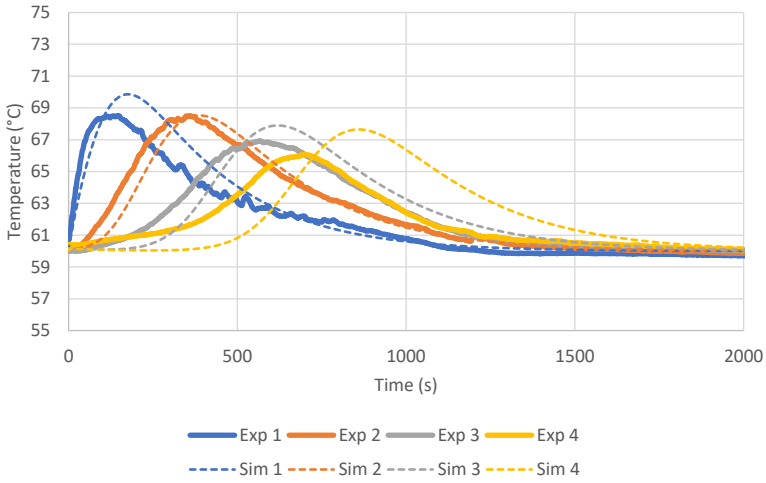

*Figure **6-4**: Comparison between simulated and experimental measurements of temperature in the four reactor stages. The numbers in the legend indicate the four reactor stages.*

The overprediction of the reduction in axial mixing when four CSTRs are used in the simulation is confirmed in *Figure **6-4***. Clearly, the temperature wave takes a longer time to travel through the reactor in the simulation than the experiment. It is also shown that the model achieves a reasonable prediction of the local temperature rise due to the exothermic reaction as the reaction front moves through the different reactor stages, heating the bed faster than the cooling oil can remove heat. Based on these results, the comparison to the full SARC cycle presented next will be carried out using only three CSTRs to correctly predict the degree of plug flow achieved in the experimental setup.

6.3.1.2 Full SARC cycle

The most important aspect that the model must capture is the degree of CO_2 capture achieved in the adsorption step. As shown in *Figure **6-5***, the CO_2 slippage during adsorption is accurately predicted. This result is achieved through a combination of three effects: 1) the rapid adsorption kinetics that justifies the assumption of equilibrium conversion in the model, 2) the correct degree of plug-flow achieved by simulating 3 CSTRs to represent the experiment 4-stages

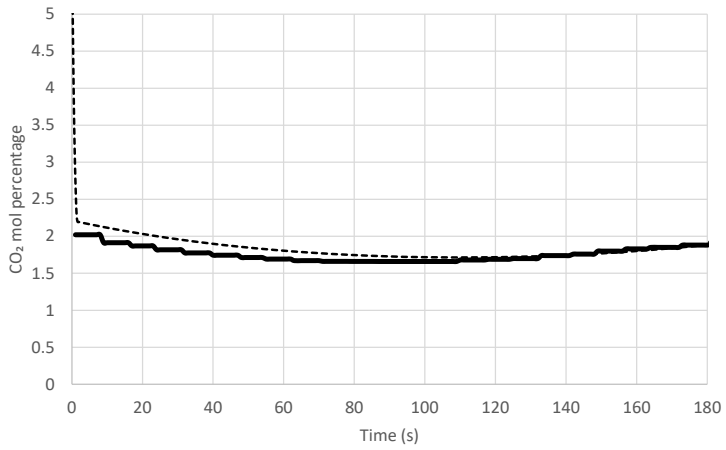

*Figure **6-5**: The simulated CO_2 mol percentage at the outlet of the adsorption step compared to experimental measurements from a full SARC cycle.*

reactor, 3) accurate heat transfer predictions to achieve the right temperatures in the different reactor stages and steps.

When considering the temperature profiles in *Figure **6-6***, a reasonable match is achieved aside from the reactor heating in the long desorption step (240-1140 s). Heat transfer in the desorption step was complicated by defluidization of the lowest reactor stage in the experiments due to an insufficient rate of CO_2 release. This is a self-strengthening effect: less fluidization causes poorer heat transfer, slowing down the temperature increase needed to drive the CO_2 release required to fluidize the reactor. Thus, a clear threshold will exist beyond which this effect is activated and the bed defluidizes.

A constant average heat transfer coefficient was derived from experimental data for each of the lower three reactor stages: 192, 338, and 343 $W/m^2/K$ from the bottom to the top. This result clearly shows the poorer fluidization in the lower stage, leading to a lower heat transfer coefficient. The second and third stages show higher heat transfer coefficients, indicating that they are successfully fluidized, aided by the CO_2 release in lower stages. Heat transfer

coefficients for the adsorption and cooling steps were measured as 508 and 393 W/m^2/K, respectively.

For most of the desorption step, the heat transfer coefficient in the bottom stage was only around 50 W/m^2/K, indicating very poor fluidization. However, at the start of the desorption step, the heat transfer coefficient was similar to the second and third stages due to the faster initial release of CO_2 when the sorbent is still highly carbonated; this results in the average heat transfer coefficient of 192 W/m^2/K that was implemented in the simulation.

The trends in *Figure* ***6-6*** during the desorption step (240-1140 s) illustrate the effects of this simplification. Initially, the first stage (blue lines) temperature rise in the experiments is much faster than the simulation prediction. This is the result of the higher heat transfer coefficient observed at the start of the desorption step when this stage was successfully fluidized. As the desorption step progresses, the experimental heat transfer coefficient sharply reduces as the first stage defluidizes and the simulation catches up due to the average heat transfer coefficient

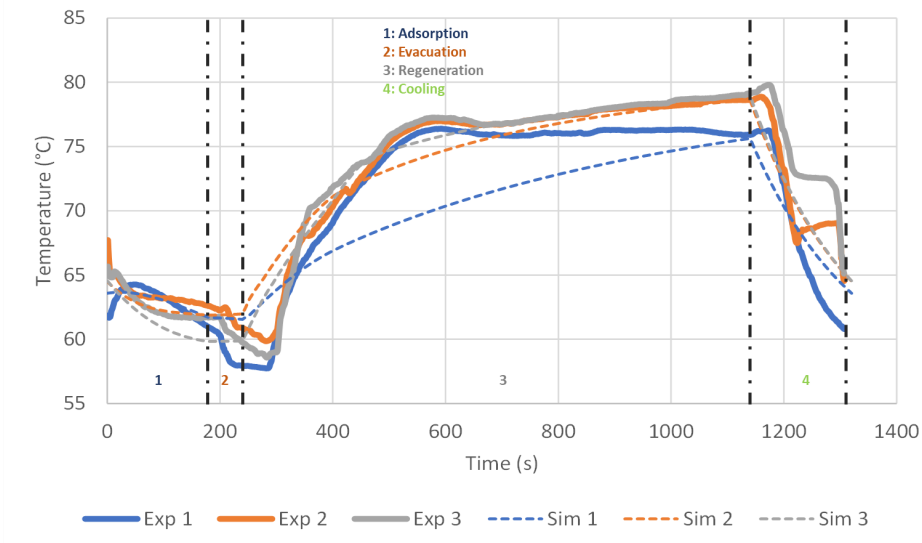

Figure ***6-6****: Comparison of simulated (Sim) temperature profiles to experimental (Exp) measurements over a full SARC cycle. The numbers in the legend indicate the three reactor stages.*

implemented. Ultimately, the correct final temperature is reached, causing the right degree of desorption in the SARC cycle.

Figure ***6-6*** also shows a delay in the experimental temperature rise at the start of the desorption step (240 s) and the temperature fall at the start of the cooling step (1140 s). This is the result of the delay in switching the heating oil pumps and displacing the cold oil with the hot oil when switching to desorption (and vice versa when switching to cooling).

Overall, these results indicate that the measured heat transfer coefficients in the experiments lead to reasonable predictions of the overall SARC cycle behaviour. In addition, the defluidization observed in the lowest reactor stage during desorption indicates that additional fluidizing gas should be added to the desorption step. This will ensure good fluidization to maximize the heat transfer coefficient and achieve a much shorter desorption step time than that was required in the experiments.

6.3.2 Economic implications of experimental observations

The simulations were completed using 6 new cases and compared to the original setup as summarized in the *Table* ***6-4***. The CO_2 avoidance cost (CAC) for the 7 cases is presented in *Figure* ***6-7***. The CAC with the standard process scheme based on the original reactor model is 51 €/ton-CO_2, which is 1 €/ton lower than the previous study [41] due to a change in the CO_2 adsorption isotherm. Correctly modelling the effect of pressure drop (PD and 400 W/m^{2}K) increased the CAC by 4.8% compared to the original setup case. This increase in CAC occurred despite increasing the heat transfer coefficient from 300 to 400 W/m^{2}K, indicating the significant negative effect that higher pressures in the lower reactor stages have on desorption performance. *Figure* ***6-8a*** shows that this increase is due to a substantial increase in heat pump power consumption required to drive the larger temperature swing needed to compensate for

the higher desorption pressures in the lower reactor stages. *Figure* ***6-8b*** shows that the increase in capital cost associated with the larger ammonia compressor is negligible.

Next, the positive effects of increasing the number of CSTR in the reactor model and further increasing the heat transfer coefficient are investigated. Both cases reduced the CAC but it remained higher by 2% and 2.8% as compared to the original setup case. Both these cases reduce the required temperature swing and thus the heat pump consumption (*Figure* ***6-8a***), but it is clear that the gains achievable from further reducing axial mixing and increasing the heat transfer coefficient are minor.

Halving the reactor height had a considerably larger effect, reducing the CAC by 9.1% compared to the original setup and 13.3% compared to the case with full pressure drop. This modification had multiple advantageous effects on the process economics. First, the consumption of the flue gas blower was reduced due to the lower reactor pressure drop. Second, heat pump consumption also reduced due to the reduced negative effect of the hydrostatic pressure increase in the lower reactor regions. Third, the cost of the reactor vessels reduced due

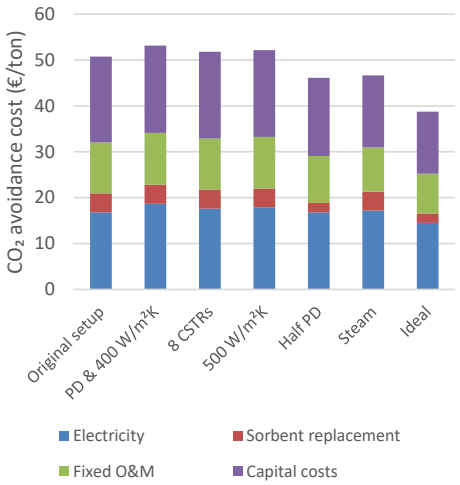

Figure ***6-7****: CO_2 avoidance cost for 7 cases detailed in Table* ***6-4***

to their lower height. Fourth, the sorbent cost was halved because only half the sorbent is used in the reactor. *Figure* ***6-8*** shows that the reduction in capital cost is significantly larger than the reduction in electricity consumption. Sorbent cost reductions also play an important role by reducing both the sorbent replacement costs in *Figure* ***6-7*** and the cost of the original batch of sorbent included in the capital costs (*Figure* ***6-8b***).

Almost similar reductions in CAC (8%) was observed with the modified process scheme (*Figure* ***6-2***) where the steam is fed to the SARC desorption step. The reduction in vacuum pump costs, enabled by an increase in desorption pressure from 0.1 to 0.2 bar, is the major benefit of this case. As shown in *Figure* ***6-8a***, the additional partial pressure swing enabled by the steam addition allowed the vacuum pump pressure to be reduced without excessive increases in heat pump consumption, keeping the total power consumption similar to prior cases. Without this added partial pressure swing, increasing the desorption pressure negatively affects the economic performance of the process [41].

When all positive effects are combined in the ideal case, a large reduction in CAC of 23.7% is

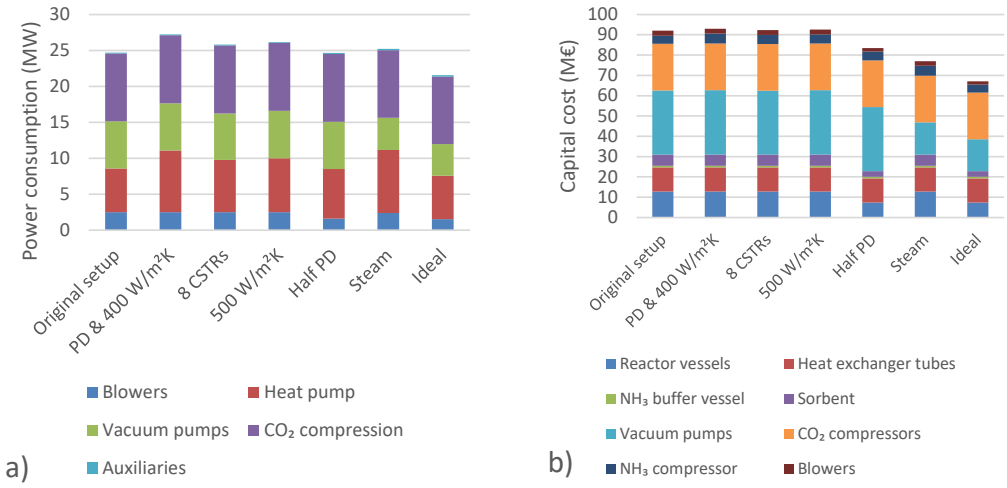

Figure ***6-8****: A breakdown of a) power consumption and b) capital cost of the 7 cases detailed in Table* ***6-4****.*

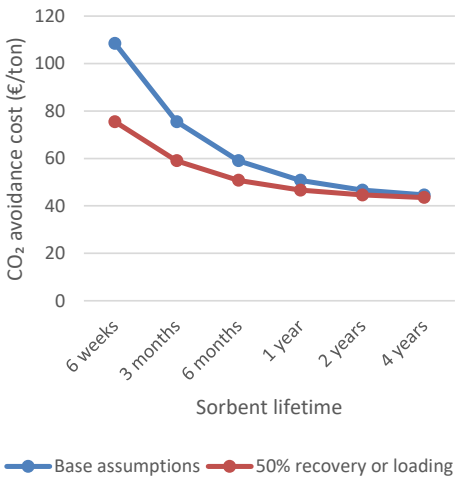

*Figure **6-9**: Sensitivity of the CAC to sorbent lifetime under the base assumptions and when 50% of the value of spent sorbent is recovered or the sorbent loading is halved. The sensitivity is completed on the penultimate case in Table **6-4**.*

observed. This brings the CAC to 38.7 €/ton, which is well below the most economical benchmark (oxyfuel combustion) at 42.4 €/ton [142]. The main contributors to this large cost reduction are the cheaper vacuum pump caused by the steam injection, the lower reactor and sorbent costs from the smaller reactor size, and the reduced power consumption from the blower.

Finally, attention should be drawn to an important economic uncertainty parameter identified from the experimental campaign. In the economic assessment, a sorbent lifetime of 2 years is assumed, but the experimental results indicated a rate of fines elutriation of 0.09%/hour, which translates into a lifetime of only 7.2 weeks at a capacity factor of 91.3%. As shown in *Figure **6-9***, such a short sorbent lifetime will render the SARC process uncompetitive, even if the half of the value of the elutriated sorbent fines can be recovered or the reactor volume can be halved.

It is therefore clear that the development of a more mechanically robust sorbent is of high priority for realizing the great techno-economic potential of the SARC concept shown in *Figure **6-7***. Furthermore, the chemical stability of the sorbent using real flue gases with high O_2

concentrations and traces of other pollutants must be demonstrated under real SARC operating conditions. The thermal stability issues of PEI sorbents are inherently avoided by the SARC process due to its mild desorption temperatures enabled by the vacuum swing.

6.4 Summary and conclusion

It is common practice to complete techno-economic assessments of new process concepts using idealized modelling assumptions such as perfect reactor mixing and chemical equilibrium. This practice was also followed in previous publications to assess the potential of the SARC post-combustion CO_2 capture technology. In this study, the reactor model used in previous works was validated against experimental data collected from a lab scale multistage fluidized bed reactor used to demonstrate the SARC concept.

In general, the comparison showed that the previously employed reactor model assumptions were reasonable. The most important correction to the reactor model that proved necessary was to account for the effect of the hydrostatic pressure gradient in the lower regions of the reactor which significantly suppressed desorption, negatively affecting reactor performance. On the positive side, the previously published experimental results showed that a substantially higher heat transfer coefficient could be achieved in practice than originally assumed in the reactor simulations, that limiting axial sorbent mixing using simple porous separators was highly effective, and that the adsorption reaction was fast enough to justify the modelling assumption of chemical equilibrium.

These learnings from the experimental campaign were used to revise the reactor model and quantify the impacts of these revisions on the projected economic performance of the SARC concept. It was shown that the negative effect of pressure drop outweighed the positive effect of increased heat transfer to increase the CO_2 avoidance cost (CAC) by 4.8% and 2.8% in the lower and upper ranges of the observed experimental heat transfer coefficient, respectively.

Capitalizing on the simplicity of further reducing axial solids mixing to delay the CO_2 breakthrough only brought small gains by reducing the CAC by 2.8%. The potential of constructing shorter reactors to capitalize on the fast adsorption kinetics observed in the experiments had a much larger effect, reducing the CAC by 13.3%, illustrating the importance of minimizing reactor size and pressure drop. Optimizing the trade-off between reactor size and gas-solid contact time is therefore an important priority for future work.

In addition, a new heat integration scheme was investigated where very low-pressure steam was raised from several low-grade heat sources in the SARC plant, still avoiding any need for heat integration with the host process. This process integration reduced the CAC almost as much as halving the reactor size, demonstrating that this relatively simple heat integration scheme should be the default configuration in future SARC plants. When this new heat integration layout was combined with all the aforementioned potential gains in economic performance, the optimal CAC emerged to be 23.7% below the case with the original SARC reactor model. This CAC of 38.7 €/ton is significantly below the most economical solution for new cement plants, oxyfuel combustion, illustrating the potential of SARC to be the preferred solution not only for retrofits but for greenfield plants as well.

Finally, attention was drawn to a key uncertainty in the economic performance of the SARC concept: sorbent durability. The observed fines generation rate from the experiments is well above the assumption in the modelling and would strongly reduce economic performance. The development of more mechanically robust sorbents should therefore be a high priority to realize the potential of this promising post-combustion CO_2 capture concept. In addition, long-term demonstration of chemical stability in real flue gases is another high sorbent-related priority.

7 Conclusion and future work

7.1 Summary and conclusion

The Swing Adsorption Reactor Cluster (SARC) concept is an adsorption-based process designed to reduce the energy requirement and cost of the CO_2 capture via a synergistic combination of vacuum and heat pumps. In this Ph.D. research, the SARC concept has been successfully demonstrated in a bench and lab scale reactors. The primary conclusions made during this research are presented below:

i. A hybrid (VTSA) regeneration mode reduces the regeneration temperature

The comparative experiments between temperature swing adsorption (TSA) and hybrid vacuum/temperature swing adsorption (VTSA) conducted in a bench scale fluidized bed reactor with PEI sorbent showed that the temperature swing required for a given sorbent working capacity was reduced by 30-40 °C by applying a partial vacuum of 50 mbar. The resulting small temperature swing is an important parameter in SARC concept as it improves the COP of the heat pump that significantly reduces the energy requirement of SARC. A full SARC cycle of carbonation, evacuation, regeneration and cooling showed a small deviation from normal behaviour, successfully proving the SARC principle.

ii. PEI sorbents were identified as the best candidate for use in the SARC concept

In the screening study conducted in the bench scale fluidized bed reactor, two PEI sorbents, a PEI sorbent functionalized with 1,2-epoxybutane supported on silica (EB-PEI) and a PEI sorbent supported on mesoporous silica containing confined metal organic framework nanocrystals (PEI-MOF) performed better than the dry sorbents (K/ZrO_2 and Na/ZrO_2) as they work well with a small temperature swing. Between the two PEI sorbents, the PEI-MOF sorbent showed a significant difference in performance and had 37 % higher working capacity than the

EB-PEI sorbent. However, the large-scale reactor simulation suggested that it did not result in an efficiency advantage relative to EB-PEI, mainly due to the higher vacuum pump power consumption of PEI-MOF sorbent as the best working adsorption capacity of the later occurred at a temperature interval 20 °C higher than the former.

The experiments with co-feeding of steam during carbonation showed no interaction of CO_2 and steam adsorption, leading to the conclusion that the single-component isotherms can safely be used in reactor modelling studies using these PEI sorbents. The addition of steam positively affected the sorbent working capacity of these sorbents as it reduces the partial pressure of CO_2 during regeneration. The working capacity obtained at a regeneration pressure of 100 mbar with steam addition in carbonation was close to the case when the regeneration was carried out at 50 mbar without steam. The partial pressure swing facilitated by the release of steam during regeneration cancels out the energy penalty of additional heat supply required to release the steam and the added gas volume that needs to be extracted through the vacuum pump of the SARC.

iii. Successful demonstration of 90% CO_2 capture in continuous SARC operation

Following the successful demonstration of the hybrid regeneration mode in the bench scale reactor, 90% CO_2 capture from a synthetic gas mixture approximating a coal power plant flue gas fed at 200 Nl/min, representing a CO_2 capture capacity up to 24 kg-CO_2/day, was demonstrated in a multistage fluidized bed lab scale reactor using the EB-PEI sorbent. A sensitivity study indicated the expected improvements of CO_2 capture efficiency with larger pressure and temperature swings and shorter carbonation times.

The comparative experiments conducted with and without perforated plate separators (used to create the physical separation in the fluidization column for the multi-staging) clearly showed that the early breakthrough of CO_2 was delayed by using these plates. This showed the ability

of perforated plate separators to limit axial mixing of the sorbent and approximate the reaction characteristics of a packed bed in a fluidized bed. Thus, this multistage reactor achieved the CO_2 capture benefits of packed beds while preserving the excellent heat transfer characteristics of fluidized beds. The controlled experiments indicated that no kinetic limitations were present during carbonation as the reactor achieved equilibrium performance even at a low gas residence time of 2.6 s. However, some mild deviations from equilibrium was observed for regeneration especially for taller beds.

The heat transfer coefficient measured along the reactor height during carbonation was 487 W/m^2K and varied in the range of 309 to 489 W/m^2 K during regeneration. Low heat transfer coefficients during regeneration in the lowest stage suggests that the amount of gas released at the bottom is rather small, resulting in poor fluidization (or a stagnant region). Thus, it is recommended to recycle part of the captured CO_2 into the regeneration step to overcome this issue and prevent defluidization in the lowest reactor regions when taller beds are used.

iv. Techno-economic evaluations using a validated reactor model yielded attractive CO_2 avoidance costs

The learnings from the experimental campaign were used to revise the initial assumptions made in the reactor and process models to quantify the impact of these revisions on the projected economic performance of the SARC concept for CO_2 capture from a cement plant. Three major learnings from the experimental studies that were incorporated in the simulation were: a) Existence of pressure gradient along the reactor height, b) Variation of the heat transfer coefficient in the range of 300 to 489 W/m^2 K and c) Effective performance of the simple perforated plates for delaying the breakthrough. The inclusion of the pressure drop increased the CO_2 avoidance cost (CAC) by 4.8% compared to the original model, despite an increase in the modelled heat transfer coefficient from 300 to 400 W/m^2 K. This increase is due to a substantial increase in heat pump power consumption required to drive the larger temperature

swing needed to compensate for the higher desorption pressures in the lower reactor stages. Increasing the heat transfer coefficient further to 500 W/m^2 K only lowed the CAC by 2%. The third learning from perforated separator for delaying the breakthrough brought small gains by reducing the CAC by 2.8%. A larger reduction in CAC (13.3%) was obtained by constructing shorter reactors to capitalize on the fast adsorption kinetics, as observed in the experimental campaign. A new heat integration scheme where very low-pressure steam was raised from several low-grade heat sources in the SARC plant yielded similarly large gains. The combination of all the above factors resulted in a CAC of 38.7 €/ton (23.4 % reduction) which is below the most economical solution for new cement plants, oxyfuel combustion. This makes SARC the most economical solution for retrofits as well as new plants. However, the observed fines generation rate (0.09% /hour) from the lab scale experiments indicated that it will strongly reduce economic performance of this concept. Thus, development of more mechanically robust sorbents is required to realize the potential of this promising post-combustion CO_2 capture concept.

7.2 Recommended future work

With the scope and the challenges encountered during this study, further research is still needed to ensure the commercialization of the proposed SARC technology as outlined below:

- It is important to confirm reliable long-term performance of the sorbent under real flue gas conditions.
- The mechanical strength of the sorbent needs to be improved.
- The positive effect of perforated plate separators needs to be further optimized and confirmed for larger diameter reactors.
- The extent to which the reactor height can be reduced, or the gas throughput rate can be increased to capitalize on the fast adsorption kinetics needs to be established.

- The next scale-up step of the SARC concept should involve a cluster of reactors with a real heat pump dynamically transferring heat between different reactors.

List of publications

1. Dhoke, C.; Zaabout, A.; Cloete, S.; Seo, H.; Park, Y.-k.; Blom, R.; Amini, S., *The swing adsorption reactor cluster (SARC) for post combustion CO_2 capture: Experimental proof-of-principle*. Chemical Engineering Journal 2019, 377, 120145.
2. Dhoke, C.; Cloete, S.; Krishnamurthy, S.; Seo, H.; Luz, I.; Soukri, M.; Park, Y.-k.; Blom, R.; Amini, S.; Zaabout, A., *Sorbents screening for post-combustion CO_2 capture via combined temperature and pressure swing adsorption*. Chemical Engineering Journal 2019, 122201.
3. Dhoke, C.; Zaabout;, A.; Cloete;, S.; Amini;, S., *Review on reactor configurations for adsorption-based CO_2 capture.* Industrial & Engineering Chemistry Research 2021.
4. Dhoke, C.; Zaabout, A.; Cloete, S.; Seo, H.; Park, Y.-k.; Demoulin, L.; Amini, S., *Demonstration of the Novel Swing Adsorption Reactor Cluster Concept in a Multistage Fluidized Bed with Heat-Transfer Surfaces for Postcombustion CO_2 Capture*. Industrial & Engineering Chemistry Research 2020.
5. Dhoke, C.; Zaabout;, A.; Cloete;, S.; Amini;, *Study of the cost reductions achievable from the novel SARC CO2 capture concept using a validated reactor model.* Industrial & Engineering Chemistry Research (under review)

Conference contribution

1. Dhoke, C.; Zaabout, A.; Cloete, S.; Seo, H.; Park, Y.-k.; Amini, S. *Demonstration of Novel Swing Adsorption Reactor Cluster (SARC) for Post Combustion CO_2 Capture*; 5th Post Combustion Capture Conference, Kyoto, Japan; 17th -19th September 2019
2. Dhoke, C.; Cloete, S.; Krishnamurthy, S.; Seo, H.; Luz, I.; Soukri, M.; Park, Y.-k.; Blom, R.; Amini, S.; Zaabout, A., *Sorbents screening for post-combustion CO_2 capture via combined temperature and pressure swing adsorption;* TCCS-10 conference, Trondheim, Norway; 17-21 June, 2019
3. Zaabout, A .; Dhoke, C.; Cloete, S.; Seo, H.; Park, Y.-k.; Amini, S., *Swing Adsorption Reactor Cluster (SARC) in post Combustion CO_2 Capture: Multistage fluidization effect on heat transfer and reactor performance*, Fluidization XVI Conference, Guilin, China; 26- 31 May, 2019
4. Dhoke, C.; Zaabout, A.; Cloete, S.; Seo, H.; Park, Y.-k.; Amini, S., et al., *The swing adsorption reactor cluster (SARC) for post combustion CO_2 capture: Experimental proof-of-principle*; ISCRE-25 Florence, Italy, 20 - 23 May 2018
5. Dhoke, C.; Zaabout, A.; Cloete, S.; Seo, H.; Park, Y.-k.; Amini, S.,*The Swing Adsorption Reactor Cluster (SARC) for Post Combustion CO_2 Capture using Polyethyleneimine (PEI) sorbent*; Nano Symposium, NTNU, Trondheim, Norway; 28 Nov, 2018

Abbreviations

ACS	Advanced carbon sorbent
ADS	Adsorber reactor in moving bed process
ads.	Adsorbent
ATMI	Advanced Technology Materials Inc.
BD	Blowdown step in PSA/VSA process
CAC	CO_2 avoidance cost
CCUS	Carbon Capture Storage and Utilization
CFB	Circulating Fluidized Bed
CHP	Combined heat and power
COL	Cooler section in moving bed reactor
COP	Coefficient of performance
CSTR	Continuous stirred tank reactor
D	Depressurization step in VSA/PSA operation
DCB	Dynamic column breakthrough
DES	Desorber/regenerator reactor in moving bed configuration
DRY	Dryer section in moving bed configuration
EB-PEI	1,2-Epoxybutane functionalized polyethyleneimine supported on SiO_2
ESA	Electric thermal swing
Expt.	Experimental
EXP 1	Temperature of the stage 1 of the reactor measured experimentally

EXP 2	Temperature of the stage 2 of the reactor measured experimentally
EXP 3	Temperature of the stage 3 of the reactor measured experimentally
EXP 4	Temperature of the stage 4 of the reactor measured experimentally
F	Feed step in VSA/PSA process
FP	Feed pressurization step in VSA/PSA process
GHG	Greenhouse Gas
HP	Heat pump
IPCC	Intergovernmental Panel on Climate Change
KCC	Kawasaki CO_2 capture
KEPRI	Korea Electric Power Research Institute
KIER	Korea Institute of Energy Research
KRICT	Korean Research Institute for Chemical Technology, South Korea
K/ZrO_2	Potassium sorbent supported on ZrO_2 (K/ZrO_2) supplied by KRICT
L_1 and L_2	Adsorption capacity (mol/kg) at low and high temperature respectively
LIF	Sorbent lift in moving bed configuration
LHV	Lower heating value
LPP	Light product purge step in VSA
LPM	Liters per minutes
L x D x H	Length x Depth x Height
MEA	Monoethanolamine absorption process
MFC	Mass flow controller

MJ	Mega joules
MOF	Metal organic framework
MWth	Megawatt thermal
N	Null
NA	Not applicable
NaUSY	Type of zeolite (adsorbent)
NH_3 HT cond.	Heat exchanger to reject heat from high temperature heat pump circuit
NH_3 LT cond.	Heat exchanger to reject heat from low temperature heat pump circuit
Na/ZrO_2	Sodium sorbent supported on ZrO_2 supplied by KRICT
Nl/min	Normal liter per minutes
P	Pressurization step in 2 step PSA process
P_h	High pressure in PSA process
PCMs	Phase change materials
PD	Pressure drop in reactor
PEI	Polyethyleneimine
PEI-MOF	Polyethyleneimine and metal organic framework supported on SiO_2
PFR	Plug flow reactor
P&ID	Process and instrumentation diagram
P_L	Low pressure in PSA process
Prod.	Productivity
PSA	Pressure swing adsorption

PTSA	Pressure temperature swing adsorption
Pu	Purge step in 2 step PSA process
P-01 & P-02	Oil pumps in the experimental setup
Q*	Equilibrium CO_2 loading on the sorbent from Isotherm
Q'	Actual CO_2 loading on the sorbent during kinetic study
R	Rise step in 2 step PSA process (Chapter 2)
RBA	Rotating bed adsorber
RVPSA	Rapid vacuum pressure swing adsorption
RTI	RTI International, Research Triangle Park, USA
SARC	Swing adsorption reactor cluster
SA-VSA	Steam-aided vacuum swing adsorption
SIM 1	Temperature of the stage 1 of the reactor estimated from reactor model
SIM 2	Temperature of the stage 2 of the reactor estimated from reactor model
SIM 3	Temperature of the stage 3 of the reactor estimated from reactor model
SIM 4	Temperature of the stage 4 of the reactor estimated from reactor model
Sorb	Sorbent (adsorbent)
SPECCA	Specific primary energy consumption for CO_2 avoided ($MJ_{LHV}/kgCO_2$)
TRA	Transition section in moving bed reactor
TRL	Technology readiness level
TSA	Temperature swing adsorption
T1-T4	Temperature of stage 1 to stage 4 of the reactor-experimentation

VFB	Vortexing fluidized bed
VPSA	Vacuum pressure swing adsorption
VSA	Vacuum swing adsorption
VTSA	Vacuum combined temperature swing adsorption
WMS	Fluidized bed with separators (for staging)
WOS	Break through experiments without water (H_2O)
WOMS	Fluidized bed without separators
WS	Break through experiments with water (H_2O)
A	Heat transfer area of heat exchanger (m^2)
b	Toth isotherm constant (Parameter of Toth isotherm)
C	Gas Phase CO_2 concentration at the section of the reactor in chapter 2
C	Fraction of theoretical maximum efficiency for heat pump in chapter 4
C_0	Gas Phase CO_2 concentration at the feed section of the reactor
$\frac{c(t)}{c_o}$	Normalized concentration in DCB experiments
$C_{p,oil}$	Oil specific heat capacity $\left(\frac{J}{kg\ K}\right)$
C_T	Total gas phase concentration in DCB experiments
D_e	Molecular diffusivity (m^2/s)
dH	Heat of adsorption in kJ/mol
h_i	Heat transfer coefficient (W/m^2k)
E_{HP}	Energy transfer by the heat pump

F	Total carrier flowrate during desorption in DCB experiments
H_i	Average heat transfer coefficient
h_i	Localized film heat transfer coefficients
k_{LDF}	LDF mass transfer coefficient for pore diffusion control (s^{-1})
k_f	Thermal conductivity of sorbent (W/mK)
m_{ads}	Mass of sorbent in DCB experiments
$\dot{m}_{oil}$	Mass flow rate of oil (kg/s)
m_{sorb}	Mass of the sorbent in the reactor (kg)
$\dot{m}$	Mass flow of streams in process simulation study
n	Parameter of Toth isotherm
$\dot{N}_{CO_2}^{in}$	CO_2 molar flowrates (mol/s) measured at the reactor inlet
$\dot{N}_{CO_2}^{out}$	CO_2 molar flowrates (mol/s) measured at the reactor outlet
p_{CO_2}	Partial pressure of CO_2
q_{CO_2} & q^*	CO_2 loading on sorbent
Q'_{Ad} & Q'_{De}	Sorbent CO_2 loadings (mol/kg) at times t_c and t_r respectively
$Q'_{Ad,end}$	Sorbent CO_2 loadings (mol/kg) at the end of carbonation step in kinetic study
q_{H_2O}	H_2O loading on sorbent
q_i	Heat transfer rate for the i^{th}stage
q_{large}	Heat transfer rate in large scale simulation
q_{lab}	Heat transfer rate in lab scale

R	Universal gas constant
t	Parameter of Toth isotherm
T_{bed}	Bed temperature (°C)
T_{oil}^{in} and T_{oil}^{out}	Oil inlet and outlet temperatures (°C)
T_0	Reference temperature in K used in Isotherm model fitting
T_{Cold} & T_C	Evaporation temperatures of the heat pump working fluid
T_{Hot} & T_H	Condensation temperatures of the heat pump working fluid
t_c	Carbonation time in kinetic study
t_r	Regeneration time in kinetic study
T_{wf}	Temperature of working fluid in heat pump circuit
W_{HP}	Heat pump power consumption
y_O	Mole fraction of CO_2 in feed of DCB experiments
τ	Contact time used in kinetic experimental runs
η_{CO_2}	CO_2 capture efficiency
φ	Relative humidity
θ	Vacant site available for the adsorption at the section of the reactor
θ_0	Equilibrium vacant site available for the adsorption at the feed CO_2 partial pressure

Reference List

[1] A. Zaabout *et al.*, "Thermodynamic assessment of the swing adsorption reactor cluster (SARC) concept for post-combustion CO2 capture," *International Journal of Greenhouse Gas Control,* vol. 60, pp. 74-92, May 2017, doi: 10.1016/j.ijggc.2017.03.001.

[2] V. Masson-Delmotte, P. Zhai, H.-O. Pörtner, D. Roberts, J. Skea, P.R. Shukla, A. Pirani, W. Moufouma-Okia, C. Péan, R. Pidcock, S. Connors, J.B.R. Matthews, Y. Chen, X. Zhou, M.I. Gomis, E. Lonnoy, T. Maycock, M. Tignor, and T. Waterfield, "IPCC, 2018: Summary for Policymakers. In: Global Warming of 1.5°C. An IPCC Special Report on the impacts of global warming of 1.5°C above pre-industrial levels and related global greenhouse gas emission pathways, in the context of strengthening the global response to the threat of climate change, sustainable development, and efforts to eradicate poverty," World Meteorological Organization, Geneva, Switzerland, 32 pp.

[3] IEA, "Global Energy Review 2020- The impacts of the Covid-19 crisis on global energy demand and CO2 emissions," 2020. [Online]. Available: https://webstore.iea.org/download/direct/2995?fileName=Global_Energy_Review_2020.pdf

[4] "IEA (2019), Global Energy & CO2 Status Report 2019, IEA, Paris," 2019.

[5] IPCC. Climate change mitigation: Summary for Policymakers

[6] H. Ahn, M. Luberti, Z. Liu, and S. Brandani, "Process configuration studies of the amine capture process for coal-fired power plants," *International Journal of Greenhouse Gas Control,* vol. 16, pp. 29-40, 8// 2013, doi: http://dx.doi.org/10.1016/j.ijggc.2013.03.002.

[7] H. M. Kvamsdal, M. C. Romano, L. van der Ham, D. Bonalumi, P. van Os, and E. Goetheer, "Energetic evaluation of a power plant integrated with a piperazine-based CO2 capture process," *International Journal of Greenhouse Gas Control,* vol. 28, pp. 343-355, Sep 2014, doi: 10.1016/j.ijggc.2014.07.004.

[8] H. M. Kvamsdal, S. Ehlers, A. Kather, P. Khakharia, M. Nienoord, and P. L. Fosbøl, "Optimizing integrated reference cases in the OCTAVIUS project," *International Journal of Greenhouse Gas Control,* vol. 50, pp. 23-36, 7// 2016, doi: http://dx.doi.org/10.1016/j.ijggc.2016.04.012.

[9] G. Manzolini, E. S. Fernandez, S. Rezvani, E. Macchi, E. L. V. Goetheer, and T. J. H. Vlugt, "Economic assessment of novel amine based CO2 capture technologies integrated in power plants based on European Benchmarking Task Force methodology," *Applied Energy,* vol. 138, pp. 546-558, Jan 15 2015, doi: 10.1016/j.apenergy.2014.04.066.

[10] M. Garcia;, N. Berghout;, and L. Herraiz, "Cost of CO2 capature in the industrial sector: Cement and Iron and Steel Industries," IEA, Septemenber 2018 2018, vol. IEAGHG technical Review.

[11] N. A. Fine, M. J. Goldman, and G. T. Rochelle, "Nitrosamine Formation in Amine Scrubbing at Desorber Temperatures," *Environmental Science & Technology,* vol. 48, no. 15, pp. 8777-8783, 2014/08/05 2014, doi: 10.1021/es501484w.

[12] S. Badr, J. Frutiger, K. Hungerbuehler, and S. Papadokonstantakis, "A framework for the environmental, health and safety hazard assessment for amine-based post combustion CO2 capture," *International Journal of Greenhouse Gas Control,* vol. 56, pp. 202-220, 2017/01/01/ 2017, doi: https://doi.org/10.1016/j.ijggc.2016.11.013.

[13] G. Shavalieva, P. Kazepidis, A. I. Papadopoulos, P. Seferlis, and S. Papadokonstantakis, "Environmental, health and safety assessment of post-combustion CO2 capture processes with phase-change solvents," *Sustainable Production and Consumption,* vol. 25, pp. 60-76, 2021/01/01/ 2021, doi: https://doi.org/10.1016/j.spc.2020.07.015.

[14] A. Samanta, A. Zhao, G. K. H. Shimizu, P. Sarkar, and R. Gupta, "Post-Combustion CO2 Capture Using Solid Sorbents: A Review," *Industrial & Engineering Chemistry Research,* vol. 51, no. 4, pp. 1438-1463, Feb 1 2012, doi: 10.1021/ie200686q.

[15] P. A. Webley, "Adsorption technology for CO2 separation and capture: a perspective," *Adsorption-Journal of the International Adsorption Society,* vol. 20, no. 2-3, pp. 225-231, Feb 2014, doi: 10.1007/s10450-014-9603-2.

[16] J. C. Abanades *et al.*, "Emerging CO2 capture systems," *International Journal of Greenhouse Gas Control,* vol. 40, pp. 126-166, 2015/09/01/ 2015, doi: https://doi.org/10.1016/j.ijggc.2015.04.018.

[17] D. M. Ruthven, *Principles of Adsorption and Adsorption Processes*

Wiley_Interscience: New York, 1984.

[18] J. C. Abanades *et al.*, "Emerging CO2capture systems," *International Journal of Greenhouse Gas Control,* 2015.

[19] F. Rezaei, A. Mosca, P. Webley, J. Hedlund, and P. Xiao, "Comparison of Traditional and Structured Adsorbents for CO2 Separation by Vacuum-Swing Adsorption," *Industrial & Engineering Chemistry Research,* vol. 49, no. 10, pp. 4832-4841, 2010/05/19 2010, doi: 10.1021/ie9016545.

[20] A. Andersen *et al.*, "On the development of Vacuum Swing adsorption (VSA) technology for post-combustion CO2 capture," in *Ghgt-11*, vol. 37, T. Dixon and K. Yamaji Eds., (Energy Procedia, 2013, pp. 33-39.

[21] F. Brandani, A. Rouse, S. Brandani, and D. M. Ruthven, "Adsorption kinetics and dynamic behavior of a carbon monolith," *Adsorption-Journal of the International Adsorption Society,* vol. 10, no. 2, pp. 99-109, Jun 2004, doi: 10.1023/B:ADSO.0000039866.37214.6a.

[22] C. Shen, Z. Liu, P. Li, and J. Yu, "Two-Stage VPSA Process for CO2 Capture from Flue Gas Using Activated Carbon Beads," *Industrial & Engineering Chemistry Research,* vol. 51, no. 13, pp. 5011-5021, 2012/04/04 2012, doi: 10.1021/ie202097y.

[23] L. Wang, Z. Liu, P. Li, J. Wang, and J. Yu, "CO2 capture from flue gas by two successive VPSA units using 13XAPG," *Adsorption,* Conference Paper vol. 18, no. 5-6, pp. 445-459, 2012, doi: 10.1007/s10450-012-9431-1.

[24] R. Veneman, N. Frigka, W. Zhao, Z. Li, S. Kersten, and W. Brilman, "Adsorption of H2O and CO2 on supported amine sorbents," *International Journal of Greenhouse Gas Control,* vol. 41, pp. 268-275, 10// 2015, doi: http://dx.doi.org/10.1016/j.ijggc.2015.07.014.

[25] T. O. Nelson, A. Kataria, P. Mobley, M. Soukri, and J. Tanthana, "RTI's Solid Sorbent-Based CO2 Capture Process: Technical and Economic Lessons Learned for Application in Coal-fired, NGCC, and Cement Plants," *Energy Procedia,* vol. 114, pp. 2506-2524, 2017/07/01/ 2017, doi: https://doi.org/10.1016/j.egypro.2017.03.1409.

[26] Y. C. Park, S.-H. Jo, C. K. Ryu, and C.-K. Yi, "Demonstration of pilot scale carbon dioxide capture system using dry regenerable sorbents to the real coal-fired power plant in Korea," *Energy Procedia,* vol. 4, pp. 1508-1512, 2011, doi: 10.1016/j.egypro.2011.02.018.

[27] M. Bui *et al.*, "Carbon capture and storage (CCS): the way forward," *Energy & Environmental Science,* vol. 11, no. 5, pp. 1062-1176, May 2018, doi: 10.1039/c7ee02342a.

[28] P. A. Webley and J. Zhang, "Microwave assisted vacuum regeneration for CO2 capture from wet flue gas," *Adsorption,* Article vol. 20, no. 1, pp. 201-210, 2014, doi: 10.1007/s10450-013-9563-y.

[29] M. Luberti, G. D. Oreggioni, and H. Ahn, "Design of a rapid vacuum pressure swing adsorption (RVPSA) process for post-combustion CO2 capture from a biomass-fuelled CHP plant,"

Journal of Environmental Chemical Engineering, vol. 5, no. 4, pp. 3973-3982, 2017/08/01/ 2017, doi: https://doi.org/10.1016/j.jece.2017.07.029.

[30] T. Gupta and R. Ghosh, "Rotating bed adsorber system for carbon dioxide capture from flue gas," *International Journal of Greenhouse Gas Control,* vol. 32, pp. 172-188, 2015/01/01/ 2015, doi: https://doi.org/10.1016/j.ijggc.2014.10.020.

[31] C. A. Grande, H. Kvamsdal, G. Mondino, and R. Blom, "Development of Moving Bed Temperature Swing Adsorption (MBTSA) Process for Post-combustion CO2 Capture: Initial Benchmarking in a NGCC Context," *Energy Procedia,* vol. 114, pp. 2203-2210, 2017/07/01/ 2017, doi: https://doi.org/10.1016/j.egypro.2017.03.1357.

[32] T. Okumura, T. Ogino, S. Nishibe, Y. Nonaka, T. Shoji, and T. Higashi, "CO2 Capture Test for A Moving-bed System Utilizi g Low-temperature Steam," *Energy Procedia,* vol. 63, pp. 2249-2254, 2014/01/01/ 2014, doi: https://doi.org/10.1016/j.egypro.2014.11.243.

[33] K. Kim, Y. Son, W. B. Lee, and K. S. Lee, "Moving bed adsorption process with internal heat integration for carbon dioxide capture," *International Journal of Greenhouse Gas Control,* vol. 17, pp. 13-24, Sep 2013, doi: 10.1016/j.ijggc.2013.04.005.

[34] J.-Y. Kim *et al.*, "Continuous testing of silica-PEI adsorbents in a lab.-scale twin bubbling fluidized-bed system," *International Journal of Greenhouse Gas Control,* vol. 82, pp. 184-191, 2019/03/01/ 2019, doi: https://doi.org/10.1016/j.ijggc.2019.01.007.

[35] C.-K. Yi, S.-H. Jo, Y. Seo, J.-B. Lee, and C.-K. Ryu, "Continuous operation of the potassium-based dry sorbent CO2 capture process with two fluidized-bed reactors," *International Journal of Greenhouse Gas Control,* vol. 1, no. 1, pp. 31-36, Apr 2007, doi: 10.1016/s1750-5836(07)00014-x.

[36] C. A. Grande, R. P. L. Ribeiro, E. L. G. Oliveira, and A. E. Rodrigues, "Electric swing adsorption as emerging CO2 capture technique," *Energy Procedia,* vol. 1, no. 1, pp. 1219-1225, 2009/02/01/ 2009, doi: https://doi.org/10.1016/j.egypro.2009.01.160.

[37] Q. Zhao *et al.*, "CO2 capture using a novel hybrid monolith (H-ZSM5/activated carbon) as adsorbent by combined vacuum and electric swing adsorption (VESA)," *Chemical Engineering Journal,* vol. 358, pp. 707-717, 2019/02/15/ 2019, doi: https://doi.org/10.1016/j.cej.2018.09.196.

[38] S. Roy, C. R. Mohanty, and B. C. Meikap, "Multistage Fluidized Bed Reactor Performance Characterization for Adsorption of Carbon Dioxide," *Industrial & Engineering Chemistry Research,* vol. 48, no. 23, pp. 10718-10727, 2009/12/02 2009, doi: 10.1021/ie901133r.

[39] H. Chalmers, M. Leach, M. Lucquiaud, and J. Gibbins, "Valuing flexible operation of power plants with CO2 capture," *Energy Procedia,* vol. 1, no. 1, pp. 4289-4296, 2009/02/01/ 2009, doi: https://doi.org/10.1016/j.egypro.2009.02.241.

[40] F. Normann, S. Ó. Garðarsdóttir, R. Skagestad, A. Mathisen, and F. Johnsson, "Partial Capture of Carbon Dioxide from Industrial Sources - A Discussion on Cost Optimization and the CO2 Capture Rate," *Energy Procedia,* vol. 114, pp. 113-121, 2017/07/01/ 2017, doi: https://doi.org/10.1016/j.egypro.2017.03.1154.

[41] S. Cloete, A. Giuffrida, M. C. Romano, and A. Zaabout, "Economic assessment of the swing adsorption reactor cluster for CO2 capture from cement production," *Journal of Cleaner Production,* vol. 275, p. 123024, 2020/12/01/ 2020, doi: https://doi.org/10.1016/j.jclepro.2020.123024.

[42] L. Riboldi and O. Bolland, "Evaluating Pressure Swing Adsorption as a CO2 separation technique in coal-fired power plants," *International Journal of Greenhouse Gas Control,* vol. 39, pp. 1-16, 2015/08/01/ 2015, doi: https://doi.org/10.1016/j.ijggc.2015.02.001.

[43] Z. Liu, L. Wang, X. Kong, P. Li, J. Yu, and A. E. Rodrigues, "Onsite CO2 Capture from Flue Gas by an Adsorption Process in a Coal-Fired Power Plant," *Industrial & Engineering Chemistry Research,* vol. 51, no. 21, pp. 7355-7363, 2012/05/30 2012, doi: 10.1021/ie3005308.

[44] T. L. P. Dantas *et al.*, "Modeling of the fixed - bed adsorption of carbon dioxide and a carbon dioxide - nitrogen mixture on zeolite 13X," *Brazilian Journal of Chemical Engineering,* vol. 28, pp. 533-544, 2011.

[45] H. Krutka, S. Sjostrom, T. Starns, M. Dillon, and R. Silverman, "Post-Combustion CO2 Capture Using Solid Sorbents: 1 MWe Pilot Evaluation," *Energy Procedia,* vol. 37, pp. 73-88, 2013/01/01/ 2013, doi: https://doi.org/10.1016/j.egypro.2013.05.087.

[46] R. E. Treybal, *Mass-transfer operations*, Third edition ed. (Ms Graw-Hill Chemical Engineering Series). Ms Graw-Hill Book Company, p. 800.

[47] J. Zhang, R. Singh, and P. A. Webley, "Alkali and alkaline-earth cation exchanged chabazite zeolites for adsorption based CO2 capture," *Microporous and Mesoporous Materials,* vol. 111, no. 1, pp. 478-487, 2008/04/15/ 2008, doi: https://doi.org/10.1016/j.micromeso.2007.08.022.

[48] Y. Park, D.-K. Moon, Y.-H. Kim, H. Ahn, and C.-H. Lee, "Adsorption isotherms of CO2, CO, N2, CH4, Ar and H2 on activated carbon and zeolite LiX up to 1.0 MPa," *Adsorption,* vol. 20, no. 4, pp. 631-647, 2014/05/01 2014, doi: 10.1007/s10450-014-9608-x.

[49] L. Hauchhum and P. Mahanta, "Carbon dioxide adsorption on zeolites and activated carbon by pressure swing adsorption in a fixed bed," *International Journal of Energy and Environmental Engineering,* vol. 5, no. 4, pp. 349-356, 2014/12/01 2014, doi: 10.1007/s40095-014-0131-3.

[50] L. Meljac, V. Goetz, and X. Py, "Isothermal composite adsorbent. Part I: Thermal characterisation," *Applied Thermal Engineering,* vol. 27, no. 5, pp. 1009-1016, 2007/04/01/ 2007, doi: https://doi.org/10.1016/j.applthermaleng.2006.07.037.

[51] F. Rezaei and P. Webley, "Structured adsorbents in gas separation processes," *Separation and Purification Technology,* vol. 70, no. 3, pp. 243-256, 2010/01/12/ 2010, doi: https://doi.org/10.1016/j.seppur.2009.10.004.

[52] D. M. Ruthven and C. Thaeron, "Performance of a parallel passage adsorbent contactor," *Gas Separation & Purification,* vol. 10, no. 1, pp. 63-73, 1996/01/01/ 1996

[53] J. Harry W. DeckmanBruce T. KelleyFrank HershkowitzRonald R. ChancePaul S. NorthropEdward W. Corcoran, "Temperature swing adsorption of CO2 from flue gas using a parallel channel contractor," US, 2011

[54] F. Rezaei and M. Grahn, "Thermal Management of Structured Adsorbents in CO2 Capture Processes," *Industrial & Engineering Chemistry Research,* vol. 51, no. 10, pp. 4025-4034, 2012/03/14 2012, doi: 10.1021/ie201057p.

[55] L. Wang *et al.*, "CO2 capture from flue gas in an existing coal-fired power plant by two successive pilot-scale VPSA units," *Industrial and Engineering Chemistry Research,* Article vol. 52, no. 23, pp. 7947-7955, 2013, doi: 10.1021/ie4009716.

[56] R. P. Lively *et al.*, "Hollow Fiber Adsorbents for CO2 Removal from Flue Gas," *Industrial & Engineering Chemistry Research,* vol. 48, no. 15, pp. 7314-7324, 2009/08/05 2009, doi: 10.1021/ie9005244.

[57] N. Querejeta, M. G. Plaza, F. Rubiera, C. Pevida, T. Avery, and S. R. Tennisson, "Carbon Monoliths in Adsorption-based Post-combustion CO2 Capture," *Energy Procedia,* vol. 114, pp. 2341-2352, 2017/07/01/ 2017, doi: https://doi.org/10.1016/j.egypro.2017.03.1366.

[58] R. Thiruvenkatachari, S. Su, H. An, and X. X. Yu, "Post combustion CO2 capture by carbon fibre monolithic adsorbents," *Progress in Energy and Combustion Science,* vol. 35, no. 5, pp. 438-455, 2009/10/01/ 2009, doi: https://doi.org/10.1016/j.pecs.2009.05.003.

[59] B. Sreenivasulu, D. V. Gayatri, I. Sreedhar, and K. V. Raghavan, "A journey into the process and engineering aspects of carbon capture technologies," *Renewable and Sustainable Energy Reviews,* vol. 41, pp. 1324-1350, 2015/01/01/ 2015, doi: https://doi.org/10.1016/j.rser.2014.09.029.

[60] B. C, *Trans. AIChE,* vol. XLII, pp. 665-680, 1946.

[61] M. D. Hornbostel *et al.*, "Characteristics of an advanced carbon sorbent for CO2 capture," *Carbon,* vol. 56, pp. 77-85, 2013/05/01/ 2013

[62] M. Hornbostel, "Pilot-Scale Evaluation of an Advanced Carbon Sorbent-Based Process for Post-Combustion Carbon Capture,"; SRI International, Menlo Park, CA (United States), 2016. [Online]. Available: https://www.osti.gov/servlets/purl/1337051

[63] G. N. Krishnan *et al.*, "CO2 Capture Using Advanced Carbon Sorbents," presented at the Carbon Management Technology Conference, Orlando, Florida, USA, 2012/1/1/, 2012.

[64] G. Mondino, C. A. Grande, R. Blom, and L. O. Nord, "Moving bed temperature swing adsorption for CO2 capture from a natural gas combined cycle power plant," *International Journal of Greenhouse Gas Control,* vol. 85, pp. 58-70, 2019/06/01/ 2019.

[65] T. Okumura, K. Yoshizawa, S. Nishibe, H. Iwasaki, M. Kazari, and T. Hori, "Parametric Testing of a Pilot-scale Design for a Moving-bed CO2 Capture System Using Low-temperature Steam," *Energy Procedia,* vol. 114, pp. 2322-2329, 2017/07/01/ 2017.

[66] K. S. Knaebel, "Temperature swing adsorption system " Patent Appl. US7594956B2, Sep. 29, 2009

[67] A. Boulet; and S. Khiavi, "Parallel passage fluid contactor structure," United States Patent Appl. US20110311761A1, 2010. .

[68] A. Boulet; and S. Khiavi, "Parallel passage fluid contactor structure," Canada Patent Appl. CA2932181A.

[69] C. Dhoke *et al.*, "Demonstration of the Novel Swing Adsorption Reactor Cluster Concept in a Multistage Fluidized Bed with Heat-Transfer Surfaces for Postcombustion CO2 Capture," *Industrial & Engineering Chemistry Research,* 2020/12/13 2020, doi: 10.1021/acs.iecr.0c05951.

[70] G. Hofer, G. Schöny, J. Fuchs, and T. Pröll, "Investigating wall-to-bed heat transfer in view of a continuous temperature swing adsorption process," *Fuel Processing Technology,* vol. 169, pp. 157-169, 2018/01/01/ 2018, doi: https://doi.org/10.1016/j.fuproc.2017.09.024.

[71] Y. C. Park, S.-H. Jo, C. K. Ryu, and C.-K. Yi, "Long-term operation of carbon dioxide capture system from a real coal-fired flue gas using dry regenerable potassium-based sorbents," *Energy Procedia,* vol. 1, no. 1, pp. 1235-1239, 2009/02/01/ 2009, doi: https://doi.org/10.1016/j.egypro.2009.01.162.

[72] R. Veneman, Z. S. Li, J. A. Hogendoorn, S. R. A. Kersten, and D. W. F. Brilman, "Continuous CO2 capture in a circulating fluidized bed using supported amine sorbents," *Chemical Engineering Journal,* vol. 207–208, pp. 18-26, 10/1/ 2012, doi: http://dx.doi.org/10.1016/j.cej.2012.06.100.

[73] Y. Seo, S.-H. Jo, H.-J. Ryu, H. Dal Bae, C. K. Ryu, and C.-K. Yi, "Effect of water pretreatment on CO2 capture using a potassium-based solid sorbent in a bubbling fluidized bed reactor," *Korean Journal of Chemical Engineering,* vol. 24, no. 3, pp. 457-460, 2007/05/01 2007, doi: 10.1007/s11814-007-0079-6.

[74] C.-K. Yi, S.-H. Jo, H.-J. Ryu, Y.-W. Yoo, J.-B. Lee, and C.-K. Ryu, "- CO2 reaction characteristics of dry sorbents in fluidized reactors," in *Greenhouse Gas Control Technologies 7*, E. S. Rubin *et al.* Eds. Oxford: Elsevier Science Ltd, 2005, pp. 1765-1769.

[75] D. Das, D. P. Samal, and B. C. Meikap, "Removal of CO2 in a multistage fluidized bed reactor by diethanol amine impregnated activated carbon," *Journal of Environmental Science and Health, Part A,* vol. 51, no. 9, pp. 769-775, 2016/07/28 2016, doi: 10.1080/10934529.2016.1170462.

[76] D. Das and B. C. Meikap, "Removal of CO2 in a multi stage fluidised bed reactor by monoethanolamine impregnated activated carbon," *Mineral Processing and Extractive Metallurgy,* pp. 1-7, 2019, doi: 10.1080/25726641.2019.1591791.

[77] J. R. McDonough, R. Law, D. A. Reay, and V. Zivkovic, "Intensified carbon capture using adsorption: Heat transfer challenges and potential solutions," *Thermal Science and Engineering Progress,* vol. 8, pp. 17-30, 2018/12/01/ 2018, doi: https://doi.org/10.1016/j.tsep.2018.07.012.

[78] Y. B. G. Varma, "Pressure drop of the fluid and the flow patterns of the phases in multistage fluidisation," *Powder Technology,* vol. 12, no. 2, pp. 167-174, 1975/09/01/ 1975, doi: https://doi.org/10.1016/0032-5910(75)80008-8.

[79] G. Schöny, F. Dietrich, J. Fuchs, T. Pröll, and H. Hofbauer, "A multi-stage fluidized bed system for continuous CO2 capture by means of temperature swing adsorption – First results from bench scale experiments," *Powder Technology,* Article vol. 316, pp. 519-527, 2017, doi: 10.1016/j.powtec.2016.11.066.

[80] E. Zehetner, G. Schöny, J. Fuchs, T. Pröll, and H. Hofbauer, "Fluid-dynamic study on a multistage fluidized bed column for continuous CO2 capture via temperature swing adsorption," *Powder Technology,* Article vol. 316, pp. 528-534, 2017, doi: 10.1016/j.powtec.2016.11.065.

[81] J. Pirklbauer, G. Schöny, T. Pröll, and H. Hofbauer, "Impact of stage configurations, lean-rich heat exchange and regeneration agents on the energy demand of a multistage fluidized bed TSA CO2 capture process," *International Journal of Greenhouse Gas Control,* Review vol. 72, pp. 82-91, 2018, doi: 10.1016/j.ijggc.2018.03.018.

[82] D. Das, S. K. Behera, and B. C. Meikap, "Removal of CO2 in a multistage fluidized bed reactor by amine impregnated activated carbon: optimization using response surface methodology," *International Journal of Coal Science & Technology,* vol. 6, no. 3, pp. 445-458, 2019/09/01 2019, doi: 10.1007/s40789-019-0261-6.

[83] T. Proell, G. Schoeny, G. Sprachmann, and H. Hofbauer, "Introduction and evaluation of a double loop staged fluidized bed system for post-combustion CO2 capture using solid sorbents in a continuous temperature swing adsorption process," *Chemical Engineering Science,* vol. 141, pp. 166-174, Feb 17 2016, doi: 10.1016/j.ces.2015.11.005.

[84] G. Schöny, E. Zehetner, J. Fuchs, T. Pröll, G. Sprachmann, and H. Hofbauer, "Design of a bench scale unit for continuous CO2 capture via temperature swing adsorption-Fluid-dynamic feasibility study," *Chemical Engineering Research and Design,* Article vol. 106, pp. 155-167, 2016, doi: 10.1016/j.cherd.2015.12.018.

[85] R. W. Breault *et al.*, "Carbon capture test unit design and development using amine-based solid sorbent," *Chemical Engineering Research and Design,* Article vol. 112, pp. 251-262, 2016, doi: 10.1016/j.cherd.2016.06.020.

[86] G. Hofer, J. Fuchs, G. Schöny, and T. Pröll, "Heat transfer challenge and design evaluation for a multi-stage temperature swing adsorption process," *Powder Technology,* vol. 316, pp. 512-518, 2017/07/01/ 2017, doi: https://doi.org/10.1016/j.powtec.2016.12.062.

[87] R. Veneman, T. Hilbers, D. W. F. Brilman, and S. R. A. Kersten, "CO2 capture in a continuous gas–solid trickle flow reactor," *Chemical Engineering Journal,* vol. 289, pp. 191-202, 2016/04/01/ 2016, doi: https://doi.org/10.1016/j.cej.2015.12.066.

[88] F. Dietrich, G. Schöny, J. Fuchs, and H. Hofbauer, "Experimental study of the adsorber performance in a multi-stage fluidized bed system for continuous CO2 capture by means of temperature swing adsorption," *Fuel Processing Technology,* Article vol. 173, pp. 103-111, 2018, doi: 10.1016/j.fuproc.2018.01.013.

[89] S. E. Zanco, M. Mazzotti, M. Gazzani, M. C. Romano, and I. Martinez, "Modeling of Circulating Fluidized Beds Systems for Post-Combustion CO2 Capture via Temperature Swing Adsorption," *Aiche Journal,* vol. 64, no. 5, pp. 1744-1759, May 2018, doi: 10.1002/aic.16029.

[90] S. Cloete, A. Giuffrida, M. C. Romano, and A. Zaabout, "The swing adsorption reactor cluster for post-combustion CO2 capture from cement plants," *Journal of Cleaner Production,* vol. 223, pp. 692-703, 2019/06/20/ 2019, doi: https://doi.org/10.1016/j.jclepro.2019.03.109.

[91] S. Cloete, A. Giuffrida, M. C. Romano, and A. Zaabout, "The effect of sorbent regeneration enthalpy on the performance of the novel Swing Adsorption Reactor Cluster (SARC) for post-combustion CO2 capture," *Chemical Engineering Journal,* 2018/08/30/ 2018, doi: https://doi.org/10.1016/j.cej.2018.08.196.

[92] C. Dhoke *et al.*, "The swing adsorption reactor cluster (SARC) for post combustion CO2 capture: Experimental proof-of-principle," *Chemical Engineering Journal,* vol. 377, p. 120145, 2019/12/01/ 2019, doi: https://doi.org/10.1016/j.cej.2018.10.082.

[93] A. Zaabout *et al.*, "A Novel Swing Adsorption Reactor Cluster (SARC) for Cost Effective Post-combustion CO2 Capture: A Thermodynamic Assessment," *Energy Procedia,* vol. 114, pp. 2488-2496, 2017/07/01/ 2017, doi: https://doi.org/10.1016/j.egypro.2017.03.1404.

[94] L. Joss, M. Gazzani, and M. Mazzotti, "Rational design of temperature swing adsorption cycles for post-combustion CO2 capture," *Chemical Engineering Science,* vol. 158, pp. 381-394, 2017/02/02/ 2017, doi: https://doi.org/10.1016/j.ces.2016.10.013.

[95] M. G. Plaza, F. Rubiera, and C. Pevida, "Evaluating the Feasibility of a TSA Process Based on Steam Stripping in Combination with Structured Carbon Adsorbents To Capture CO2 from a Coal Power Plant," *Energy & Fuels,* vol. 31, no. 9, pp. 9760-9775, 2017/09/21 2017, doi: 10.1021/acs.energyfuels.7b01508.

[96] G. Mondino *et al.*, "Production of MOF Adsorbent Spheres and Comparison of Their Performance with Zeolite 13X in a Moving-Bed TSA Process for Postcombustion CO2 Capture," *Industrial & Engineering Chemistry Research,* vol. 59, no. 15, pp. 7198-7211, 2020/04/15 2020, doi: 10.1021/acs.iecr.9b06387.

[97] W. Jung, J. Park, and K. S. Lee, "Moving bed adsorption process based on a PEI-silica sorbent for CO2 capture," *International Journal of Greenhouse Gas Control,* vol. 67, pp. 10-19, 2017/12/01/ 2017, doi: https://doi.org/10.1016/j.ijggc.2017.10.004.

[98] Q. Wang, J. Luo, Z. Zhong, and A. Borgna, "CO2 capture by solid adsorbents and their applications: current status and new trends," *Energy & Environmental Science,* 10.1039/C0EE00064G vol. 4, no. 1, pp. 42-55, 2011, doi: 10.1039/C0EE00064G.

[99] W. Zhang, H. Liu, Y. Sun, J. Cakstins, C. Sun, and C. E. Snape, "Parametric study on the regeneration heat requirement of an amine-based solid adsorbent process for post-combustion carbon capture," *Applied Energy,* vol. 168, pp. 394-405, 2016/04/15/ 2016, doi: https://doi.org/10.1016/j.apenergy.2016.01.049.

[100] J. Park, W. Won, W. Jung, and K. S. Lee, "One-dimensional modeling of a turbulent fluidized bed for a sorbent-based CO 2 capture process with solid–solid sensible heat exchange," *Energy,* Article pp. 1168-1180, 2019, doi: 10.1016/j.energy.2018.11.152.

[101] Y. K. Park *et al.*, "An Energy Exchangeable Solid-sorbent Based Multi-stage Fluidized Bed Process for CO 2 Capture," in *Energy Procedia*, 2017, vol. 114, pp. 2410-2420, doi: 10.1016/j.egypro.2017.03.1388.

[102] J. Bonjour, J.-B. Chalfen, and F. Meunier, "Temperature Swing Adsorption Process with Indirect Cooling and Heating," *Industrial & Engineering Chemistry Research,* vol. 41, no. 23, pp. 5802-5811, 2002/11/01 2002, doi: 10.1021/ie011011j.

[103] A. Ntiamoah, J. Ling, P. Xiao, P. A. Webley, and Y. Zhai, "CO2 Capture by Temperature Swing Adsorption: Use of Hot CO2-Rich Gas for Regeneration," *Industrial & Engineering Chemistry Research,* vol. 55, no. 3, pp. 703-713, 2016/01/27 2016, doi: 10.1021/acs.iecr.5b01384.

[104] N. Tlili, G. Grévillot, and C. Vallières, "Carbon dioxide capture and recovery by means of TSA and/or VSA," *International Journal of Greenhouse Gas Control,* vol. 3, no. 5, pp. 519-527, 2009/09/01/ 2009, doi: https://doi.org/10.1016/j.ijggc.2009.04.005.

[105] D. Tondeur, G. Grevillot, J. Granger, and M. Mitrović, "Temperature-Swing Gas Separation with Electrothermal Desorption Step AU - Petkovska, M," *Separation Science and Technology,* vol. 26, no. 3, pp. 425-444, 1991/03/01 1991, doi: 10.1080/01496399108050482.

[106] S. Lillia, D. Bonalumi, C. Grande, and G. Manzolini, "A comprehensive modeling of the hybrid temperature electric swing adsorption process for CO2 capture," *International Journal of Greenhouse Gas Control,* vol. 74, pp. 155-173, 2018/07/01/ 2018, doi: https://doi.org/10.1016/j.ijggc.2018.04.012.

[107] P. A. Webley, "Adsorption technology for CO2 separation and capture: a perspective," *Adsorption,* vol. 20, no. 2, pp. 225-231, 2014/02/01 2014, doi: 10.1007/s10450-014-9603-2.

[108] S. Krishnamurthy *et al.*, "CO2 capture from dry flue gas by vacuum swing adsorption: A pilot plant study," vol. 60, no. 5, pp. 1830-1842, 2014, doi: doi:10.1002/aic.14435.

[109] S. P. Reynolds, A. Mehrotra, A. D. Ebner, and J. A. Ritter, "Heavy reflux PSA cycles for CO2 recovery from flue gas: Part I. Performance evaluation," *Adsorption,* journal article vol. 14, no. 2, pp. 399-413, June 01 2008, doi: 10.1007/s10450-008-9102-4.

[110] Z. Liu, C. A. Grande, P. Li, J. Yu, and A. E. Rodrigues, "Multi-bed Vacuum Pressure Swing Adsorption for carbon dioxide capture from flue gas," *Separation and Purification Technology,* vol. 81, no. 3, pp. 307-317, 2011/10/10/ 2011, doi: https://doi.org/10.1016/j.seppur.2011.07.037.

[111] S. Krishnamurthy, R. Haghpanah, A. Rajendran, and S. Farooq, "Simulation and Optimization of a Dual-Adsorbent, Two-Bed Vacuum Swing Adsorption Process for CO2 Capture from Wet Flue Gas," *Industrial & Engineering Chemistry Research,* vol. 53, no. 37, pp. 14462-14473, 2014/09/17 2014, doi: 10.1021/ie5024723.

[112] K. T. Leperi, R. Q. Snurr, and F. You, "Optimization of Two-Stage Pressure/Vacuum Swing Adsorption with Variable Dehydration Level for Postcombustion Carbon Capture," *Industrial & Engineering Chemistry Research,* vol. 55, no. 12, pp. 3338-3350, 2016/03/30 2016, doi: 10.1021/acs.iecr.5b03122.

[113] M. Ishibashi *et al.*, "Technology for removing carbon dioxide from power plant flue gas by the physical adsorption method," *Energy Conversion and Management,* vol. 37, no. 6, pp. 929-933, 1996/06/01/ 1996, doi: https://doi.org/10.1016/0196-8904(95)00279-0.

[114] C. Dhoke *et al.*, "The swing adsorption reactor cluster (SARC) for post combustion CO2 capture: Experimental proof-of-principle," *Chemical Engineering Journal,* 2018/10/09/ 2018, doi: https://doi.org/10.1016/j.cej.2018.10.082.

[115] K. Warmuzinski, M. Tanczyk, and M. Jaschik, "Experimental study on the capture of CO2 from flue gas using adsorption combined with membrane separation," *International Journal of Greenhouse Gas Control,* vol. 37, pp. 182-190, 2015/06/01/ 2015, doi: https://doi.org/10.1016/j.ijggc.2015.03.009.

[116] J. A. Wurzbacher, C. Gebald, and A. Steinfeld, "Separation of CO2 from air by temperature-vacuum swing adsorption using diamine-functionalized silica gel," *Energy & Environmental Science,* 10.1039/C1EE01681D vol. 4, no. 9, pp. 3584-3592, 2011, doi: 10.1039/C1EE01681D.

[117] J. Fujiki, F. A. Chowdhury, H. Yamada, and K. Yogo, "Highly efficient post-combustion CO2 capture by low-temperature steam-aided vacuum swing adsorption using a novel polyamine-

based solid sorbent," *Chemical Engineering Journal,* vol. 307, pp. 273-282, 2017/01/01/ 2017, doi: https://doi.org/10.1016/j.cej.2016.08.071.

[118] C. Dhoke *et al.*, "Sorbents screening for post-combustion CO2 capture via combined temperature and pressure swing adsorption," *Chemical Engineering Journal,* p. 122201, 2019/07/11/ 2019, doi: https://doi.org/10.1016/j.cej.2019.122201.

[119] M. G. Plaza and F. Rubiera, "Evaluation of a novel multibed heat-integrated vacuum and temperature swing adsorption post-combustion CO2 capture process," *Applied Energy,* vol. 250, pp. 916-925, 2019/09/15/ 2019, doi: https://doi.org/10.1016/j.apenergy.2019.05.079.

[120] S. Sengupta *et al.*, "Circulating Fluid-Bed Studies for CO2 Capture from Flue Gas using K2CO3/Al2O3 Adsorbent," *Energy & Fuels,* vol. 32, no. 8, pp. 8594-8604, 2018/08/16 2018, doi: 10.1021/acs.energyfuels.8b01383.

[121] R. Zhao, L. Zhao, S. Wang, S. Deng, H. Li, and Z. Yu, "Solar-assisted pressure-temperature swing adsorption for CO2 capture: Effect of adsorbent materials," *Solar Energy Materials and Solar Cells,* vol. 185, pp. 494-504, 2018/10/01/ 2018, doi: https://doi.org/10.1016/j.solmat.2018.06.004.

[122] Y. Lara, A. Martínez, P. Lisbona, and L. M. Romeo, "Energy Integration of High and Low Temperature Solid Sorbents for CO2 Capture," *Energy Procedia,* vol. 114, pp. 2380-2389, 2017/07/01/ 2017, doi: https://doi.org/10.1016/j.egypro.2017.03.1384.

[123] K. Kim, D. Kim, Y.-K. Park, and K. S. Lee, "A solid sorbent-based multi-stage fluidized bed process with inter-stage heat integration as an energy efficient carbon capture process," *International Journal of Greenhouse Gas Control,* vol. 26, pp. 135-146, Jul 2014, doi: 10.1016/j.ijggc.2014.03.012.

[124] H. Vogtenhuber, R. Hofmann, F. Helminger, and G. Schöny, "Process simulation of an efficient temperature swing adsorption concept for biogas upgrading," *Energy,* vol. 162, pp. 200-209, 2018/11/01/ 2018, doi: https://doi.org/10.1016/j.energy.2018.07.193.

[125] W. Jung, J. Park, W. Won, and K. S. Lee, "Simulated moving bed adsorption process based on a polyethylenimine-silica sorbent for CO2 capture with sensible heat recovery," *Energy,* vol. 150, pp. 950-964, 2018/05/01/ 2018, doi: https://doi.org/10.1016/j.energy.2018.03.022.

[126] W. Zhang *et al.*, "Process simulations of post-combustion CO2 capture for coal and natural gas-fired power plants using a polyethyleneimine/silica adsorbent," *International Journal of Greenhouse Gas Control,* Article vol. 58, pp. 276-289, 2017, doi: 10.1016/j.ijggc.2016.12.003.

[127] M. Clausse, J. Merel, and F. Meunier, "Numerical parametric study on CO2 capture by indirect thermal swing adsorption," *International Journal of Greenhouse Gas Control,* vol. 5, no. 5, pp. 1206-1213, 2011/09/01/ 2011, doi: https://doi.org/10.1016/j.ijggc.2011.05.036.

[128] S. Sjostrom, H. Krutka, T. Starns, and T. Campbell, "Pilot test results of post-combustion CO2 capture using solid sorbents," *Energy Procedia,* vol. 4, pp. 1584-1592, 2011/01/01/ 2011, doi: https://doi.org/10.1016/j.egypro.2011.02.028.

[129] W. J. Morris *et al.*, "ADA's Solid Sorbent CO2 Capture process: Developing Solid Sorbent Technology to Provide the Necessary Flexible CO2 Capture Solutions for a Wide Range of Applications," *Energy Procedia,* vol. 63, pp. 1536-1545, 2014/01/01/ 2014, doi: https://doi.org/10.1016/j.egypro.2014.11.163.

[130] S. Sjostrom and C. Senior, "Pilot testing of CO2 capture from a coal-fired power plant—Part 2: Results from 1-MWe pilot tests," *Clean Energy,* vol. 4, no. 1, pp. 12-25, 2020, doi: 10.1093/ce/zkz034.

[131] Y. C. Park *et al.*, "Test Operation Results of the 10 MWe-scale Dry-sorbent CO2 Capture Process Integrated with a Real Coal-fired Power Plant in Korea," *Energy Procedia,* vol. 63, pp. 2261-2265, 2014/01/01/ 2014, doi: https://doi.org/10.1016/j.egypro.2014.11.245.

[132] F. Raganati, P. Ammendola, and R. Chirone, "CO2 adsorption on fine activated carbon in a sound assisted fluidized bed: Effect of sound intensity and frequency, CO2 partial pressure and fluidization velocity," *Applied Energy,* vol. 113, pp. 1269-1282, 2014/01/01/ 2014, doi: https://doi.org/10.1016/j.apenergy.2013.08.073.

[133] D. Danaci, M. Bui, N. Mac Dowell, and C. Petit, "Exploring the limits of adsorption-based CO2 capture using MOFs with PVSA – from molecular design to process economics," *Molecular Systems Design & Engineering,* 10.1039/C9ME00102F vol. 5, no. 1, pp. 212-231, 2020, doi: 10.1039/C9ME00102F.

[134] B. Verougstraete, A. Martin-Calvo, S. Van der Perre, G. Baron, V. Finsy, and J. F. M. Denayer, "A new honeycomb carbon monolith for CO2 capture by rapid temperature swing adsorption using steam regeneration," (in Multi-Language), *Chemical Engineering Journal,* vol. 383, 2020, doi: 10.1016/j.cej.2019.123075.

[135] W. Jung *et al.*, "Rapid thermal swing adsorption process in multi-beds scale with sensible heat recovery for continuous energy-efficient CO2 capture," *Chemical Engineering Journal,* p. 123656, 2019/12/02/ 2019, doi: https://doi.org/10.1016/j.cej.2019.123656.

[136] Y.-K. Park *et al.*, "An Energy Exchangeable Solid-sorbent Based Multi-stage Fluidized Bed Process for CO2 Capture," *Energy Procedia,* vol. 114, pp. 2410-2420, 2017/07/01/ 2017, doi: https://doi.org/10.1016/j.egypro.2017.03.1388.

[137] W. Choi *et al.*, "Epoxide-functionalization of polyethyleneimine for synthesis of stable carbon dioxide adsorbent in temperature swing adsorption," *Nature Communications,* Article vol. 7, p. 12640, 08/30/online 2016, doi: 10.1038/ncomms12640

[138] I. Luz, M. Soukri, and M. Lail, "Confining Metal–Organic Framework Nanocrystals within Mesoporous Materials: A General Approach via "Solid-State" Synthesis," *Chemistry of Materials,* vol. 29, no. 22, pp. 9628-9638, 2017/11/28 2017, doi: 10.1021/acs.chemmater.7b02042.

[139] I. Luz, M. Soukri, and M. Lail, "Flying MOFs: polyamine-containing fluidized MOF/SiO2 hybrid materials for CO2 capture from post-combustion flue gas," *Chemical Science,* 10.1039/C7SC05372J vol. 9, no. 20, pp. 4589-4599, 2018, doi: 10.1039/C7SC05372J.

[140] C. Dhoke *et al.*, "Sorbents screening for post-combustion CO2 capture via combined temperature and pressure swing adsorption," *Chemical Engineering Journal,* vol. 380, p. 122201, 2020/01/15/ 2020, doi: https://doi.org/10.1016/j.cej.2019.122201.

[141] S. Cloete, A. Giuffrida, M. C. Romano, and A. Zaabout, "The effect of sorbent regeneration enthalpy on the performance of the novel Swing Adsorption Reactor Cluster (SARC) for post-combustion CO2 capture," *Chemical Engineering Journal,* vol. 377, p. 119810, 2019/12/01/ 2019, doi: https://doi.org/10.1016/j.cej.2018.08.196.

[142] S. O. D. L. Gardarsdottir, E.; Romano, M.; Roussanaly, S.; Voldsund, M.; Pérez-Calvo, J.-F.; Berstad, D.; Fu, C.; Anantharaman, R.; Sutter, D.; Gazzani, M.; Mazzotti, M.; Cinti, G. , "Comparison of Technologies for CO2 Capture from Cement Production—Part 2: Cost Analysis," *Energies* vol. 12, p. 542, 2019, doi: 10.3390/en12030542